rec'd
10/1/01

Simulation of a Long-Term Aquifer Test Conducted near the Rio Grande, Albuquerque, New Mexico

---

U.S. DEPARTMENT OF THE INTERIOR
U.S. GEOLOGICAL SURVEY

Water-Resources Investigations Report 99-4260

Prepared in cooperation with the

CITY OF ALBUQUERQUE PUBLIC WORKS DEPARTMENT

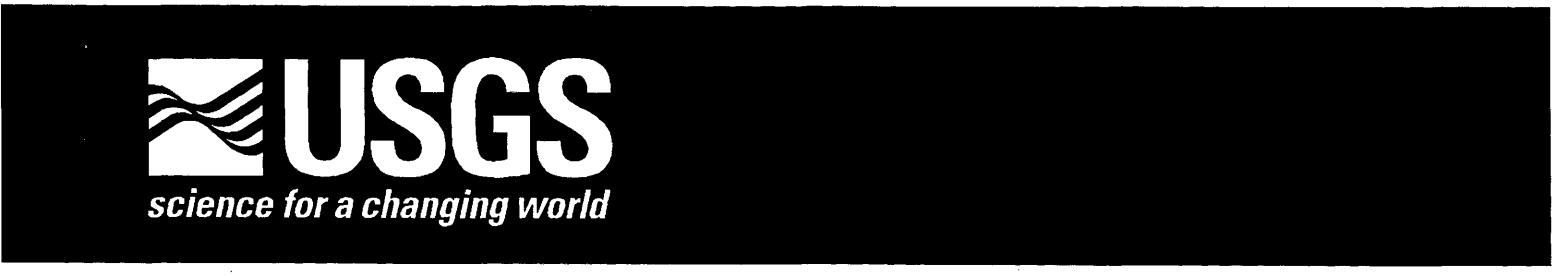

Simulation of a Long-Term Aquifer Test Conducted near the Rio Grande, Albuquerque, New Mexico

By Douglas P. McAda

U.S. GEOLOGICAL SURVEY

Water-Resources Investigations Report 99-4260

Prepared in cooperation with the

CITY OF ALBUQUERQUE PUBLIC WORKS DEPARTMENT

Albuquerque, New Mexico
2001

U.S. DEPARTMENT OF THE INTERIOR
GALE A. NORTON, Secretary

U.S. GEOLOGICAL SURVEY
Charles G. Groat, Director

For additional information write to:

District Chief
U.S. Geological Survey
Water Resources Division
5338 Montgomery Blvd. NE, Suite 400
Albuquerque, NM 87109-1311

Copies of this report can be purchased from:

U.S. Geological Survey
Information Services
Box 25286
Denver, CO 80225-0286

Information regarding research and data-collection programs of the U.S. Geological Survey is available on the Internet via the World Wide Web. You may connect to the home page for the New Mexico District Office using the URL *http://nm.water.usgs.gov.*

CONTENTS

PLATE

FIGURES

TABLES

CONVERSION FACTORS AND VERTICAL DATUM

Multiply	By	To obtain
inch	2.54	centimeter
foot	0.3048	meter
mile	1.609	kilometer
per foot	3.281	per meter
square foot	0.09290	square meter
square mile	2.590	square kilometer
gallon	3.785	liter
cubic foot	0.02832	cubic meter
acre-foot	1,233	cubic meter
cubic foot per second	0.02832	cubic meter per second
cubic foot per day	0.02832	cubic meter per day
acre-foot per day	0.01427	cubic meter per second
foot per day	0.3048	meter per day
gallon per minute	0.06309	liter per second
foot squared	0.09290	meter squared
foot squared per day	0.09290	meter squared per day

Sea level: In this report, "sea level" refers to the National Geodetic Vertical Datum of 1929—a geodetic datum derived from a general adjustment of the first-order level nets of the United States and Canada, formerly called Sea Level Datum of 1929.

SIMULATION OF A LONG-TERM AQUIFER TEST CONDUCTED NEAR THE RIO GRANDE, ALBUQUERQUE, NEW MEXICO

By Douglas P. McAda

ABSTRACT

A long-term aquifer test was conducted near the Rio Grande in Albuquerque during January and February 1995 using 22 wells and piezometers at nine sites, with the City of Albuquerque Griegos 1 production well as the pumped well. Griegos 1 discharge averaged about 2,330 gallons per minute for 54.4 days. A three-dimensional finite-difference ground-water-flow model was used to estimate aquifer properties in the vicinity of the Griegos well field and the amount of infiltration induced into the aquifer system from the Rio Grande and riverside drains as a result of pumping during the test. The model was initially calibrated by trial-and-error adjustments of the aquifer properties. The model was recalibrated using a nonlinear least-squares regression technique.

The aquifer system in the area includes the middle Tertiary to Quaternary Santa Fe Group and post-Santa Fe Group valley- and basin-fill deposits of the Albuquerque Basin. The Rio Grande and adjacent riverside drains are in hydraulic connection with the aquifer system.

The hydraulic-conductivity values of the upper part of the Santa Fe Group resulting from the model calibrated by trial and error varied by zone in the model and ranged from 12 to 33 feet per day. The hydraulic conductivity of the inner-valley alluvium was 45 feet per day. The vertical to horizontal anisotropy ratio was 1:140. Specific storage was 4×10^{-6} per foot of aquifer thickness, and specific yield was 0.15 (dimensionless). The sum of squared errors between the observed and simulated drawdowns was 130 feet squared.

Not all aquifer properties could be estimated using nonlinear regression because of model insensitivity to some aquifer properties at observation locations. Hydraulic conductivity of the inner-valley alluvium, middle part of the Santa Fe Group, and riverbed and riverside-drain bed and specific yield had low sensitivity values and therefore could not be estimated. Of the properties estimated, hydraulic conductivity of the upper part of the Santa Fe Group was estimated to be 12 feet per day, the vertical to horizontal anisotropy ratio was estimated to be 1:82, and specific storage was estimated to be 1.2×10^{-6} per foot of aquifer thickness. The overall sum of squared errors between the observed and simulated drawdowns was 87 feet squared, a significant improvement over the model calibrated by trial and error.

At the end of aquifer-test pumping, induced infiltration from the Rio Grande and riverside drains was simulated to be 13 percent of the total amount of water pumped. The remainder was water removed from aquifer storage. After pumping stopped, induced infiltration continued to replenish aquifer storage. Simulations estimated that 5 years after pumping began (about 4.85 years after pumping stopped), 58 to 72 percent of the total amount of water pumped was replenished by induced infiltration from the Rio Grande surface-water system.

INTRODUCTION

Ground water withdrawn from the Santa Fe Group aquifer system is the principal source of water for municipal, domestic, and industrial uses (Wilson, 1992) in the Albuquerque Basin (fig. 1). The aquifer system, composed of middle Tertiary to Quaternary Santa Fe Group and Quaternary post-Santa Fe Group deposits, is hydraulically connected to the Rio Grande and a system of canals and drains through the alluvium in the Rio Grande inner valley. Because water in the Rio Grande is fully appropriated, it is important to evaluate the effects of ground-water withdrawal from wells on the flow of the river (McAda, 1996, p. 3).

A long-term aquifer test was conducted near the Rio Grande in Albuquerque during January and February 1995 using 22 wells and piezometers at nine sites, with the City of Albuquerque Griegos 1 production well used as the pumped well (fig. 2). The purpose of this test was to estimate aquifer properties in the vicinity of the Griegos well field and the amount of water induced into the aquifer system as a result of pumping during the test. The aquifer test and analysis of aquifer properties using conventional analytical curve-matching techniques are described by Thorn (2001). Although these techniques can be used to

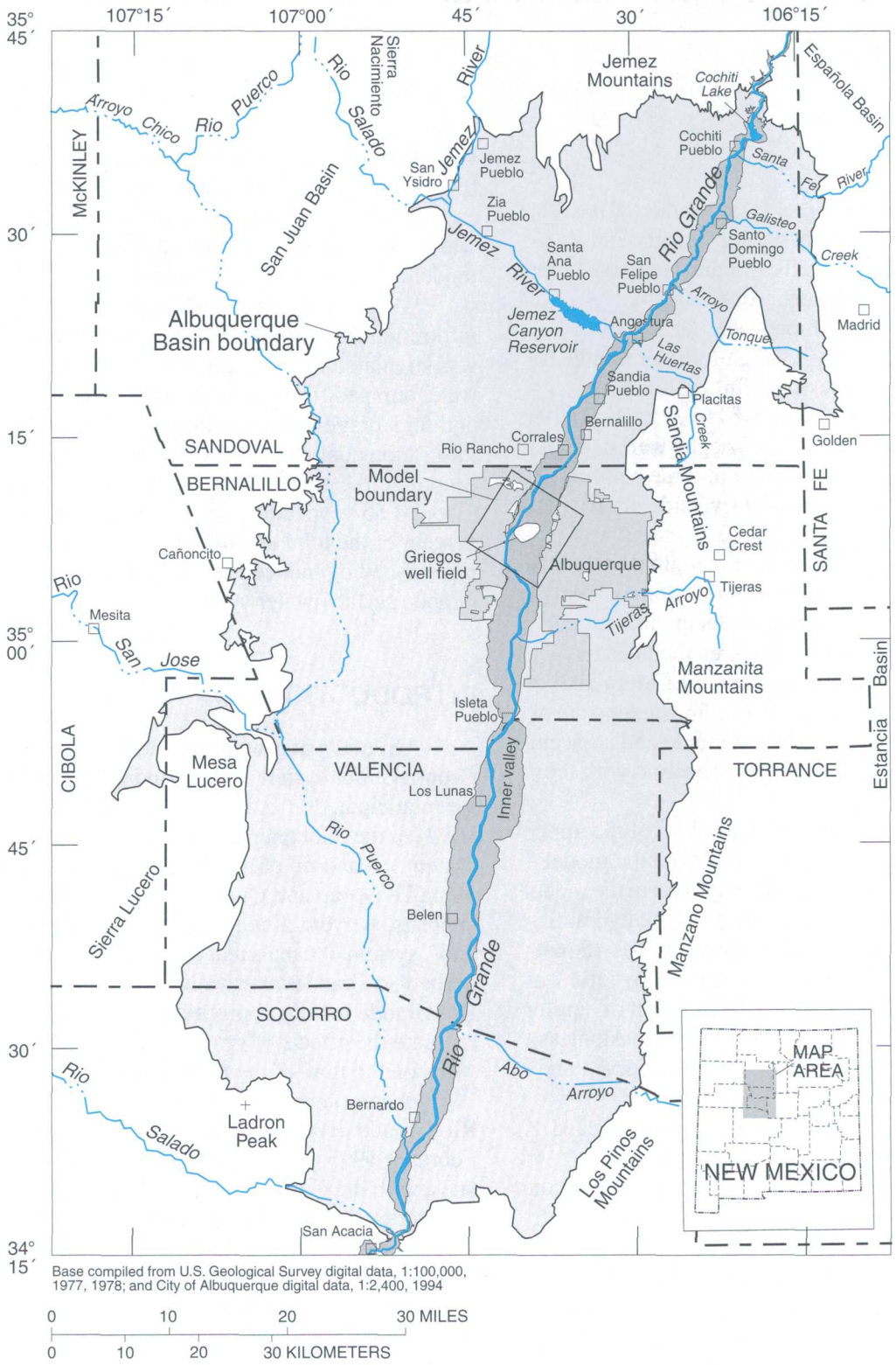

Figure 1. Location of the modeled area in the Albuquerque Basin, central New Mexico.

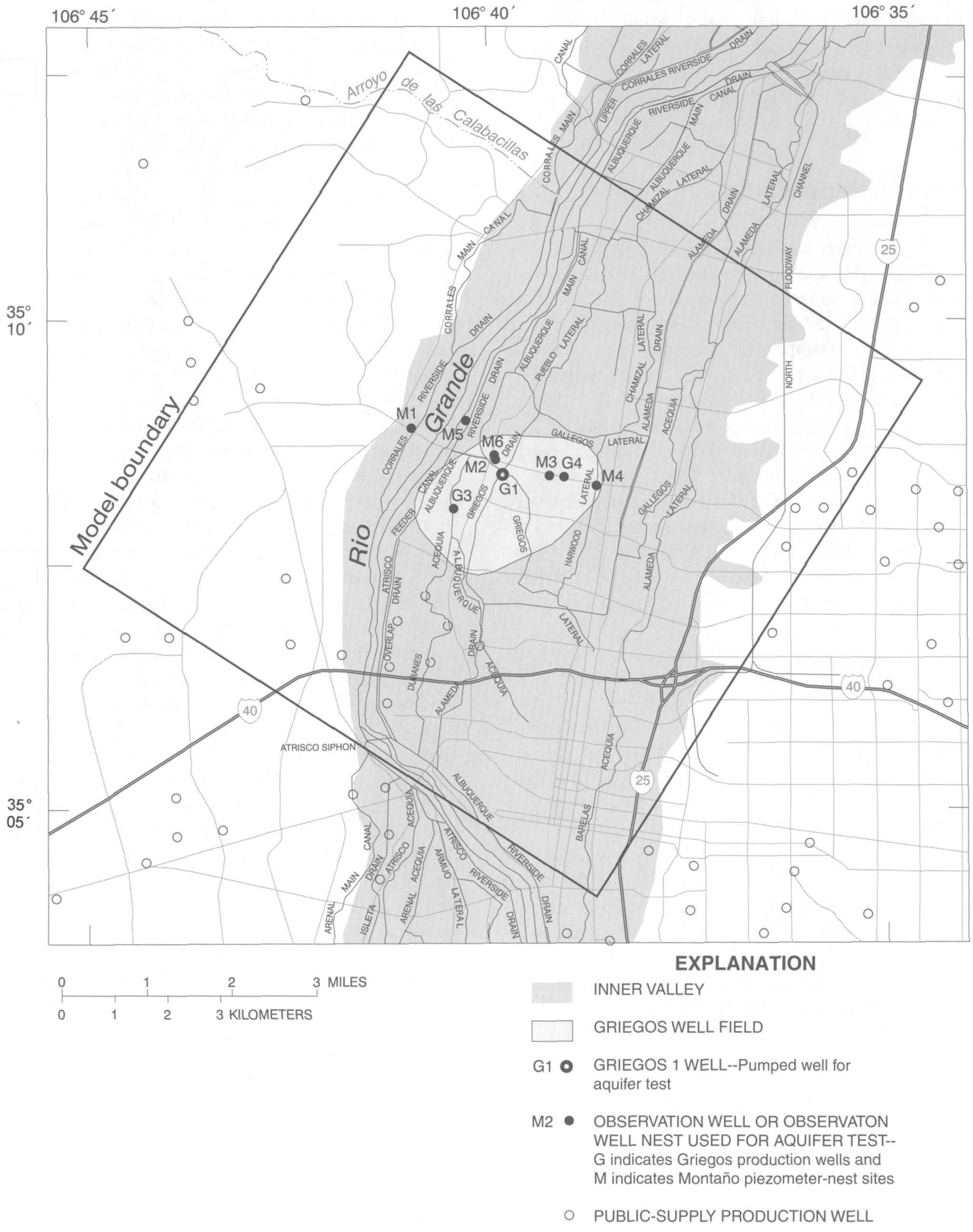

Figure 2. Vicinity of aquifer test.

estimate aquifer properties, they cannot be used to estimate the amount and timing of infiltration of water from the river/canal/drain system resulting from ground-water withdrawal. A ground-water-flow model is a tool that can be used for that purpose. This study was conducted to analyze this aquifer test using numerical-modeling techniques.

Acknowledgments

This study was conducted in cooperation with the City of Albuquerque Public Works Department. The author thanks the numerous Water Utility Division employees of the Public Works Department for modifying City supply-well pumping schedules to accomodate this aquifer test and for providing well production records. Claire Tiedeman of the U.S. Geological Survey (USGS) provided essential guidance in the application of the nonlinear regression method. She and Mike Roark (USGS) technically reviewed this report. Jim Basler and Chuck Heywood (USGS) installed monitoring instrumentation and collected the monitoring data for this test. Condé Thorn and Chuck Heywood (USGS) compiled and corrected those data for use in aquifer-test analyses.

Purpose and Scope

This report describes a finite-difference ground-water flow-model analysis of the aquifer test, the resulting estimates of aquifer properties and infiltration from the river/canal/drain system, and the comparison of the infiltration estimates to estimates derived by analytical solution. The ground-water-flow model was calibrated by trial-and-error adjustments of the aquifer's hydraulic properties using the computer program MODFLOW developed by McDonald and Harbaugh (1988). The model was further calibrated using the nonlinear-regression technique implemented in the computer program MODFLOWP developed by Hill (1992).

Study-Area Description

The study area is the vicinity of the City of Albuquerque Griegos well field in the Rio Grande inner valley (fig. 2) and is within the Albuquerque Basin (fig. 1). The basin is defined for this report as the extent of Cenozoic deposits within the structural Rio Grande Rift between Cochiti Pueblo and San Acacia (Thorn and others, 1993, p. 10). The inner valley is a broad flood plain along the Rio Grande and is about 4 miles wide near the Griegos well field. The river lies on the west side of the flood plain in this area. The Rio Grande is perennial and has a mean annual flow of about 1,055,000 acre-feet (Rio Grande at Albuquerque, New Mexico, after closure of Cochiti Dam, water years 1974-97; Ortiz and others, 1998, p. 216).

The Rio Grande surface-water system in the Albuquerque area consists of the Rio Grande and a series of canals and drains in the Rio Grande inner valley (fig. 2). Water is diverted from the Rio Grande to canals for irrigation within the inner valley. Riverside drains, installed in the 1920's and 1930's, intercept seepage from the Rio Grande that previously contributed to waterlogging of irrigated land in the inner valley. These drains are open channels dug to a level below the water table. Interior drains, most of which are also open channels, were installed beginning at the same time as the riverside drains. The interior drains were installed to lower the water table and prevent waterlogging of land as a result of seepage from canals and irrigation in the inner valley. The interior drains discharge to the riverside drains, which then return the water to the river downstream. The interior drains in the vicinity of the Griegos well field no longer function as water-table drains because ground-water withdrawal and the transfer of irrigated land to other uses have resulted in the water table dropping below drain level. However, the interior and riverside drains receive canal tail water during the irrigation season and storm runoff.

The Albuquerque Riverside Drain on the east side of the Rio Grande also functions as a feeder canal during the irrigation season (Atrisco Feeder Canal, fig. 2), but functions as a drain the rest of the year. The altitude of the Albuquerque Riverside Drain rises relative to the river toward the south in the modeled area so that drain water may be returned to the river at a wasteway near the Atrisco Siphon. An overlap drain takes over the drain function about 2 miles north of the wasteway (fig. 2). This overlap drain continues south to become the Albuquerque Riverside Drain.

The Corrales Riverside Drain on the west side of the Rio Grande extends only through the northern part of the modeled area (fig. 2). Water is returned to the river at the southern terminus of the drain. The river is on the western edge of the flood plain in the southern part of the modeled area. An escarpment on the west side of the flood plain in this area makes a drain impractical and unnecessary.

Geohydrologic Setting

The geologic framework of the Albuquerque Basin was described by Hawley and Haase (1992) and by Hawley and others (1995). These reports also provide references to additional geologic reports and information about the basin. McAda (1996) described components of the Santa Fe Group aquifer system and provided references describing various aspects of hydrologic conditions in the basin.

The Santa Fe Group aquifer system in the Albuquerque Basin is composed of middle Tertiary to Quaternary Santa Fe Group and Quaternary post-Santa Fe Group valley and basin-fill deposits. The Santa Fe Group is as much as about 15,000 feet thick in the Albuquerque Basin (Hawley and others, 1995, p. 47). The upper part of the Santa Fe Group is the primary water-yielding zone in the vicinity of the aquifer test and is about 850 feet thick in this area (Hawley and others, 1995, p. 8; Hawley, 1996, app. F). The middle part of the Santa Fe Group, about 5,000 feet thick in this area (Hawley and Haase, 1992, fig. III-4), and the lower part of the Santa Fe Group, about 3,000 feet thick in this area (Hawley and Haase, 1992, fig. III-3), do not provide significant quantities of water to wells in the vicinity of the aquifer test.

The alluvium in the inner valley consists of post-Santa Fe Group deposits from the most recent erosion and deposition sequence of the Rio Grande (Hawley and Haase, 1992, p. II-7). These channel and flood-plain sediments average about 70 to 80 feet thick in the vicinity of the well field (Hawley, 1996, app. F).

Aquifer-Test Description

The aquifer test was conducted in the City of Albuquerque Griegos well field (figs. 1 and 2). A detailed description of the test can be found in Thorn (2001). The Griegos 1 production well was the well pumped for the test. Nineteen piezometers at six sites and the Griegos 3 and 4 production wells were used as observation wells. Water levels were also measured in the pumped well. In preparation for the test, all public-supply wells within 2.8 miles of Griegos 1 were shut down on October 1, 1994, 3 months prior to the beginning of aquifer-test pumping. This allowed water levels in the test area to come to a relatively static condition and pretest water levels in the observation and pumped wells to be measured. Water levels in each well were continuously monitored with pressure transducers or floats and recorded at preset intervals, which varied with time during the test. Stage in the Rio Grande and Albuquerque Riverside Drain and barometric pressure were also monitored. Pretest water-level trends and effects of changes in stage and barometric pressure on water levels in each well were determined from measurements made during the pretest period. The drawdown measured in each well during the test was then corrected on the basis of pretest water-level trends and on the changes in stage and barometric pressure (Thorn, 2001). Except for additional corrections made to the drawdown measured in Griegos 1 (described later in this report), these corrected measurements are the observed drawdowns used in this report.

Griegos 1 began pumping the morning of January 4, 1995. Except for a 27-minute power failure on January 5, it pumped continuously until the evening of February 27, 1995. The average discharge was about 2,330 gallons per minute over the 54-day, 9-hour period. Water-level recovery from the aquifer-test pumping was monitored for 3 weeks. A well-bore flow test was conducted during the last week of March 1995 to help determine the distribution of water production along the well screen (Thorn, 2001). Normal operation of all public-supply wells in the test area resumed on April 1, 1995.

MODEL DESCRIPTION

Ground-water flow during the Griegos well field aquifer test was simulated in three dimensions using the MODFLOW finite-difference ground-water-flow model developed by McDonald and Harbaugh (1988). By assuming that the Cartesian coordinate axes x, y, and z are aligned with the principal components of hydraulic conductivity, three-dimensional ground-water flow through a porous medium can be expressed as (McDonald and Harbaugh, 1988, p. 2-1):

$$\frac{\partial}{\partial x}\left(K_{xx}\frac{\partial h}{\partial x}\right)+\frac{\partial}{\partial y}\left(K_{yy}\frac{\partial h}{\partial y}\right)+\frac{\partial}{\partial z}\left(K_{zz}\frac{\partial h}{\partial z}\right)-W = S_s\frac{\partial h}{\partial t} \quad (1)$$

where K_{xx}, K_{yy}, and K_{zz} = values of hydraulic conductivity along the x, y, and z coordinate axes (LT^{-1});

h = potentiometric head (L);
W = a volumetric flux per unit volume and represents sources and (or) sinks of water (T^{-1});
S_s = specific storage of the porous material (L^{-1}); and
t = time (T).

The partial-differential flow equation (eq. 1) can be approximated by replacing the derivatives with finite differences. The aquifer is divided into a series of cells by a sequence of layers and a series of rows and columns extending through each layer. Aquifer properties are assumed to be uniform within each cell. Hydraulic heads are assumed to be at the center of each model cell. For a model with N cells, N simultaneous equations are formulated with the hydraulic heads as unknowns. The finite-difference equations are then solved simultaneously using one of several numerical-solver algorithms. The preconditioned conjugate-gradient method (Hill, 1990) is used as the algorithm to solve the equations. The rate and direction of ground-water flow between model cells and from model boundaries are then calculated on the basis of the hydraulic heads and the assigned aquifer properties.

A solution of the flow equation using this method is not unique—that is, any number of reasonable representations of the aquifer system can produce equally good results. However, a ground-water-flow model is a valuable tool that can be used to help understand an aquifer system and project responses to stresses on the aquifer system. Assumptions and simplifications are made in the formulation and solution of the mathematical equations; therefore, a ground-water-flow model is only an approximation of the aquifer system, and simulated results need to be interpreted carefully.

The model analysis described in this report uses the principle of superposition for simulating the aquifer test. The principle of superposition is applicable to a linear problem and as applied to a ground-water system means that the result of multiple stresses on an aquifer system is equal to the sum of the results of the individual stresses. Because the aquifer system is unconfined, transmissivity changes with drawdown of the water table and the differential equations describing the problem are not strictly linear. Reilly and others (1987) suggested that if drawdown is small relative to aquifer saturated thickness (about 10 percent or less), the error associated with this nonlinearity generally is acceptably small. Because drawdown during the aquifer test was substantially less than 10 percent of aquifer thickness, the error introduced as a result of using the superposition approach is considered small. For a detailed discussion of the application of superposition to ground-water problems, the reader is referred to Reilly and others (1987).

To apply the principle of superposition to a ground-water-flow model, the initial simulated hydraulic head for the aquifer and all model boundaries are set equal to zero, making all initial fluxes in the model also equal to zero. Layer top and bottom altitudes are specified in the model relative to the initial water-table altitude to conform with the zero initial head values and to assure that layer thicknesses are calculated correctly within the model code. All simulated changes in hydraulic head and water fluxes result from the simulated ground-water withdrawal of the aquifer-test pumping, and influences outside the pumped well are avoided. The adjusted drawdown from the actual test, which to the extent possible has been corrected for influences from stresses other than the aquifer-test pumping (Thorn, 2001), is then directly comparable to the simulated drawdown for use in model calibration.

Model Grid and Layers

The modeled area was divided by a grid containing 57 rows and 65 columns (pl. 1). The rows are oriented N. 33° E., which aligns the grid with the Rio Grande and with the general direction of major fault trends in the area (Hawley, 1996). This allows the model to effectively represent the river, while orienting the grid in the direction of the assumed principal hydraulic-conductivity tensor. The horizontal grid-cell dimensions vary from a column width of 100 feet and a row width of 200 feet along the Rio Grande and riverside drains in the central part of the model to a column width of 2,800 feet and a row width of 1,500 feet at the margins of the model. The grid is situated so that the pumped well, Griegos 1, is represented at the center of the model—the center of row 29, column 40 (pl. 1). The horizontal dimensions of the model are 7.2 miles on each side, covering an area of about 52 square miles.

The aquifer system in the test area is represented in the model by eight layers (fig. 3). Altitudes in figure 3 are shown relative to sea level; because superposition has been applied to the model, however, altitude values entered into the model are relative to the water table. The uppermost active cell at each row-column location in the model is simulated as unconfined. All other active cells are simulated as confined. The top of layer 1 is defined as the water table prior to the beginning of pumping during the aquifer test (zero altitude in the model), and the bottom of layer 1 is defined as 30 feet below the altitude of the Rio Grande. The maximum thickness of layer 1 is 30 feet directly under the Rio Grande. Layer-1 thickness decreases away from the river in both directions, corresponding with a decrease in the difference between the water-table altitude and the layer-1bottom altitude (fig. 3). Where the water table is below the bottom of layer 1, layer-1 cells are inactive and the top of layer 2 is the water table. The thickness of layer 2 is 50 feet except where the water table is below the bottom of layer 1. The water table is below the bottom of layer 2 in six cells along the west model boundary; therefore, layer 2 is inactive at those cells, and the top of layer 3 is the water table. Layers 3 through 8 range from 110 feet to 500 feet in thickness (fig. 3). Except for the six cells in layer 3 where the water table is below the bottom of layer 2, thicknesses of layers 3 through 8 are each constant throughout the model. The total model thickness simulated is 1,440 feet.

The model layers were defined to correspond with lithologic descriptions from the Montano 1-6 piezometer nests and the Griegos 1 production well (from Hawley, 1996, app. F; and Thorn, 2001) and the screened interval and flow distribution measured by well-bore flow tests in the Griegos 1 production well (fig. 4; Thorn, 2001). The top two model layers represent the post-Santa Fe Group river alluvium in the inner valley. Layer 3 is 150 feet thick and represents the portion of the upper part of the Santa Fe Group above the Griegos 1 well screen. Layer 4 is 190 feet thick and represents the upper part of the screened interval of Griegos 1. This interval contributes the most water to the Griegos 1 well, approximately 48 percent of the total, based on the well-bore flow test reported by Thorn (2001) and shown in figure 4. Layer 5 is 110 feet thick and represents the next lower section of well screen in Griegos 1. On the basis of the lithology described for Griegos 1 (Thorn, 2001), the sediments near the borehole in this interval contain a greater amount of finer grained sediments than the intervals above and below (layers 4 and 6). The effect of the finer grained sediments is reflected in the contribution of water from this interval, approximately 16 percent of the total (fig. 4). Layer 6 is 110 feet thick and represents the next lower portion of the well screen and the lowermost portion that contributed a significant amount of water to Griegos 1 in the well-bore flow test, approximately 36 percent of the total. Layer 7 is 300 feet thick and represents the lowest part of the upper Santa Fe Group. Although the Griegos well screen extends about 160 feet into this interval, the well-bore flow test indicated that this interval contributes a small amount of water to the well relative to the other screened portions. This interval of the aquifer is reported to contain a significant amount of sand and gravel and was thought to be the most productive interval of the well when it was drilled in 1955 (Norman Gaume, City of Albuquerque, oral commun., 1995). Thorn (2001) suggested that the small contribution may be the result of mineral deposits accumulating on the screen, which were seen in video monitoring of the well bore. Layer 8, the bottom layer of the model, represents the upper 500 feet of the middle part of the Santa Fe Group in the vicinity of the Griegos well field.

Boundary Conditions

The lateral model boundaries are located about 3.6 miles from the Griegos 1 production well (pl. 1). Initially simulated as no flow, the lateral boundaries were changed to head-dependent-flux boundaries to test the sensitivity of the simulated results to the boundary conditions. During the aquifer-test pumping used for the model-calibration period, there was no difference in simulated hydraulic heads at the water-level-observation points using the two boundary conditions. However, the water-budget flux rates differ between the two simulations (see discussion in the "Water budget" sections later in this report). In addition, the amount and timing of induced infiltration from the surface-water system are sensitive to the boundary conditions in simulations significantly longer than the aquifer-test pumping period (see "Amount and timing of induced infiltration from the Rio Grande surface-water system" section). The model with no-flow lateral boundaries estimates a greater effect of

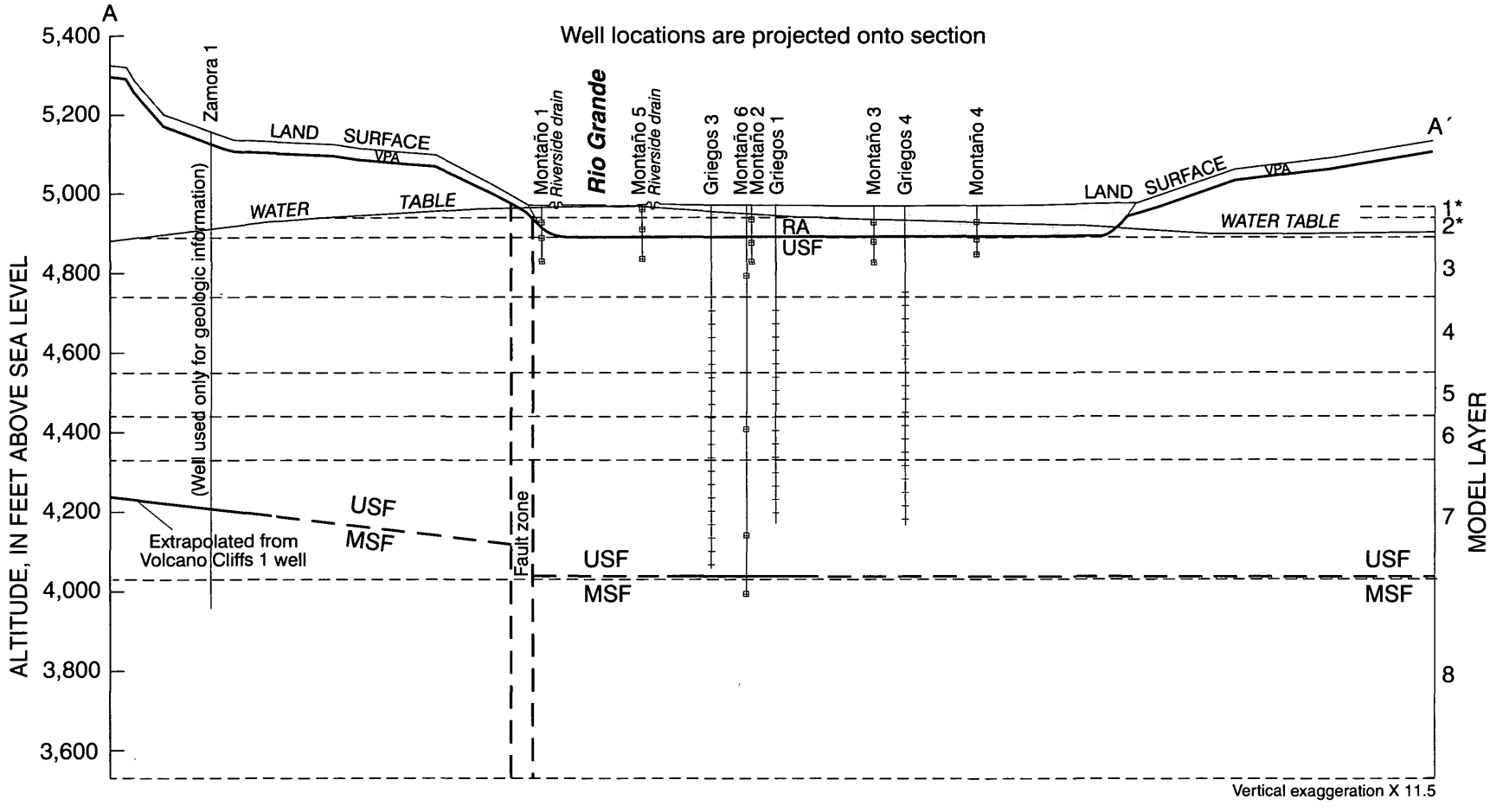

EXPLANATION

HYDROSTRATIGRAPHIC UNITS--Based on units described by Hawley and others (1995, p. 49)

- RA RIVER ALLUVIUM (shaded)
- VPA VALLEY-BORDER AND PIEDMONT-SLOPE ALLUVIUM
- USF UPPER PART OF THE SANTA FE GROUP
- MSF MIDDLE PART OF THE SANTA FE GROUP

— — — GEOLOGIC CONTACT--Dashed where approximately located. USF and MSF contacts based on hydrostratigraphic-unit descriptions for wells Volcano Cliffs 1, Zamora 1, and Montaño 6 from Hawley (1996, appendix F)

– – – – – BOUNDARY BETWEEN MODEL LAYERS

SCREENED INTERVAL OF PRODUCTION WELL

SCREENED INTERVAL OF PIEZOMETER--Screen lengths are 5 to 10 feet

* Top of layer 1 is the water table. Where the water table is below the base altitude of layer 1, layer-1 cells are inactive and the top of layer 2 is the water table. Where the water table is below the base altitude of layer 2, layer-2 cells are inactive and the top of layer 3 is the water table

Figure 3. Schematic vertical profile along section A - A´ (location of section shown on plate 1).

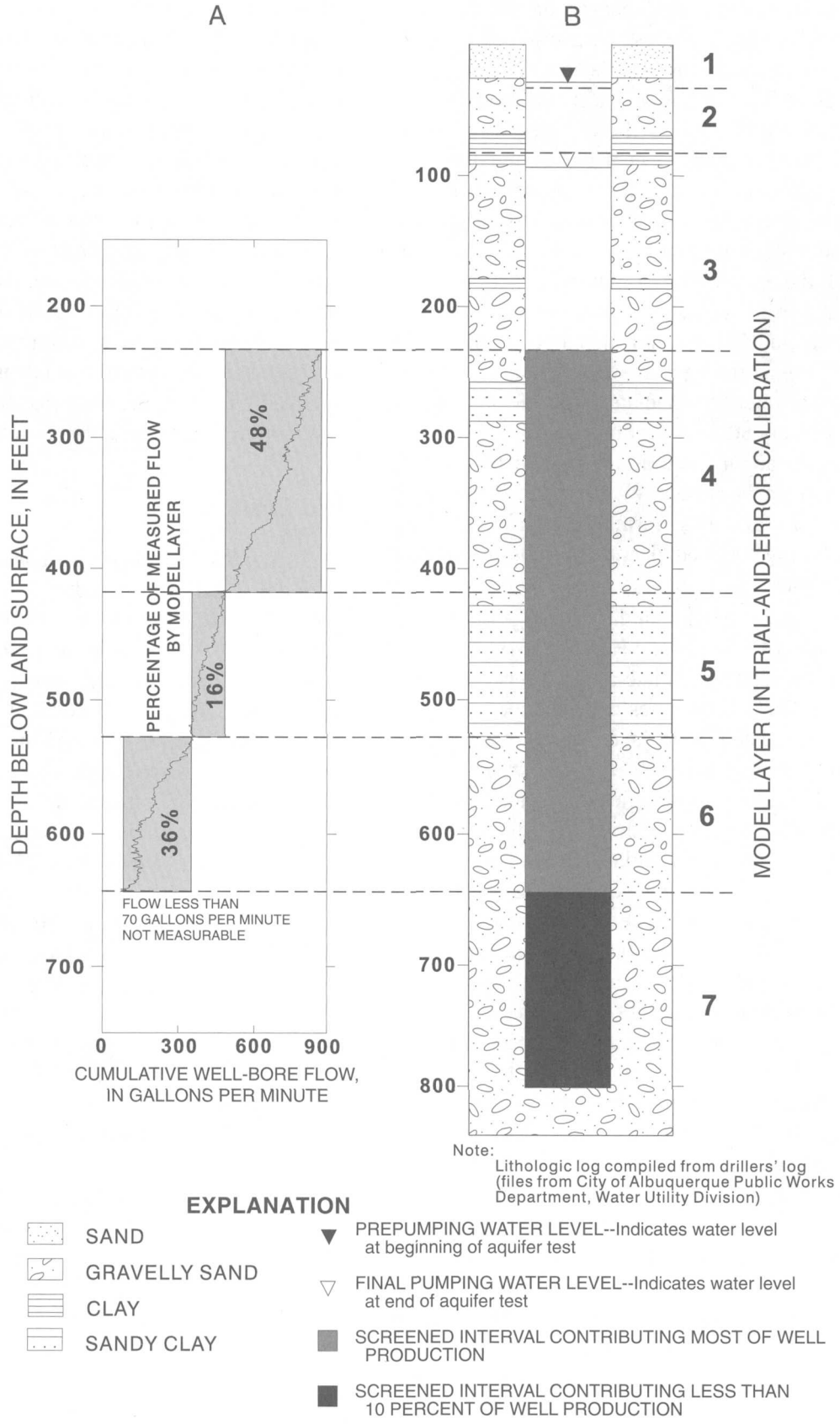

Figure 4. Cumulative flow measured during well-bore flow test (A) and lithologic log and completion (B) of Griegos 1 production well (modified from Thorn, 2001).

pumping on induced infiltration from the surface-water system than the model with head-dependent-flux boundaries. The only sources of water to compensate for ground-water withdrawal in the model with no-flow boundaries are aquifer storage within the modeled area and induced infiltration from the surface-water system. The model with head-dependent-flux boundaries allows an additional simulated source of water from aquifer storage outside the modeled area to compensate for ground-water withdrawal. Several faults are in the vicinity of the modeled area (Hawley, 1996, pl. 2) that may act as partial barriers to ground-water flow between the modeled area and other areas of the aquifer system. These partial barriers would likely affect the system in a manner intermediate to the effects resulting from the two boundary conditions discussed above. Therefore, the amount and timing of induced infiltration from the surface-water system as a result of ground-water withdrawal during the aquifer test were calculated using both boundary conditions to define the likely extremes.

The general-head-boundary package of MODFLOW (McDonald and Harbaugh, 1988, chap. 11) was used for the lateral head-dependent-flux boundaries. These boundaries were applied to perimeter model cells in all layers of the model except those that contained a river or riverside-drain cell in layer 1. The values of hydraulic conductance (area times hydraulic conductivity divided by distance) used for the boundaries were calculated as the horizontal hydraulic conductivity of the cell times the cross-sectional area of the outside cell face divided by the distance of 3 miles to an assumed constant head of zero. Although the 3-mile distance of the assumed constant head from the model boundary is somewhat arbitrary, it was chosen to effectively double the distance between the well-field area and the effective model boundary. In addition, the characteristics of the general-head boundary and the no-flow boundary were chosen to represent the likely extremes in the response of the aquifer system to aquifer-test pumping.

The base of the model is the bottom of layer 8, about 1,440 feet below the Rio Grande. The depth of the model was chosen to include a significant section of aquifer below the pumped well screen (640 feet) and at least one model layer below the screen (500-foot-thick layer 8; fig. 3). Layer 8 represents the middle part of the Santa Fe Group, which contains a significantly greater proportion of fine-grained sediments than the upper part of the Santa Fe Group in the Griegos well field area (Hawley and Haase, 1992, table VI-1; Hawley, 1996, app. F), resulting in a relatively lower horizontal hydraulic conductivity than the upper part of the Santa Fe Group. Because vertical hydraulic conductivity is commonly two or more orders of magnitude less than horizontal hydraulic conductivity (Freeze and Cherry, 1979, p. 34), the section of the aquifer to a depth 640 feet below the Griegos 1 well screen was considered to include most of the aquifer transmitting water vertically to the well. Therefore, the bottom of layer 8 is assumed to be a no-flow boundary. Although a relatively small amount of water may be contributed in the actual aquifer system from depths below this assumed boundary, the error associated with this assumption is considered to be small.

Rio Grande

The Rio Grande is simulated in the model as a head-dependent-flux boundary (pl. 1) using the river package of MODFLOW (McDonald and Harbaugh, 1988, chap. 6). Seepage between the river and the aquifer is a function of river stage, simulated head in the aquifer, and hydraulic conductance (area times hydraulic conductivity divided by thickness) of the riverbed. The riverbed hydraulic conductivity in the trial-and-error calibrated model was 1 foot per day. The riverbed is assumed to be 3 feet below river stage and 1 foot thick. This assumed depth of the riverbed below river stage allows the simulated river and aquifer hydraulic connection to be maintained during the simulations as the actual connection was maintained during the aquifer test; therefore, a specified depth below river stage other than 3 feet would not influence the simulated results. A geographic information system (GIS) polygon coverage showing the Rio Grande channel based on 1989 digital data from the National Biological Survey (Roelle and Hagenbuck, 1994) at a source scale of 1:24,000 was used to determine the area of the riverbed assigned to each model cell by intersecting the coverage with a GIS polygon coverage of the model grid. The area of the Rio Grande in this coverage represents the part of the channel where water normally flows. The flow of the Rio Grande during the aquifer test (January 4 through February 27, 1995) ranged from 945 to 1,800 cubic feet per second (Ortiz and Lange, 1996, p. 206), whereas the average flow for the period of record is 1,456 cubic feet per second (Rio

Grande at Albuquerque, New Mexico, after closure of Cochiti Dam, water years 1974-97; Ortiz and others, 1998, p. 216). Therefore, the GIS coverage reasonably represents the midrange of flow conditions of the Rio Grande during the aquifer test. As discussed in the "Model description" section, the stage of the river and the head in the aquifer are set equal to zero at the beginning of the simulations so that only changes in seepage resulting from aquifer-test pumping are simulated.

Simulated drawdown at the observation locations was insensitive to the hydraulic conductance of the riverbed. Therefore, neither the hydraulic conductivity nor the hydraulic conductance of the riverbed could be calibrated in the model. They were fixed at the initial values.

Drains

The riverside drains are simulated as head-dependent-flux boundaries (pl. 1) using the general-head boundary package of MODFLOW (McDonald and Harbaugh, 1988, chap. 11). As in the river package, seepage between the drains and aquifer is a function of drain stage, simulated head in the aquifer, and hydraulic conductance of the drain bed. Because the model uses the principle of superposition, the simulated drain stage and initial simulated head in the aquifer are both zero. Therefore, the initial simulated flow between the aquifer and drains is zero, and simulated drawdown near the drain cannot reduce simulated flow from the aquifer to the drain. Because direct hydraulic connection between the aquifer and the riverside drains was maintained during the aquifer test, however, the boundary condition is linear and simulated drawdown has the same effect on capture of flow from the drains whether it is a reduction of seepage to the drain from the aquifer or an increase in seepage from the riverside drain to the aquifer. The general-head boundary package is used instead of the drain package (McDonald and Harbaugh, 1988, chap. 9) so that seepage is allowed both to and from the drains rather than only to the drains. The drain-bed hydraulic conductivity in the trial-and-error-calibrated model was 4 feet per day. The thickness of the drain bed is assumed to be 1 foot. A GIS line coverage containing the riverside drain locations from the Bureau of Reclamation based on 1992 digital data at a source scale of 1:12,000 was used to determine the length of each drain reach within each model cell by intersecting the coverage with a GIS polygon coverage of the model grid. During the aquifer test, the width of the water surface in the Albuquerque Riverside Drain was measured to average about 26 feet near the northern part of the modeled area and about 35 feet near the point where the overlap drain starts (Thorn, 2001). A width of 30 feet was assumed for the Albuquerque Riverside Drain and the Corrales Riverside Drain (pl. 1). The overlap drain is narrower and was assumed to be 15 feet wide. A representation of the drain-bed altitude is not applicable to the general-head boundary package. Interior drains are not simulated in the model because the water table is below the level of these drains in the area simulated by the model, and further lowering of the water table cannot significantly influence infiltration of any water that may be in the drain.

Simulated drawdown at the observation locations was insensitive to the hydraulic conductance of the riverside-drain bed. Therefore, neither the hydraulic conductivity nor the hydraulic conductance of the drain bed could be calibrated in the model. They were fixed at the initial values.

Canals

Canals are not simulated in the model. The aquifer test was conducted during the winter when no water was in the canals, so canal seepage could not influence water-level measurements during the test. The water table in the area simulated by the model is below the level of the canal beds; therefore, further lowering of the water table cannot significantly influence the amount of infiltration of water from the canals when they do contain water.

Ground-Water Withdrawal from Griegos 1

Ground-water withdrawal from the Griegos 1 production well during the aquifer test was simulated using the well package of MODFLOW (McDonald and Harbaugh, 1988, chap. 8). Although a power failure stopped withdrawal for 27 minutes on the second day of the test, withdrawal was assumed to be constant at the average production rate (2,330 gallons per minute) throughout the length of the pumping test (54 days and 9 hours). The proportion of withdrawal applied to each layer of the model was based on the well-bore flow test

(Thorn, 2001) conducted in the Griegos 1 production well following the aquifer test, described in the "Model grid and layers" section of this report. Forty-eight percent was assumed to come from layer 4, 16 percent from layer 5, and 36 percent from layer 6 (fig. 4).

Preliminary models simulating the aquifer test indicated that a better match between observed and simulated drawdowns could be obtained by reapportioning pumpage so that a significant amount of withdrawal was taken from layer 7. This result could indicate that a significant amount of water from the zone thought initially to be the most productive, but is adjacent to the clogged section of well screen, could still be contributing to well production. Some of the water originating from this zone could be entering the well above the clogged screen, possibly transmitted through the gravel-packed well annulus or in permeable sediments near the well. Because the horizontal dimensions of the cell in which the well is represented (row 29, column 40) are 200 feet on a side compared with about a 2-foot-diameter well bore, withdrawal would be from the zone represented by layer 7 if water moves from that zone into the well. Rather than simulating withdrawal from the layer-7 cell in which the well is represented, the vertical to horizontal anisotropy ratio was increased in the trial-and-error-calibrated model to account for the tendency of the well bore to allow greater vertical movement of water than the rest of the model (see the "Aquifer hydraulic conductivity" section of this report).

Hydraulic Properties

Aquifer Hydraulic Conductivity

Initial values of horizontal hydraulic conductivity assigned in the model were based on the lithofacies descriptions from borehole analyses reported by Hawley (1996, app. F) and the relative hydraulic conductivity of each lithofacies reported by Hawley and Haase (1992, table VI-1). The borehole analyses in the model vicinity were used to obtain relative hydraulic-conductivity values at each borehole location for each aquifer interval represented by a model layer. Similar hydraulic-conductivity values were then grouped into zones using fault zones and other geologic subdivisions of the Albuquerque Basin reported by Hawley (1996, pl. 2) as the boundaries between each hydraulic-conductivity zone. The hydraulic-conductivity values were then adjusted during the trial-and-error model calibration. The resulting horizontal hydraulic-conductivity values are shown in figure 5. Within each hydraulic-conductivity zone, the aquifer material was assumed to be isotropic in the horizontal dimension. The simulated hydraulic conductivity for the zones representing the upper part of the Santa Fe Group ranges from 12 to 33 feet per day. The simulated hydraulic conductivity for the zones representing the middle part of the Santa Fe Group were 4 and 11 feet per day. The simulated hydraulic conductivity of the inner-valley alluvium was 45 feet per day.

Vertical hydraulic conductivity in the aquifer system is substantially less than horizontal hydraulic conductivity. Layers or lenses of low-permeability material (silts and clays) restrict the movement of water in the vertical direction. In addition, coarse sediments in an alluvial system (sands and gravels) tend to be deposited flat side down, limiting vertical relative to horizontal hydraulic conductivity within the coarse sediments. Except for the cell where the production well is located (row 29, column 40), the vertical to horizontal anisotropy ratio (ratio of vertical to horizontal hydraulic conductivity) was assumed to be uniform throughout the model calibrated by trial and error. The resulting value of vertical to horizontal anisotropy from model calibration is 1:140. Because the Griegos 1 well bore and gravel pack increase the vertical to horizontal anisotropy ratio in the near vicinity of the well, the vertical to horizontal anisotropy ratio was assumed to be 1:5 in the cells representing the well.

Specific Storage and Specific Yield

Specific storage was assumed to be uniform throughout the confined parts of the model (all of layers 4-8 and parts of layers 2 and 3). The value of specific storage resulting from the trial-and-error calibration was 4×10^{-6} per foot of aquifer thickness. Specific yield was assumed to be uniform for the unconfined layers of the model (all of layer 1 and parts of layers 2 and 3). The value of specific yield resulting from the trial-and-error calibration was 0.15 (dimensionless).

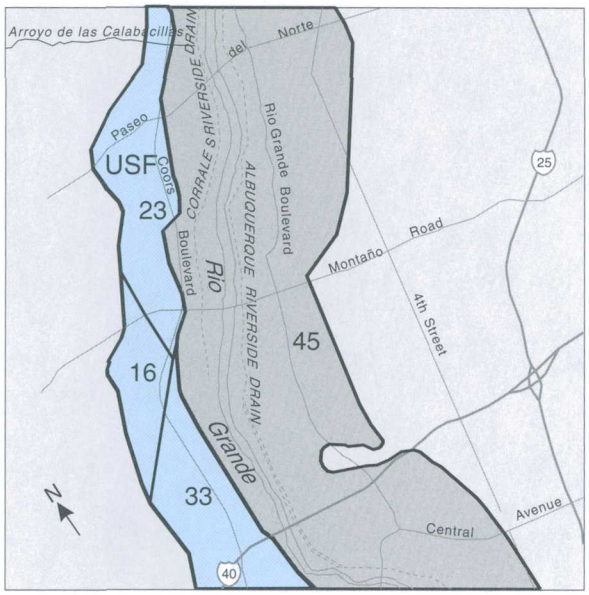

LAYER 1

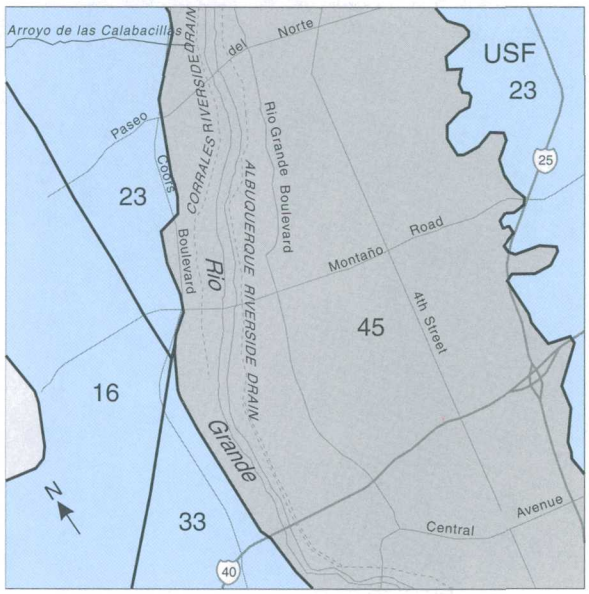

LAYER 2

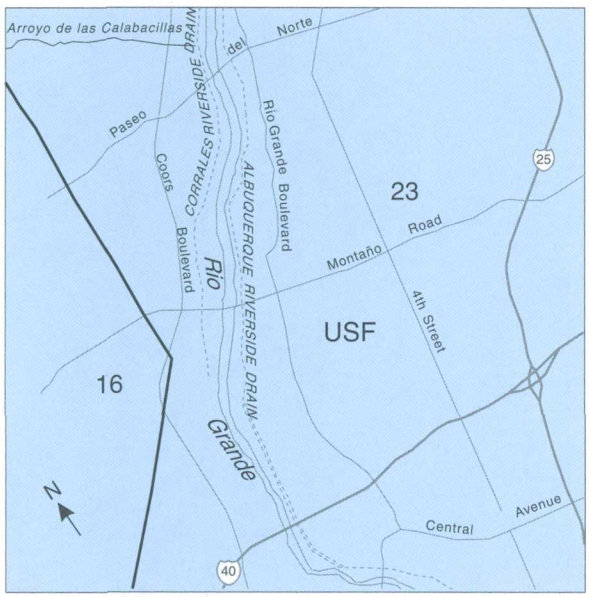

LAYER 3

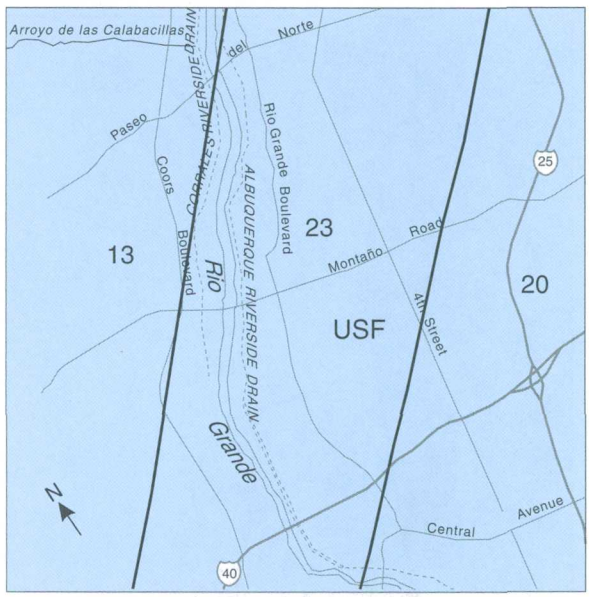

LAYER 4

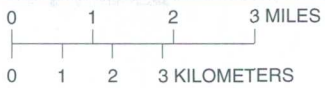

EXPLANATION

HYDROSTRATIGRAPHIC UNITS--Based on units described by Hawley and others (1995, p. 49)

- RA — RIVER ALLUVIUM
- USF — UPPER PART OF THE SANTA FE GROUP
- USF and MSF — CONTAINS BOTH UPPER AND MIDDLE PARTS OF THE SANTA FE GROUP
- MSF — MIDDLE PART OF THE SANTA FE GROUP

- 16 — ZONE OF EQUAL HYDRAULIC CONDUCTIVITY--Number is hydraulic conductivity, in feet per day
- INACTIVE PART OF MODEL--Part of model layer that represents an unsaturated part of the aquifer

Figure 5. Distribution of hydraulic conductivity in the model calibrated by trial and error.

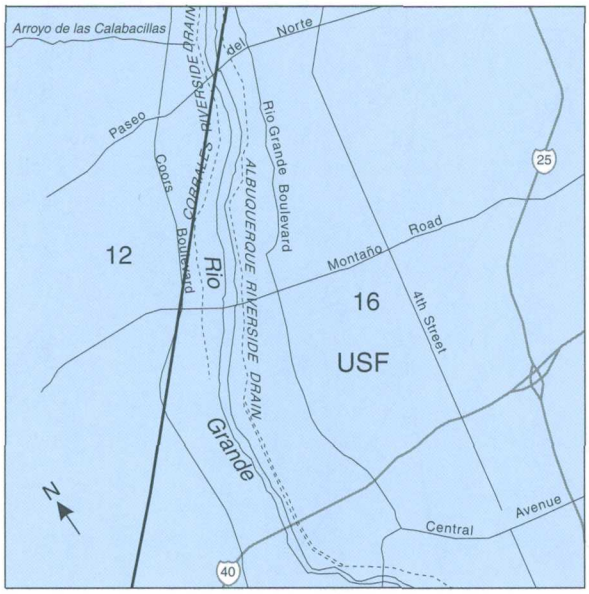

LAYER 5

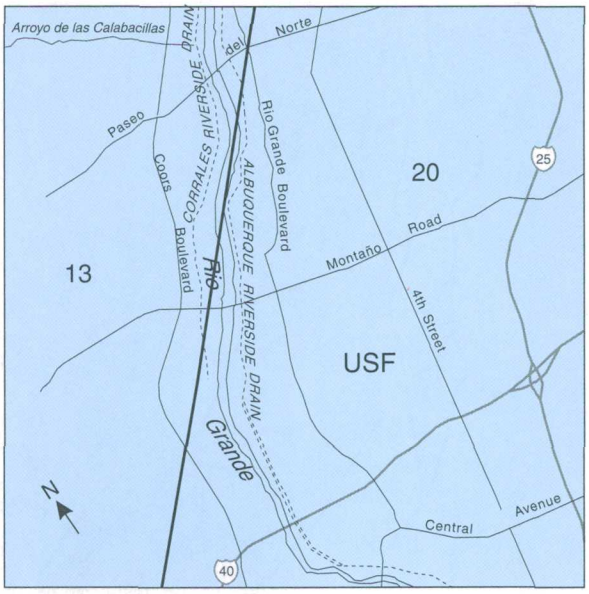

LAYER 6

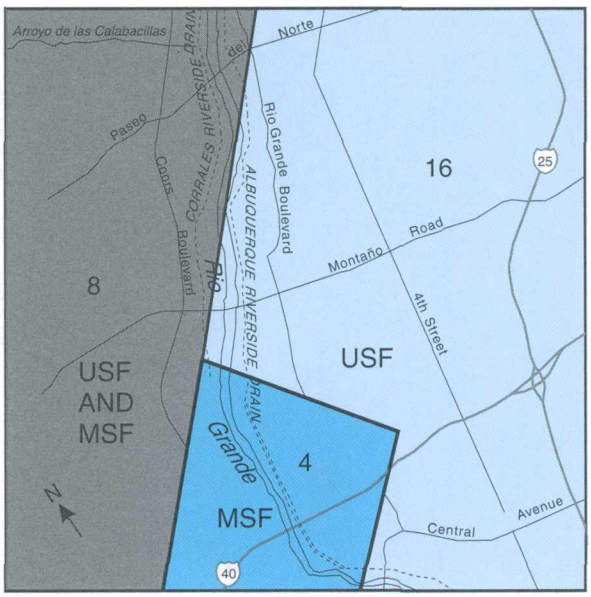

LAYER 7

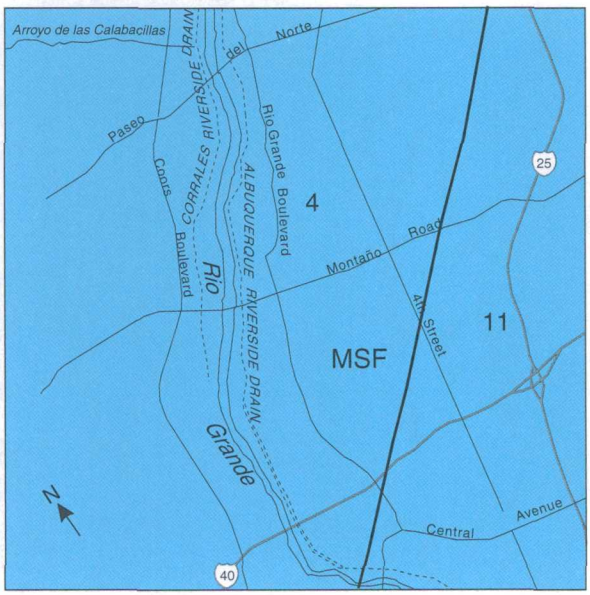

LAYER 8

Figure 5. Distribution of hydraulic conductivity in the model calibrated by trial and error--Concluded.

MODEL CALIBRATION BY TRIAL AND ERROR

The pumping period of the aquifer test was used to calibrate the simulated aquifer properties in an effort to match the simulated drawdown in the model with the observed drawdown from the observation wells. The observed drawdowns are the drawdowns measured in the observation wells, corrected to account for trends from influences other than the aquifer-test pumped well (for example, prepumping trend, barometric pressure, and change in river stage). Other than pumping from Griegos 1 during the aquifer test, no public-supply wells within the inner valley in the modeled area (fig. 2) were pumped from October 1, 1994 (3 months prior to the start of aquifer-test pumping), to April 1, 1995 (1 month after aquifer-test pumping stopped). The closest public-supply well in operation during the test is about 2.8 miles from Griegos 1. Aquifer characteristics were adjusted by a judgmental trial-and-error procedure in an effort to minimize the difference between simulated drawdown and corrected drawdown from the observation wells.

The observation wells (fig. 2; pl. 1) consist of production wells and piezometers. The production wells in which drawdown was measured are Griegos 3 and 4, which were used only for observation during the test, and Griegos 1, which was the pumped well for the test. The 19 piezometers are located at six sites, Montaño 1 through 6. Montaño 1 through 5 each contain three single piezometers, and Montaño 6 contains four nested piezometers. The depths, screened intervals, model layers that represent the screened intervals, and weighting factors used in interpolation of simulated drawdown are listed in table 1. Simulated drawdown at model cell centers was interpolated both horizontally and vertically to obtain simulated drawdown at the position of each piezometer screen. Simulated drawdown at the production wells was calculated as the average of the simulated drawdown from the cells in each model layer representing the well screen, weighted by the proportion of screen in each layer. Because simulated drawdown in the cells representing the pumped well is not representative of drawdown at the well bore, it was further corrected to estimate drawdown at the borehole using the following form of the Thiem (1906) equation (modified from Trescott and others, 1976, eq. 15, p. 10):

$$d_w = d_{mc} + \frac{Q}{2\pi T_{mc}} \ln(r_e / r_w) \qquad (2)$$

where d_w = estimated drawdown in hydraulic head at the well radius (L);

d_{mc} = simulated drawdown in hydraulic head weighted by the proportion of screen in each layer (L);

Q = average withdrawal rate of the pump well (L^3/T);

T_{mc} = combined transmissivity of model cells representing the well screen (L^2/T);

r_e = effective radius of a hypothetical well for which the simulated drawdown in the cells representing the pumped well would apply (L), and is equal to the x or y dimension of the cell divided by 4.81 (Trescott and others, 1976, eq. 12, p. 9); and

r_w = radius of the well (L).

Transmissivity is constant in equation 2, representative of a confined aquifer. Under unsaturated conditions, transmissivity would change on the basis of changes in saturated thickness. Although conditions are unconfined in the shallow part of the aquifer system, the upper extent of the Griegos 1 well screen is about 200 feet below the prepumped water table near the well. The aquifer material over this distance between the water table and the top of the screen acts as a confining unit. Therefore, drawdown at the water table will be significantly less than drawdown at the well screen. Although no measurement of drawdown of the water table during the aquifer test is available at the pumped well, the reduction in saturated thickness during the aquifer test compared with the thickness of the aquifer system will likely have little effect on the effective aquifer transmissivity in the vicinity of the screen. Therefore, the assumption of constant transmissivity is reasonable for this situation.

The values used in equation 2 for estimating d_w were 449,000 cubic feet per day (2,330 gallons per minute, the average well discharge for the aquifer test) for Q; 8,400 feet squared per day (the sum of the transmissivities of model layers 4, 5, and 6) for T_{mc}; 200 feet (the x and y dimensions of the model cell containing Griegos 1) for r_e; and 1 foot for r_w. Although the radius of the Griegos 1 well screen is 7 inches (14-inch diameter; Groundwater Management, Inc., 1988, p. B-2), r_w was assumed to be 1 foot for the calculation to account for the influence of the gravel pack in the well bore.

Table 1. Depths, screened intervals, and model representation of observation wells used in the Griegos aquifer test

Well name (fig. 2)	Well depth, in feet below land surface	Screened interval, in feet below land surface	Depth to water measured in well prior to start of test, in feet below land surface	Model-grid location		Layers and weighting factors for each layer used in interpolation of simulated drawdown							
				Row	Column	Layer	Factor	Layer	Factor	Layer	Factor	Layer	Factor
Griegos 1	824	232 - 802	26.47	29	40	4	0.465	5	0.270	6	0.265		
Griegos 3	916	260 - 916	15.39	42	33	4	0.418	5	0.289	6	0.290	7	0.003
Griegos 4	804	218 - 804	36.37	25	53	3	0.027	4	0.450	5	0.261	6	0.262
Montaño 1:													
Shallow	48	38 - 43	7.60	32	7	1	0.326	2	0.674				
Intermediate	93	83 - 88	9.99	32	7	2	0.721	3	0.279				
Deep	152	142 - 147	10.03	32	7	2	0.131	3	0.869				
Montaño 2:													
Shallow	40	30 - 35	13.29	26	36	1	1.000						
Intermediate	99	89 - 94	15.14	26	36	2	0.613	3	0.387				
Deep	147	137 - 142	16.99	26	36	2	0.132	3	0.867				
Montaño 3:													
Shallow	50	40 - 45	27.34	22	50	2	1.000						
Intermediate	99	89 - 94	29.29	22	50	2	0.644	3	0.356				
Deep	150	140 - 145	29.13	22	50	2	0.124	3	0.876				
Montaño 4:													
Shallow	50	40 - 45	41.51	18	57	2	1.000						
Intermediate	93	83 - 88	41.40	18	57	2	0.746	3	0.254				
Deep	131	121 - 126	43.58	18	57	2	0.345	3	0.655				
Montaño 5:													
Shallow	25	10 - 20	6.94	22	21	1	1.0000						
Intermediate	75	60 - 70	7.08	22	21	2	0.930	3	0.070				
Deep	150	135 - 145	9.69	22	21	2	0.180	3	0.820				
Montaño 6:													
Shallow	182	172 - 177	21.54	26	35	3	0.872	4	0.128				
Intermediate	568	558 - 563	28.58	26	35	5	0.202	6	0.798				
Medium deep	836	826 - 831	30.34	26	35	7	0.898	8	0.102				
Deep	983	973 - 978	31.49	26	35	7	0.531	8	0.469				

The Griegos 1 production well began pumping the morning of January 4, 1995. Except for a power failure resulting in a 27-minute lapse of pumping on January 5, the well pumped continuously until the evening of February 27, 1995. The average pumping rate over that 54.4-day time period was 2,330 gallons per minute. Because the trial-and-error calibration was based primarily on calculated differences between observed and simulated drawdown at the end of pumping and visual comparison of observed and simulated drawdown hydrographs over the entire period, the pumping lapse was considered to be insignificant relative to the entire pumping period. Therefore, the aquifer test was simulated with a single stress period of 16 time steps using the average pumping rate.

Drawdown of Hydraulic Head

Comparisons between observed and simulated drawdown using the model calibrated by trial and error are listed in table 2. The table shows comparisons and summary statistics for three times during the aquifer test: early time (1,000 minutes or 0.69 day of pumping), intermediate time (10,000 minutes or 6.9 days of pumping), and at the end of pumping (78,300 minutes or 54.4 days of pumping). The summary statistics for comparisons over all three time periods are shown at the end of table 2. The sum of squared error for all observations is 130 feet squared. The increase in this statistic as the time in pumping increases (about 24 feet squared for early time, 50 feet squared for intermediate time, and 56 feet squared for late time) reflects the increasing drawdown with time, which resulted in a general increase in the magnitude of differences between observed and simulated drawdown.

Curves of drawdown as a function of time in the observation wells are shown in figure 6. As discussed above, simulated drawdown in the Griegos 1 pumped well was calculated using equation 2 to adjust the model-simulated drawdown. Water-level trends from influences other than the aquifer test completely overwhelmed drawdown that could be attributed to test pumping in piezometers Montaño 4-shallow, Montaño 5-shallow, and Montaño 5-intermediate; therefore, no observed data are shown in figure 6M, P, and Q. Water levels measured in Montaño 4-intermediate (fig. 6N) during the early and intermediate times were determined to be unreliable; therefore, only the late-time observation was used for comparison. Water levels measured in Montaño 4-shallow and Montaño 4-intermediate were likely affected by ground-water withdrawal from other than the aquifer-test pumped well. Water levels measured in Montaño 5-shallow and -intermediate were likely affected by fluctuations in river stage. The decrease in the rate of observed drawdown in the Montaño 3-intermediate and -deep piezometers (fig. 15K and L) about 200 minutes after pumping began is most likely a result of a nearby private well shutting off, allowing a small amount of drawdown recovery. With some exceptions, reasonable matches between simulated and observed drawdown were obtained for most of the observation wells (fig. 6). Major exceptions are Griegos 3, Montaño 1-intermediate, and Montaño 1-deep. These are discussed in subsequent paragraphs.

A poor match was obtained for the Griegos 3 well (fig. 6B). Maximum drawdown in the Griegos 3 well was 0.95 foot at the end of pumping, whereas the model simulated 4 feet of drawdown (table 2). Single-well aquifer tests have been conducted on all the original five Griegos production wells (Bjorklund and Maxwell, 1961, p. 74; Groundwater Management, Inc., 1988, p. 15). Values of transmissivity from these tests indicate that the average hydraulic conductivity of sediments in the vicinity of the Griegos 3 well is about one-quarter to one-third that of sediments in the vicinity of all the other Griegos production wells (Thorn and others, 1993, p. 40). Because of this significant difference, it is possible that the hydraulic connection between Griegos 3 and the well pumped for this aquifer test, Griegos 1, is less than that to the other observation wells, resulting in the small amount of drawdown measured in Griegos 3. Changes in the representation of the aquifer system in the model to try to replicate the Griegos 3 drawdown were unsuccessful and reduced the overall match between observed and simulated drawdown. No other observation wells are in the general direction of Griegos 3 (fig. 2) to substantiate this response or to help guide changes in model representation in this vicinity; therefore, changes in the model to better simulate the response in Griegos 3 were not pursued further.

Table 2. Comparison between observed drawdown and drawdown simulated using the model calibrated by trial and error, by time of pumping

[--, data not used]

Well (fig. 2)	Observed drawdown, in feet	Simulated drawdown, in feet	Difference (observed-simulated), in feet
Early time--1,000 minutes after pumping began			
Griegos 1	64.73	[1]63.33	1.40
Griegos 3	0.27	0.68	-0.41
Griegos 4	0.65	0.80	-0.15
Montaño 1-deep	0.00	0.03	-0.03
Montaño 1-intermediate	0.00	0.01	-0.01
Montaño 1-shallow	0.00	0.00	0.00
Montaño 2-deep	4.17	1.49	2.68
Montaño 2-intermediate	1.19	0.79	0.40
Montaño 2-shallow	0.00	0.01	-0.01
Montaño 3-deep	0.39	0.30	0.09
Montaño 3-intermediate	0.26	0.12	0.14
Montaño 3-shallow	0.00	0.00	0.00
Montaño 4-deep	0.01	0.02	-0.01
Montaño 4-intermediate	--	0.01	--
Montaño 4-shallow	--	0.00	--
Montaño 5-deep	0.20	0.12	0.08
Montaño 5-intermediate	--	0.03	--
Montaño 5-shallow	--	0.00	--
Montaño 6-deep	2.72	0.97	1.75
Montaño 6-medium deep	4.55	1.62	2.93
Montaño 6-intermediate	6.88	8.21	-1.33
Montaño 6-shallow	3.52	2.51	1.01
Root-mean-square error			1.04
Sum of squared errors, in feet squared			23.96
Mean difference, in feet			0.47
Mean absolute difference, in feet			0.69
Intermediate time--10,000 minutes after pumping began			
Griegos 1	66.33	[1]67.01	-0.68
Griegos 3	0.67	3.11	-2.44

Table 2. Comparison between observed drawdown and drawdown simulated using the model calibrated by trial and error, by time of pumping--Continued

Well (fig. 2)	Observed drawdown, in feet	Simulated drawdown, in feet	Difference (observed-simulated), in feet
Griegos 4	3.13	3.43	-0.30
Montaño 1-deep	0.10	0.40	-0.30
Montaño 1-intermediate	0.07	0.19	-0.12
Montaño 1-shallow	0.06	0.07	-0.01
Montaño 2-deep	5.79	2.93	2.86
Montaño 2-intermediate	2.05	1.64	0.41
Montaño 2-shallow	0.13	0.18	-0.05
Montaño 3-deep	1.24	0.99	0.25
Montaño 3-intermediate	1.03	0.45	0.58
Montaño 3-shallow	0.13	0.08	0.05
Montaño 4-deep	0.16	0.25	-0.09
Montaño 4-intermediate	--	0.11	--
Montaño 4-shallow	--	0.02	--
Montaño 5-deep	0.69	0.59	0.10
Montaño 5-intermediate	--	0.18	--
Montaño 5-shallow	--	0.02	--
Montaño 6-deep	7.59	3.87	3.72
Montaño 6-medium deep	9.23	5.87	3.36
Montaño 6-intermediate	11.00	14.05	-3.05
Montaño 6-shallow	5.27	4.72	0.55
Root-mean-square error			1.67
Sum of squared errors, in feet squared			50.11
Mean difference, in feet			0.27
Mean absolute difference, in feet			1.05
Late time (end of pumping)--78,300 minutes after pumping began			
Griegos 1	64.63	[1]67.91	-3.28
Griegos 3	0.95	4.02	-3.07
Griegos 4	4.22	4.44	-0.22
Montaño 1-deep	0.17	0.66	-0.49
Montaño 1-intermediate	0.17	0.36	-0.19
Montaño 1-shallow	0.11	0.17	-0.06

Table 2. Comparison between observed drawdown and drawdown simulated using the model calibrated by trial and error, by time of pumping--Concluded

Well (fig. 2)	Observed drawdown, in feet	Simulated drawdown, in feet	Difference (observed-simulated), in feet
Montaño 2-deep	6.77	3.88	2.89
Montaño 2-intermediate	3.17	2.69	0.48
Montaño 2-shallow	1.28	1.40	-0.12
Montaño 3-deep	1.92	1.60	0.32
Montaño 3-intermediate	1.71	1.08	0.63
Montaño 3-shallow	0.65	0.72	-0.07
Montaño 4-deep	0.57	0.57	0.00
Montaño 4-intermediate	0.36	0.40	-0.04
Montaño 4-shallow	--	0.29	--
Montaño 5-deep	1.00	0.85	0.15
Montaño 5-intermediate	--	0.30	--
Montaño 5-shallow	--	0.04	--
Montaño 6-deep	8.68	6.07	2.61
Montaño 6-medium deep	10.24	7.86	2.38
Montaño 6-intermediate	11.88	15.58	-3.70
Montaño 6-shallow	6.21	5.80	0.41
Root-mean-square error			1.72
Sum of squared errors, in feet squared			55.97
Mean difference, in feet			-0.07
Mean absolute difference, in feet			1.11
Summary statistics for all observations			
Root-mean-square error			1.48
Sum of squared errors			130.05
Mean difference			0.20
Mean absolute difference			0.89

[1]Simulated drawdown adjusted to represent drawdown in the pumped well.

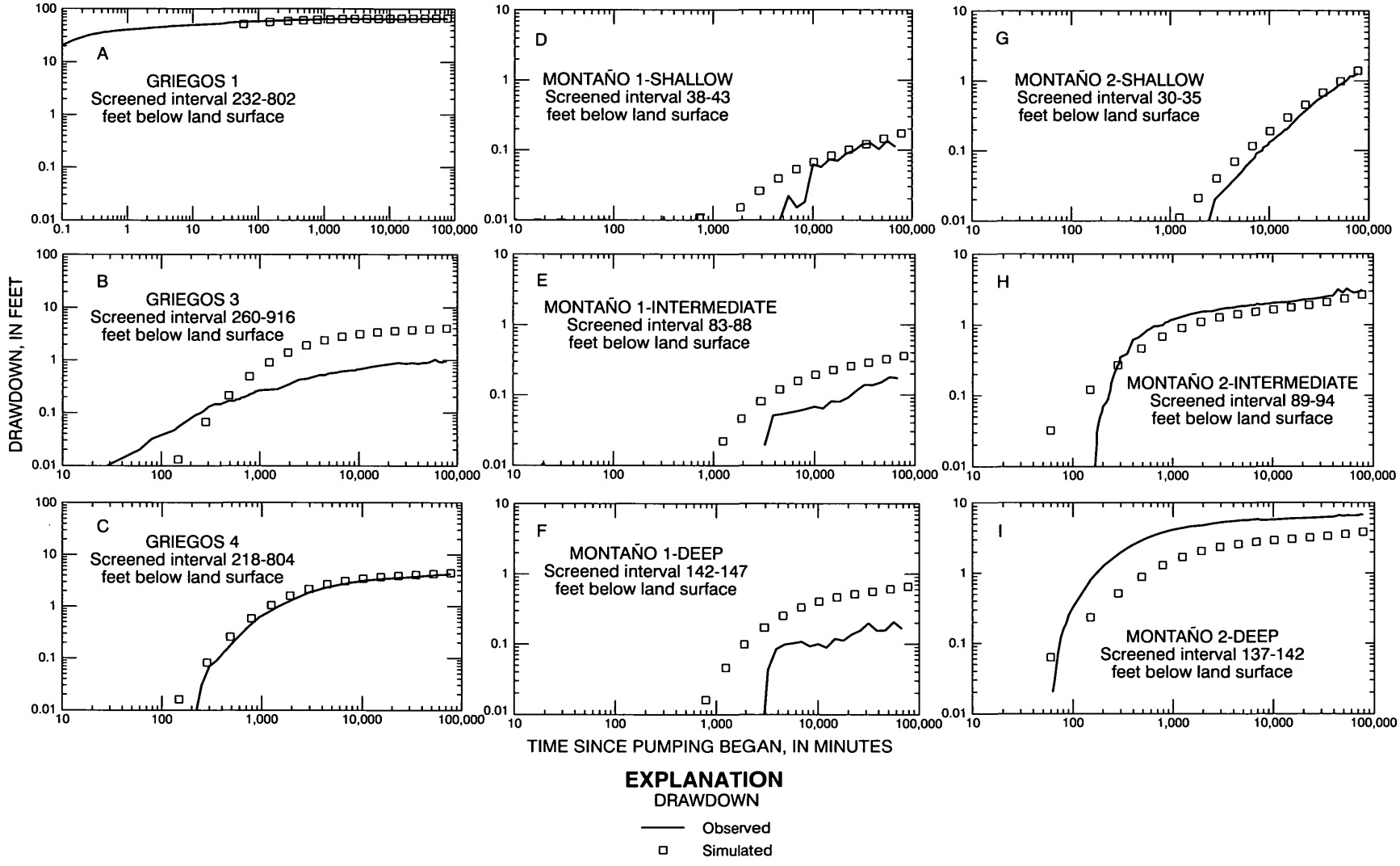

Figure 6. Comparison between observed drawdown and drawdown simulated using the model calibrated by trial and error.

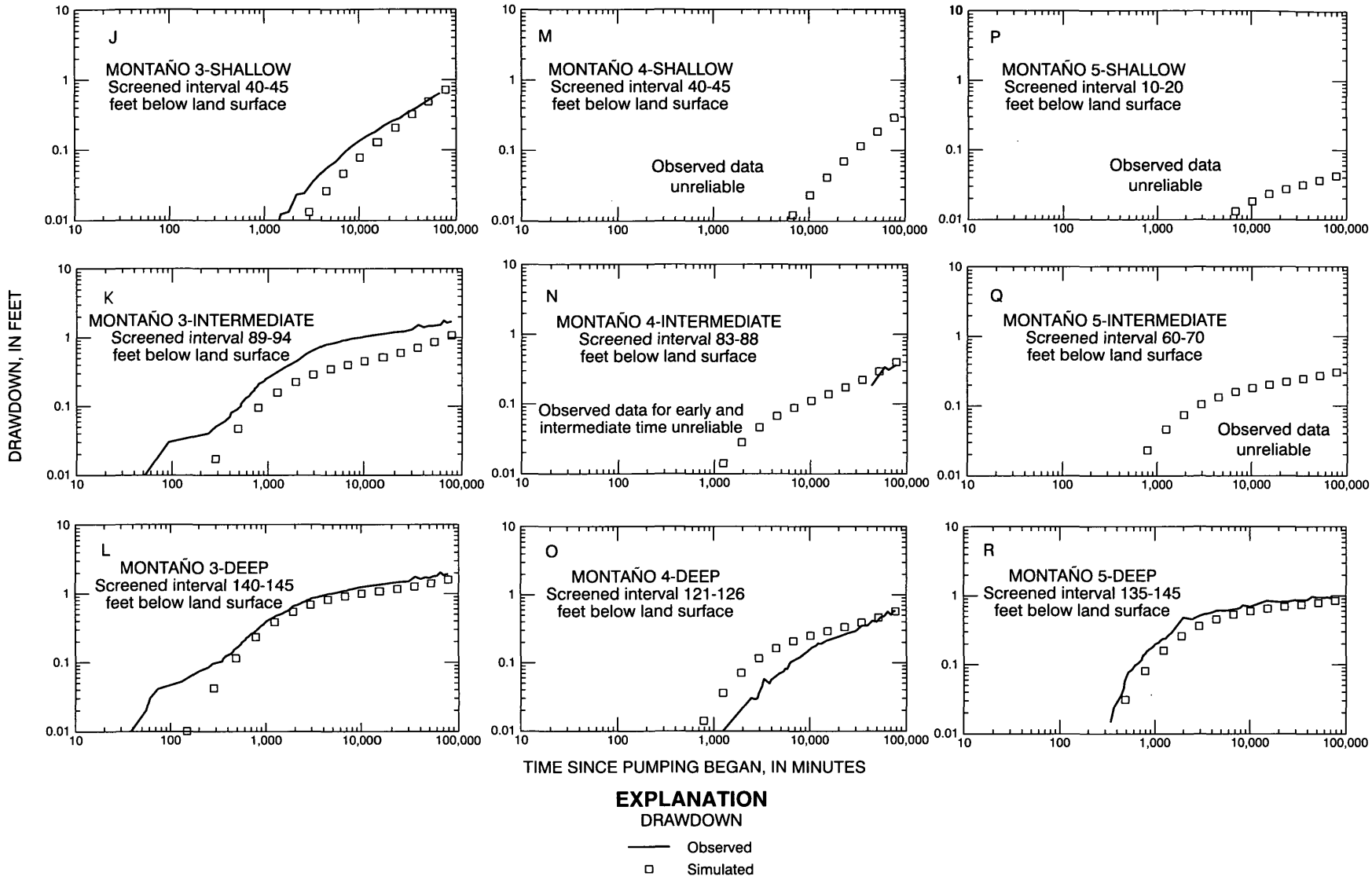

Figure 6. Comparison between observed drawdown and drawdown simulated using the model calibrated by trial and error--Continued.

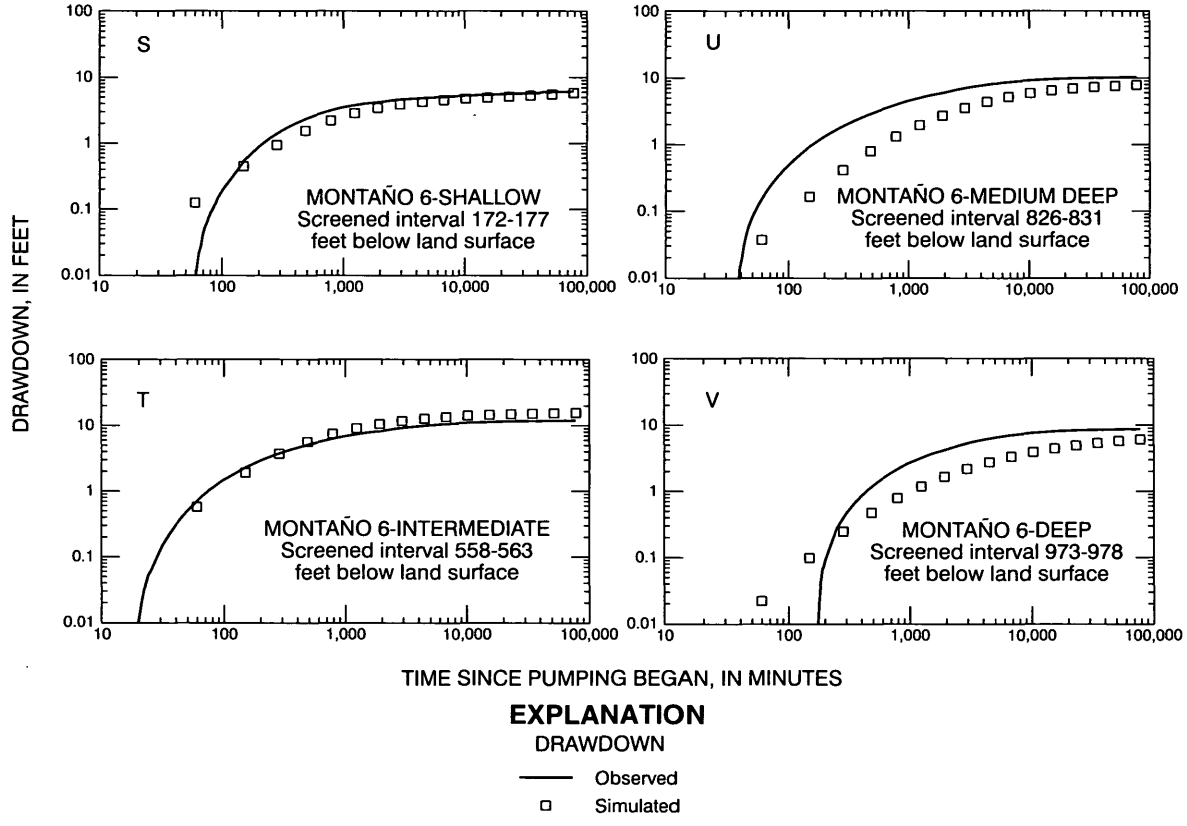

Figure 6. Comparison between observed drawdown and drawdown simulated using the model calibrated by trial and error--Concluded.

Observed drawdown in some wells was relatively small. For example, drawdown at the end of pumping was 0.17 foot in both Montaño 1-intermediate and Montaño 1-deep (figs. 6E and F; table 2). With these small amounts of drawdown, changes in local water-level trends resulting from influences on the flow system other than 54-day pumping from Griegos 1 contributed significant error to the observed drawdown. These changes in water-level trends at least partially account for the relatively poor match between observed and simulated drawdown for these piezometers.

The simulated declines in hydraulic head (drawdown) for all layers in the model and the observed drawdown at the observation wells are shown at the end of the aquifer-test pumping period in figure 7. Drawdowns for the models with no-flow and head-dependent-flux lateral boundaries are both shown. Simulated drawdown for both models is the same at the observation-well locations, as discussed in the "Boundary conditions" section of this report. The vertical distribution of simulated drawdown and observed drawdown in the observation wells along a section through the aquifer-test area is shown in figure 8. The boundaries of the Rio Grande and riverside drains buffer the amount of drawdown in the upper two layers of the model by providing infiltration of water into the aquifer system. This is shown by the flexures in the 0.1- and 0.5-foot lines of equal drawdown in figure 7 (layers 1 and 2) and in figure 8. These boundaries do not show much influence in the lines of equal drawdown for layers 3 through 8 (figs. 7 and 8).

Water Budget

The simulated water budget at the end of pumping is listed in table 3 for the model with a no-flow boundary and for the model with a head-dependent-flux boundary. The rates of simulated leakage from the river and riverside drains differ by about 1 to 2 percent between the two models. These differences are not significant at the end of pumping; however, these differences increase and become significant for longer simulation times (see discussion in "Amount and timing of induced infiltration from the Rio Grande surface-water system" section of this report). The main difference between the two simulated water budgets is the amount of water coming from storage at the end of pumping. Use of the head-dependent-flux boundary condition results in water coming from aquifer storage both within (aquifer-storage mechanism) and outside (head-dependent model-boundary mechanism) the modeled area. However, the difference between the models in the total amount of water coming from aquifer storage (aquifer storage and head-dependent model-boundary mechanisms) is less than 1 percent. At the end of pumping, about 82 to 83 percent of the ground-water withdrawal rate was compensated by water from aquifer storage (aquifer storage inside and outside the model boundary), 7 to 8 percent by river leakage, and 10 percent by riverside-drain leakage (table 3). Of the cumulative amount pumped during the test, about 87 percent was simulated to have come from aquifer storage, 6 percent from river leakage, and 7 percent from riverside-drain leakage.

The change in the simulated water budget during and after the aquifer test is shown in figure 9 for the model with a no-flow model boundary. Because of the similarity of the water budgets between the two models at the end of pumping as described in the previous paragraph, only the model with a no-flow model boundary is shown. Differences between the two models for longer simulation times are discussed in the "Amount and timing of induced infiltration from the Rio Grande surface-water system" section of this report. As pumping begins, 100 percent of the water pumped comes from aquifer storage (fig. 9A). Within the first day of pumping, leakage from the river and riverside drains is induced into the aquifer as the cone of depression reaches these boundaries. As pumping continues, the total amount of water withdrawn from storage continues to increase (fig. 9B); however, the rate of water coming from aquifer storage decreases and the rates of water leaking from the river and drains increase (fig. 9A). After the pump is turned off, aquifer storage is replenished by leakage from the river and riverside drains.

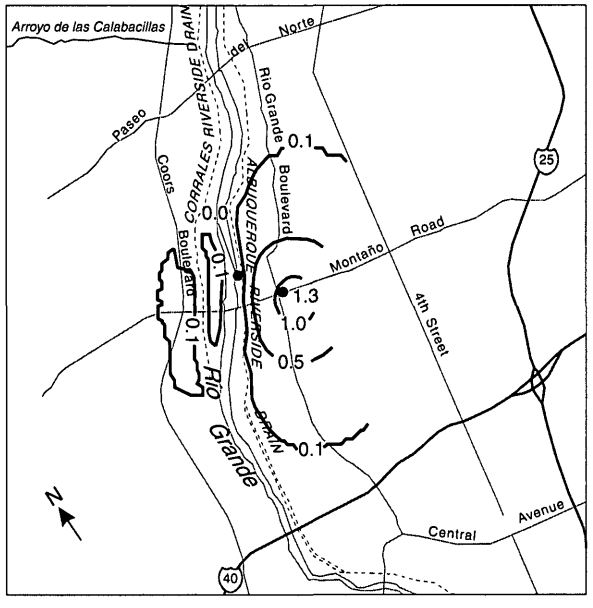

LAYER 1

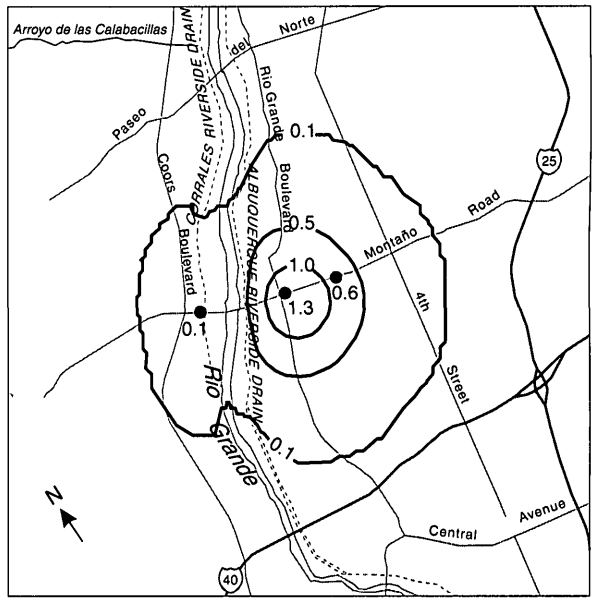

LAYER 2

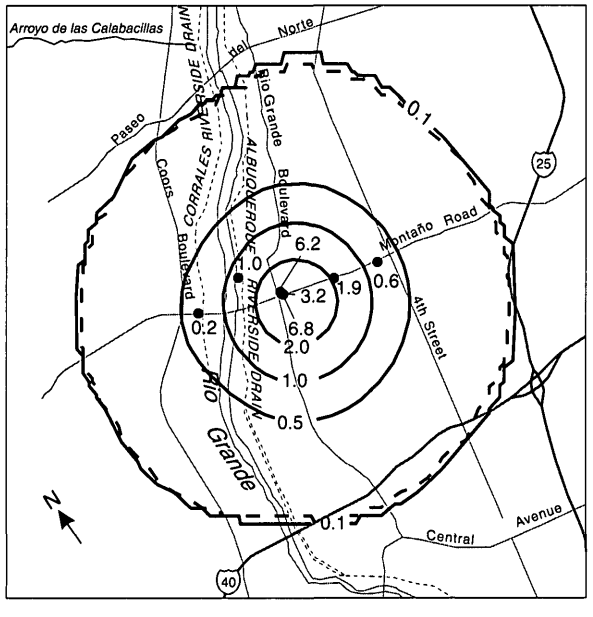

LAYER 3

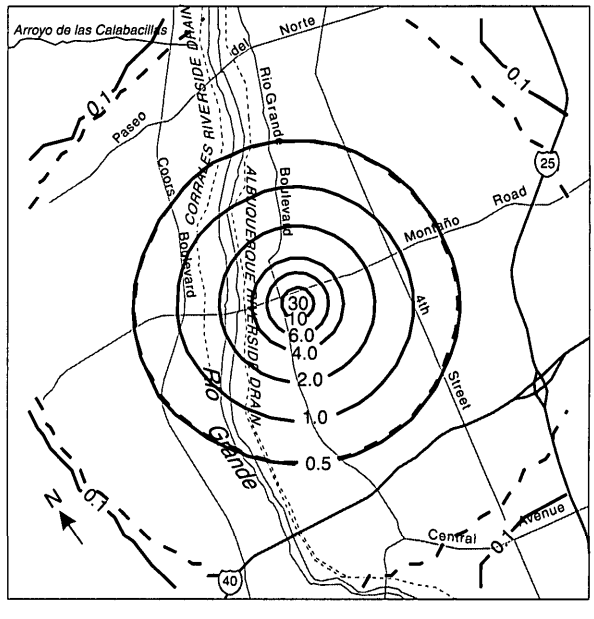

LAYER 4

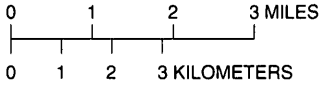

EXPLANATION

INACTIVE PART OF MODEL--Part of model layer that represents an unsaturated part of the aquifer

—0.5— LINE OF EQUAL SIMULATED DRAWDOWN WITH A NO-FLOW MODEL BOUNDARY-- Interval, in feet, is variable

– –0.5– – LINE OF EQUAL SIMULATED DRAWDOWN WITH A HEAD-DEPENDENT-FLUX MODEL BOUNDARY--Interval, in feet, is variable

•1.9 OBSERVATION WELL--Number is observed drawdown, in feet

Figure 7. Observed drawdown and distribution of drawdown in the model calibrated by trial and error.

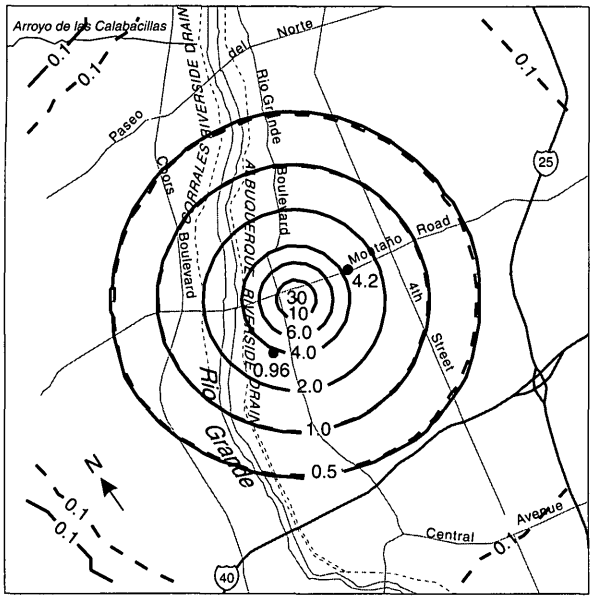

LAYER 5

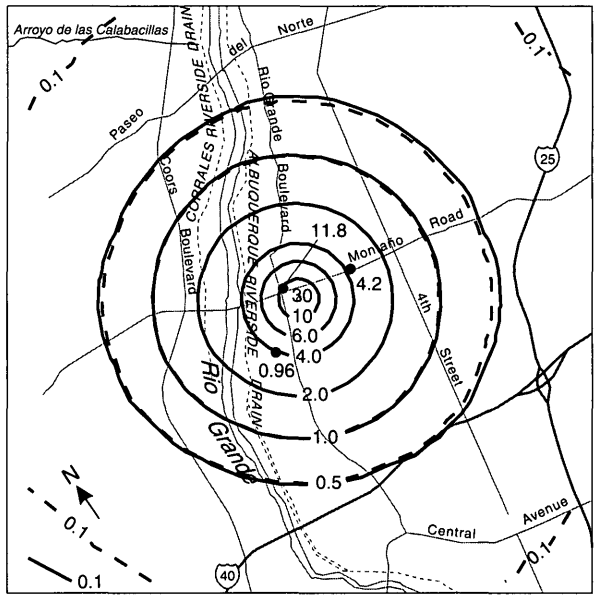

LAYER 6

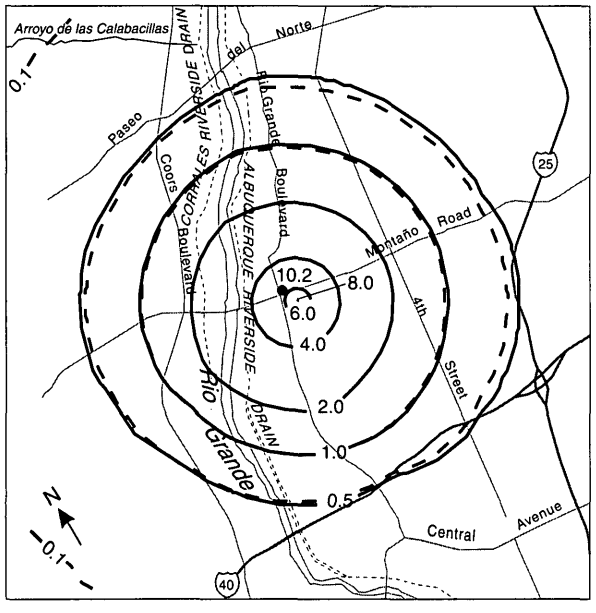

LAYER 7

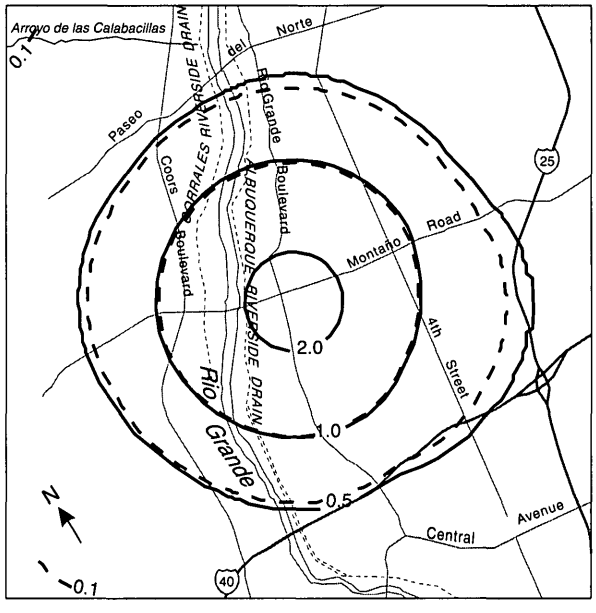

LAYER 8

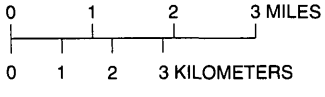

Figure 7. Observed drawdown and distribution of drawdown in the model calibrated by trial and error--Concluded.

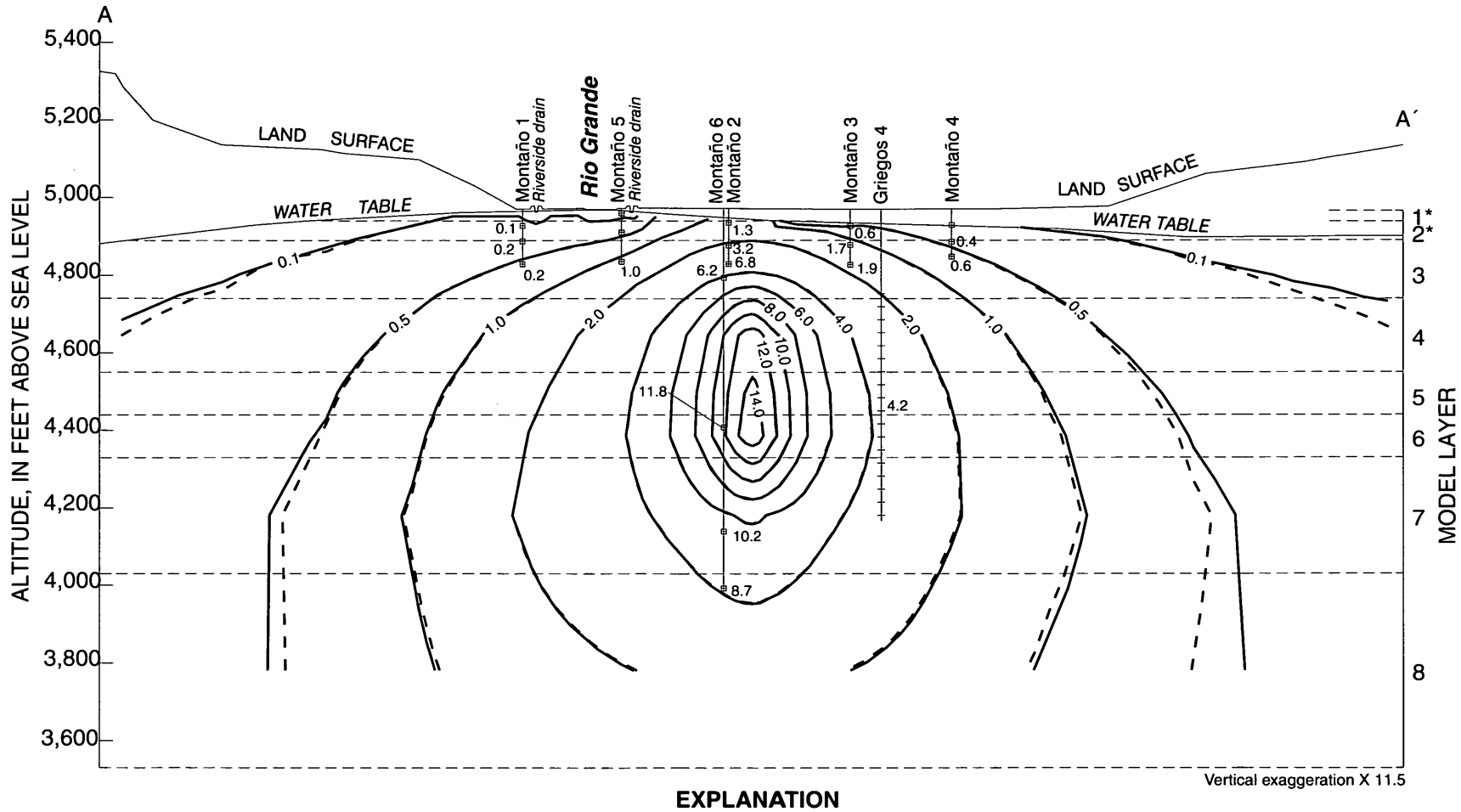

Figure 8. Generalized section A-A´ showing the vertical distribution of drawdown simulated at the end of pumping using the model calibrated by trial and error (location of section shown on plate 1).

Table 3. Simulated water budget at the end of pumping for the model calibrated by trial and error

[Positive numbers indicate a source of water and negative numbers indicate a discharge of water]

Mechanism	Model with no-flow boundary				Model with head-dependent-flux boundary			
	Net flow rate		Cumulative net flow		Net flow rate		Cumulative net flow	
	Acre-feet per day	Sources as percentage of withdrawal	Acre-feet	Sources as percentage of withdrawal	Acre-feet per day	Sources as percentage of withdrawal	Acre-feet	Sources as percentage of withdrawal
Ground-water withdrawal	-10.25		-557.44		-10.25		-557.44	
River leakage	0.78	7.6	32.17	5.8	0.76	7.4	31.85	5.7
Riverside-drain leakage	1.06	10.3	40.73	7.3	1.05	10.2	40.35	7.2
Aquifer storage	8.44	82.3	485.49	87.1	8.01	78.1	470.71	84.4
Head-dependent model boundary	0.00	0.00	0.00	0.00	0.46	4.5	15.49	2.8
Total	0.03	100.2	0.95	100.2	0.03	100.2	0.96	100.1
Percent discrepancy	0.29	0.20	0.17	0.20	0.29	0.20	0.17	0.10

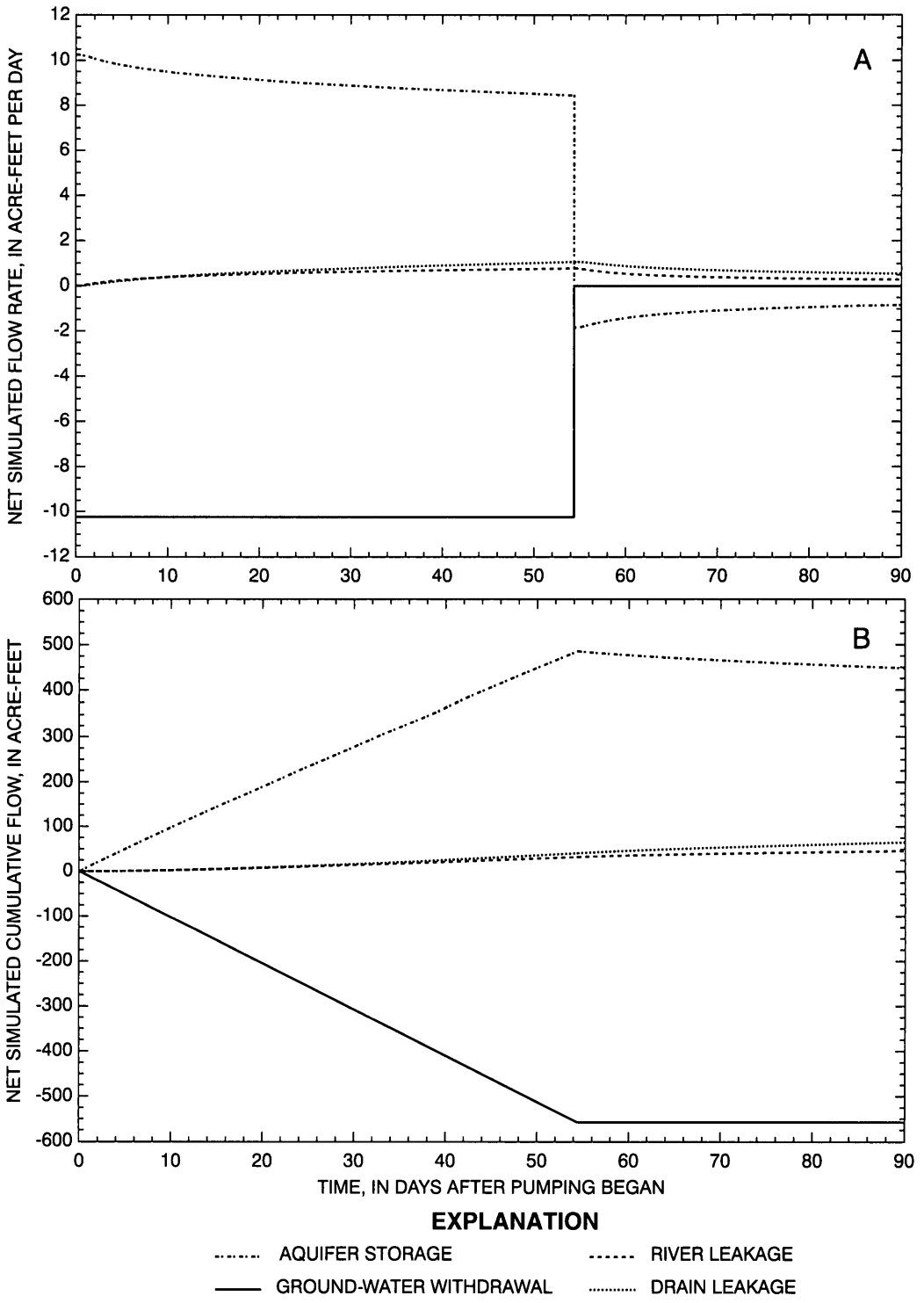

Figure 9. Net simulated flow rates (A) and cumulative flow (B) from the model calibrated by trial and error. Positive numbers indicate a source of water and negative numbers indicate a discharge of water.

MODEL CALIBRATION BY NONLINEAR LEAST-SQUARES REGRESSION

The trial-and-error-calibrated model described in the previous sections was further calibrated using a nonlinear-regression technique developed by Cooley and Naff (1990). The MODFLOWP computer program (Hill, 1992), which applies this technique for use with MODFLOW (McDonald and Harbaugh, 1988), was used for this study. The technique estimates optimal parameter values by minimizing the squared-weighted difference between observed and simulated values as shown in equation 3:

$$S(\boldsymbol{b}) = \sum_{i=1}^{n} [w_i^{1/2} e_i]^2 \qquad (3)$$

where $\boldsymbol{b}$ = vector of parameters to be estimated;
n = number of observations;
w_i = weight, calculated as the inverse of the estimated variance of the measurement error; and
e_i = difference between simulated and observed values of measurement i.

The modified Gauss-Newton optimization method is used to minimize equation 3 (Hill, 1992, p. 76-82). The observations can be hydraulic heads, flows, or prior information on parameters. In this study, only hydraulic heads and prior information are used. No flow observations were available.

The weight applied to each observation is used to compensate for differences in the reliability of the observations. Because superposition is applied to this model, the head observations are drawdown of head corrected for trends in head caused by influences other than aquifer-test pumping. In this case, because similarly accurate equipment and procedures were used for all observation wells, differences in the reliability of the drawdown observations are less related to the accuracy of the measurements themselves, than to the time since pumping began and the magnitude of drawdown. As time of pumping increases, the prepumping trend in head, which is used to correct the measured drawdown, becomes less certain. After a few days or weeks of pumping, this adds a considerable uncertainty to the observed drawdown. In addition, observed drawdown that is relatively small, such as that from observation wells distant from the pumped well, is potentially affected to a proportionately greater degree by outside influences than by aquifer-test pumping.

Additionally, the weight applied to each observation is used to put observations of heads, flows, and prior information, which have different units of measurement, on a comparable basis. The square root of weight ($w_i^{1/2}$) is the inverse of the estimated standard deviation of the measurement error associated with the observation. Therefore, the weighted difference between observed and simulated values ($w_i^{1/2} e_i$) is dimensionless, thus eliminating the discrepancy between units.

The sensitivity of the simulated values at each observation location to each model parameter is calculated by MODFLOWP and used in minimizing equation 3 (Hill, 1992, p. 90-94). These sensitivity values are a measure of the change in simulated head at the observation location resulting from a change in the parameter, and they indicate how much information each observation contributes in estimating the parameter.

Adjustments in Model Representation

Several adjustments in the representation of the aquifer system were necessary to apply MODFLOWP to the model. Except for the changes described in the following sections, the zonation patterns used for the hydraulic properties in the trial-and-error-calibrated model were assumed to correctly represent those in the aquifer system.

Model Layers

The version of MODFLOWP used for this study (version 2.13) does not support estimation of parameters for models of transient flow with layers that are convertible from confined to unconfined. Because the second layer of the trial-and-error-calibrated model was convertible, the configuration of the top two model layers (layers 1 and 2) was modified for compatibility with MODFLOWP. Rather than defining the bottom of layer 1 (and the top of layer 2) as 30 feet below the altitude of the Rio Grande, as described in the previous "Model grid and layers" section and shown in figure 3, the bottom of layer 1 was defined as three-eighths of the depth from the initial water table to 80 feet below the Rio Grande. The bottom of layer 2, defined as 80 feet below the Rio Grande, is the same as in the trial-

and-error-calibrated model. With this configuration, the maximum thickness of layer 1 is 30 feet, the maximum thickness of layer 2 is 50 feet, and the proportionate thickness of the two layers is maintained throughout the model. For example, where the distance between the water table and the base of layer 2 is 32 feet, the thickness of layer 1 is 12 feet (three-eighths of 32 feet) and the thickness of layer 2 is 20 feet (five-eighths of 32 feet). The configuration of the rest of the model, including the area where the water table is in layer 3, was not changed. With this adjustment in layer configuration, no cells in the model go dry; therefore, convertible layers are not needed.

Vertical to Horizontal Anisotropy

For the trial-and-error-calibrated model, the vertical to horizontal anisotropy ratio was assumed to be smaller between cells where the production well screen is located than in the rest of the model (1:5 compared with 1:140) because of the influence of the well bore and gravel pack. The MODFLOWP program allows the vertical to horizontal anisotropy ratio to vary between different layers, but the only way it allows this ratio to vary spatially between the same layers is by separate specification or estimation of the horizontal and vertical hydraulic conductivities. Although attempts were made to estimate different vertical to horizontal anisotropy ratios between selected model layers, they were unsuccessful. Therefore, a uniform ratio was assumed throughout the model.

Ground-Water Withdrawal from Griegos 1

The distribution of pumping in the Griegos 1 well was modified from the trial-and-error-calibrated model. For the calibration by nonlinear regression, pumping by layer was a candidate for estimation because of uncertainty in the pumping rate due to measurement error and variation of the rate with time. Additional uncertainty is associated with the distribution of pumping to the model layers because of measurement error associated with the well-bore flow test and the uncertainty in whether the pumping rate during the flow test (less than 900 gallons per minute; fig. 4) resulted in the same relative distribution of well production as the pumping rate during the aquifer test (2,330 gallons per minute, not including the 27-minute power failure). Although no flow was measured from the zone represented by layer 7 during the flow test, the instrument used (an impeller-type flow meter) could not measure flow less than about 70 gallons per minute in the well bore. Additionally, preliminary models indicated the possibility of more water from the zone represented by layer 7 entering the borehole outside the well screen than the flow test showed (refer to the discussion of ground-water withdrawal from Griegos 1 in the "Model description" section). It was therefore assumed that at least 10 percent of the total flow could be produced from layer 7, and, therefore, about 43 percent of the flow comes from layer 4, about 14 percent from layer 5, and about 32 percent from layer 6.

Aquifer-Test Simulation

The aquifer-test simulation was modified from the simulation used during the trial-and-error calibration. Drawdown observations throughout the aquifer-test pumping period were used for the parameter-estimation calibration. Therefore, the 27-minute lapse of pumping resulting from the power failure could be significant for these simulations. Three stress periods were used for this simulation rather than the single stress period used for the model calibrated by trial and error. The first stress period, representing the pumping time prior to the power failure, was 1.134 days with three time steps. The second stress period, representing the no-pumping period during the power failure, was 0.01875 day (27 minutes) with one step. The third stress period, representing the time from when the pump was restarted after the power failure to the end of aquifer-test pumping, was 53.222 days with 11 steps.

Observations of Drawdown

Fifty-two drawdown observations were used for the nonlinear-regression model calibration. Observations from Griegos 3 were not included as data in the nonlinear-regression calibration for the reasons described previously in the "Model calibration by trial and error" section of this report. With the exception of Griegos 3, the observations used included those shown in table 2 for the intermediate and late time periods and those for the early time period with measured drawdown greater than zero. The early time measurements with zero drawdown shown in table 2 were replaced with observations of drawdown from the same wells at a later time (between 4,000 and 5,630

minutes after pumping began). Observations from Montaño 4-shallow, Montaño 5-shallow, and Montaño 5-intermediate and the early and intermediate observations from Montaño 4-intermediate were omitted from the data set for the same reasons described in the "Model calibration by trial and error" section. Therefore, the data set contains three observations from 17 wells, one each at early time (1,000 to 5,630 minutes after pumping began), intermediate time (10,000 minutes after pumping began), and late time (78,300 minutes after pumping began) and one observation from Montaño 4-intermediate at late time.

Initial regression runs excluded observations of drawdown in the production well, Griegos 1, because the simulated drawdown in a model cell is not representative of drawdown measured in the borehole of an operating production well (see previous discussion in the "Model calibration by trial and error" section). However, when observations from Griegos 1 were excluded, the model produced unreasonable simulated drawdown in the vicinity of the production well. Observations from Griegos 1 were therefore modified as described in subsequent paragraphs and included as data in the calibration by nonlinear regression.

As described previously, the reliability of the drawdown observations decreases as the time of pumping increases because of the increasing uncertainty of trends in hydraulic heads from influences other than aquifer-test pumping. The weighting of the observations from the nonpumped wells was calculated to reflect this increasing uncertainty. However, the quantitative effect of this increasing uncertainty on the measurement of drawdown is not known; therefore, assumptions were made. At the beginning of pumping, the error of drawdown observations was assumed to be associated only with the ability of the instruments to accurately measure water levels in the wells and the interpreted representation of the three-dimensional locations of the observation-well screens in the model. The standard deviation of measurement error at the beginning of pumping was assumed to be 0.17 foot (error variance of 0.03 foot squared). As the aquifer test continued, the standard deviation of measurement error was assumed to increase as the uncertainty of trends from outside influences increases. The increase in standard deviation of the measurement error with time was assumed to not be linear because 1 more day at early time (for example, from 6 to 7 days of pumping, a 17-percent increase in time) may have a greater effect on uncertainty than 1 more day at late time (for example, from 52 to 53 days of pumping, a 2-percent increase in time). Therefore the square of the standard deviation (variance) was used in the increasing error function. The initial error variance of 0.03 foot squared was increased at the rate of 0.01 foot squared for each day that pumping continued. In this manner, the average increase in the standard deviation of measurement error in the first 10 days of the test was about 0.02 foot/day and in the last 10 days of the test was about 0.007 foot/day. Thus, the standard deviation of measurement error would be 0.20 foot 1 day after pumping began (square root of [[1 day x 0.01 foot squared/day] + 0.03 foot squared]), 0.55 foot halfway through the aquifer test (square root of [[27.2 days x 0.01 foot squared/day] + 0.03 foot squared]), and 0.76 foot at the end of the test (square root of [[54.4 days x 0.01 foot squared/day] + 0.03 foot squared]). The weight applied to the difference between observed and simulated values is the inverse of the standard deviation of the measurement error associated with the observation.

Because the increase in measurement error with time (decrease in weight with time) applied to the observations is somewhat arbitrary, regression runs were made using one-half the increase in standard deviation of measurement error with time (smaller decrease in weight with time) to test the sensitivity of the weights on the resulting parameter values. A single estimated parameter value (pumpage from model layer 5) changed by 18 percent with the change. The rest of the estimated parameter values changed by 0.7 to 4 percent. Because pumpage from layer 5 is relatively small compared with total pumpage from Griegos 1, the 18-percent change amounted to 38 gallons per minute (less than 2 percent of total pumpage). Therefore, the weighting scheme does have some effect on the estimated values of parameters, but these effects are small compared to the change in weighting factor.

With the same weights applied to all observations at a given time, locations with larger drawdown residuals will have a greater influence on the regression than those with small drawdown residuals. Because the magnitude of drawdown decreases with distance from the pumped well, drawdown residuals are likely to be larger at locations closer to the pumped well. This is consistent with the potential for greater measurement error with distance from the pumped well. Although public-supply wells in the vicinity of

the test were shut down prior to and during the test, many private wells exist in the area that could not be controlled. As the amount of withdrawals from these wells changed and the river and riverside drain stages changed during the test, they influenced the measured drawdown in the observation wells. These influences have a greater proportionate effect and therefore a greater potential measurement error on small drawdowns than on large drawdowns.

The reliability in drawdown measurements is less in the production well than in the nonpumped observation wells. As described previously, the drawdown calculated by the model for a cell (200 feet on a side) representing the pumped well is not equivalent to the drawdown that would be measured in the borehole. For comparison to the model-derived drawdown, the "observed" drawdown was calculated using equation 2 by solving for the term d_{mc} and substituting the measured drawdown in Griegos 1 for the term d_w. The transmissivity calculated from a previous aquifer test of Griegos 1 (10,720 feet squared per day; Groundwater Management, Inc., 1988, p. 15; Thorn and others, 1993, table 2) was substituted for T_{mc}, and the average measured pumping rate for the aquifer test (449,000 cubic feet per day or 2,330 gallons per minute) was substituted for Q. The terms r_e and r_w are as defined for equation 2. This procedure of estimating the drawdown increases the uncertainty. In addition, slight changes in the pumping rate can cause significant fluctuations in the measured drawdown in the well. Therefore, the reliability of observations from Griegos 1 is less than that of observations from nonpumped observation wells. The errors associated with these components of uncertainty are unknown. The standard deviation of measurement error associated with observations from Griegos 1 was assumed to be 1.4 feet throughout the aquifer test, a factor about eight times that of the initial values for the observation wells. Because the observed drawdown in Griegos 1 is large compared with that in the observation wells (about 65 feet compared with the largest drawdown of about 12 feet measured in an observation well; table 2), influences outside the test would affect the drawdown observations in the pumped well proportionately less than in the observation wells. No increase in measurement error with time was assumed for Griegos 1 because the initial standard deviation of measurement error assumed for Griegos 1 (1.4 feet) is significantly larger than that for the observation wells at the end of pumping (0.76 foot).

The standard deviation of measurement error for drawdown in Griegos 1 (and thus the weighting) is somewhat arbitrary because the degree of uncertainty of the measurements is unknown. The sensitivity of the resulting parameter values to the weight applied to drawdown in Griegos 1 was tested by doing an additional nonlinear-regression run using smaller weights. The weight applied to the Griegos 1 observations was halved (standard deviation of the measurement error was doubled). The change in estimated parameters was 31 percent less pumpage from model layer 6 and 23 percent smaller transmissivity in the upper part of the Santa Fe Group. Changes in the remaining parameters ranged from 3 to 12 percent. Therefore, some parameters are intermediately sensitive to the weight applied to the drawdown observations from Griegos 1. This could introduce some error into estimation of the parameters.

Prior Information

Prior information was used for the well discharge parameters. Information from the well-bore flow test described previously was used to assign initial values for the well discharge parameters based on the assumption that the relative distribution of well production with depth during the borehole flow test is the same that resulted from the larger pumping rate during the aquifer test (less than 900 compared with 2,330 gallons per minute). As described in the "Adjustments in model representation" section, the initial discharge from model layer 4 is about 43 percent of total well discharge (about 1,000 gallons per minute), the initial discharge from model layer 5 is about 14 percent of total well discharge (about 330 gallons per minute), the initial discharge from model layer 6 is about 32 percent of total well discharge (about 750 gallons per minute), and the initial discharge from model layer 7 is about 10 percent of total well discharge (about 230 gallons per minute). These initial discharge values were used as prior information in the regression procedure. The error associated with this prior information is a result of measurement error in the discharge during the aquifer test, measurement error during the borehole flow test, and error associated with the assumption that the relative distribution of well production with depth during the borehole flow test is the same that resulted from the aquifer test. The coefficient of variation

associated with the pumping rates applied to model layers 4, 5, and 6 was assumed to be 0.2. Because the flow contribution from the part of the well screen represented by model layer 7 was about equal to the lower detection limit of the flow meter and, therefore, less certain than the pumping rates for the other model layers, the coefficient of variation associated with the pumping rate applied to layer 7 was assumed to be 0.3.

Selection of Parameters for Estimation

As described previously, the sensitivity of the simulated value at each observation location to each model parameter is calculated by MODFLOWP (Hill, 1992). The composite scaled sensitivity is a measure of how much information all observations contribute to estimating each of the parameters and is calculated as:

$$CSS_j = \left\{ \frac{\sum_{i=1}^{n} w_i \left(\frac{\partial \hat{y}_i}{\partial b_j} b_j \right)^2}{n} \right\}^{\frac{1}{2}} \quad (4)$$

where CSS_j = composite scaled sensitivity for parameter j;
n = number of observations;
w_i = weight applied to observation location i;
$\hat{y}_i$ = simulated value at observation location i; and
b_j = model parameter j.

Because the composite scaled sensitivity values are scaled by the parameter value (eq. 4), they are comparable among different parameters. Therefore, they are good indicators for selecting which parameters are reasonable candidates for estimation. Parameters with large composite scaled sensitivity values are more likely to be estimated because the simulated values used for comparison with the observations are more sensitive to those parameters.

The set of hydraulic properties considered initially as candidates for parameter estimation were the aquifer hydraulic-conductivity values for each zone shown in figure 5, vertical to horizontal anisotropy ratio, specific yield, specific storage, riverbed hydraulic conductivity, drain-bed hydraulic conductivity, and pumping rate by layer. Of the candidate aquifer hydraulic-conductivity parameters, only those zones representing the upper part of the Santa Fe Group in the vicinity of the pumped well and observation wells have relatively high composite scaled sensitivity values (the zones representing the center part of the modeled area in layers 3-7; fig. 5). Zones outside the immediate area of the aquifer test had very low composite scaled sensitivity values, which is not surprising because no observations are available for those zones. Initial regression runs aimed at separately estimating those zones with relatively high composite scaled sensitivity values were unsuccessful. Without the addition of prior information on these parameters, reasonable estimates of hydraulic conductivity for these zones were not obtained. These results indicate that the observed data are not sufficient to estimate hydraulic conductivity for these zones separately. Therefore, all hydraulic-conductivity zones representing the upper part of the Santa Fe Group were combined into a single zone for estimating the hydraulic conductivity of the upper part of the Santa Fe Group in the aquifer-test area. Initial nonlinear-regression runs were also done to test the possibility of estimating the vertical to horizontal anisotropy ratio by layer or by separating it into that for the Santa Fe Group and that for the post-Santa Fe Group inner-valley alluvium. These runs also indicated that the observed data are not sufficient for estimating the anisotropy ratio separately. Composite scaled sensitivity values indicated that simulated values at the observation locations were most sensitive to the anisotropy ratio in the Santa Fe Group as a whole and least sensitive to the anisotropy ratio in the inner-valley alluvium. Therefore, a single anisotropy ratio was used for all layers in the model. The candidates for parameter estimation were then hydraulic conductivity of the inner-valley alluvium (zones labeled RA in fig. 5), the upper part of the Santa Fe Group (zones labeled USF in fig. 5), and each zone representing the middle part of the Santa Fe Group (zones labeled MSF and USF + MSF in fig. 5); riverbed hydraulic conductivity; drain-bed hydraulic conductivity; vertical to horizontal anisotropy ratio; specific storage; specific yield; and pumping rate by layer. The values of composite scaled sensitivity for these candidate parameters are shown in table 4.

Table 4. Composite scaled sensitivity values for aquifer properties and pumping rates that are candidates for parameter estimation

Candidate for parameter estimation	Parameter identifier	Value resulting from trial-and-error-calibrated model	Initial value for nonlinear regression (used for sensitivity calculation)	Composite scaled sensitivity (dimensionless)
Hydraulic conductivity of the inner-valley alluvium (zone labeled RA in fig. 5)	K_{RA}	45 feet per day	45 feet per day	0.524
Hydraulic conductivity of the upper part of the Santa Fe Group (zones labeled USF in fig. 5)	K_{USF}	Variable (see fig. 5)	15 feet per day[1]	9.34
Hydraulic conductivity of zone 4 from figure 5 (zones labeled 4 and MSF in fig. 5)	K_4	4 feet per day	4 feet per day	0.410
Hydraulic conductivity of zone 8 from figure 5 (zone labeled USF + MSF in fig. 5)	K_8	8 feet per day	8 feet per day	6.44×10^{-2}
Hydraulic conductivity of zone 11 from figure 5 (zone labeled 11 and MSF in fig. 5)	K_{11}	11 feet per day	11 feet per day	9.48×10^{-3}
Riverbed hydraulic conductivity	K_{RB}	1 foot per day	2 feet per day[2]	2.06×10^{-4}
Riverside drain-bed hydraulic conductivity	K_{DB}	4 feet per day	4 feet per day	1.69×10^{-3}
Vertical to horizontal anisotropy ratio	A_V	1:140	1:140	2.79
Specific storage	S_s	4×10^{-6} per foot	4×10^{-6} per foot	2.85
Specific yield	S_y	0.15	0.15	0.334
Pumpage from model layer 4	P_4	1,110 gallons per minute	1,000 gallons per minute	4.05
Pumpage from model layer 5	P_5	370 gallons per minute	330 gallons per minute	1.67
Pumpage from model layer 6	P_6	840 gallons per minute	770 gallons per minute	6.06
Pumpage from model layer 7	P_7	0	230 gallons per minute	1.46

[1]Average hydraulic conductivity from the original five wells in the Griegos well field (Thorn and others, 1993, p. 40).

[2]Changed in nonlinear-regression model to be 1/2 the value of K_{DB}. Because of the insensitivity of simulation results at the observation locations to values of K_{RB} and K_{DB}, neither value of K_{RB} is preferred over the other.

Table 5. Values of aquifer properties and pumping rates estimated by nonlinear regression

Estimated parameter	Parameter estimate	Standard deviation of the estimate	Coefficient of variation, in percent	Approximate linear 95-percent confidence interval for parameter[1]	
				Lower limit	Upper limit
Hydraulic conductivity of the upper part of the Santa Fe Group, in feet per day (K_{USF})	12	1.95	16	8.2	16
Vertical to horizontal anisotropy ratio (A_V)	1:82	1:14.6	1:18	1:52	1:111
Specific storage, in per foot of aquifer thickness (S_s)	1.2×10^{-6}	2.4×10^{-7}	20	7.1×10^{-7}	1.7×10^{-6}
Pumping rate in model layer 4, in gallons per minute (P_4)	1,390	211	15	965	1,810
Pumping rate in model layer 5, in gallons per minute (P_5)	197	121	62	0	440
Pumping rate in model layer 6, in gallons per minute (P_6)	353	119	34	115	591
Pumping rate in model layer 7, in gallons per minute (P_7)	542	74	14	394	690

[1]See "Model linearity and normality of weighted residuals" section for explanation of why confidence intervals are considered to be approximate.

The composite scaled sensitivity values for the candidate parameters range from 2.06×10^{-4} for riverbed hydraulic conductivity (K_{RB}), the least sensitive parameter, to 9.34 for hydraulic conductivity of the upper part of the Santa Fe Group (K_{USF}), the most sensitive parameter (table 4). The parameters K_8, K_{11}, K_{RB}, and K_{DB} (table 4) have significantly smaller composite scaled sensitivities than those for the other parameters; thus, it is unlikely that they can be successfully estimated by the regression procedure with the data available. Regression runs were made with the remaining parameters to determine whether the parameters with intermediate composite scaled sensitivity values (between about 0.3 and 0.6; table 4) could be realistically estimated. Estimates of these parameters (K_{RA}, K_4, and S_y) and their confidence intervals were outside the reasonable range for these aquifer properties. Either these parameters are not sensitive enough to the observed information to produce realistic estimates by nonlinear regression or the conceptual model may contain errors. K_4 is represented in a part of the model where no observations are available, and K_{RA} and S_y are represented in the upper part of the model where no pumping occurs. Therefore, these parameters likely are not sensitive enough to the observed information, so changes in the conceptual model were not attempted. The remaining parameters, hydraulic conductivity of the upper part of the Santa Fe Group (K_{USF}), vertical to horizontal anisotropy ratio (A_V), specific storage (S_s), and pumping rate from layers 4 through 7 (P_4, P_5, P_6, and P_7) are the parameters selected for estimation. The parameters not estimated (K_{RA}, K_4, K_8, K_{11}, K_{RB}, K_{DB}, and S_y) were fixed at the initial values shown in table 4.

Estimation of Parameters

The nonlinear least-squares regression method was applied to the ground-water-flow model of the Griegos aquifer test using MODFLOWP to estimate the seven parameters selected on the basis of their composite scaled sensitivity values. The parameter estimates, standard deviations of the estimates, coefficients of variation, and approximate linear 95-percent confidence intervals are shown in table 5. The distribution of hydraulic conductivity with these estimates is shown in figure 10.

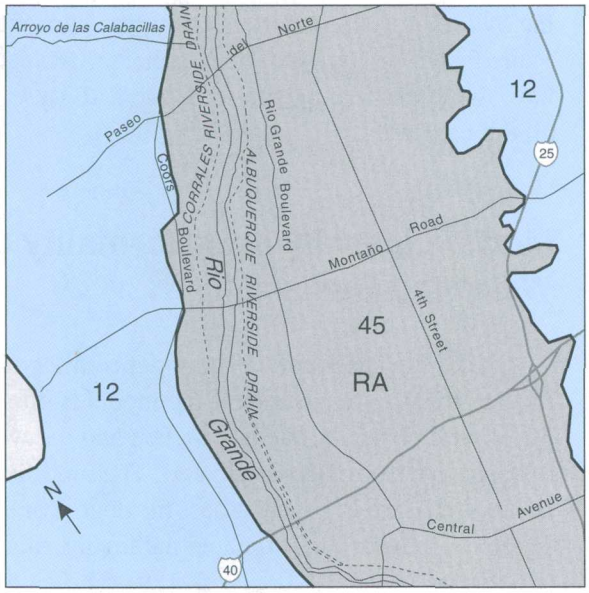

LAYER 1

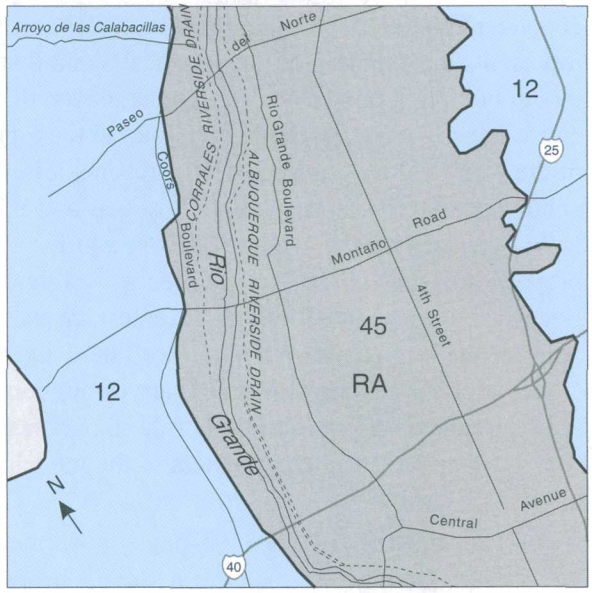

LAYER 2

HYDRAULIC CONDUCTIVITY THROUGHOUT LAYERS 3, 4, 5, AND 6 IS 12 FEET PER DAY

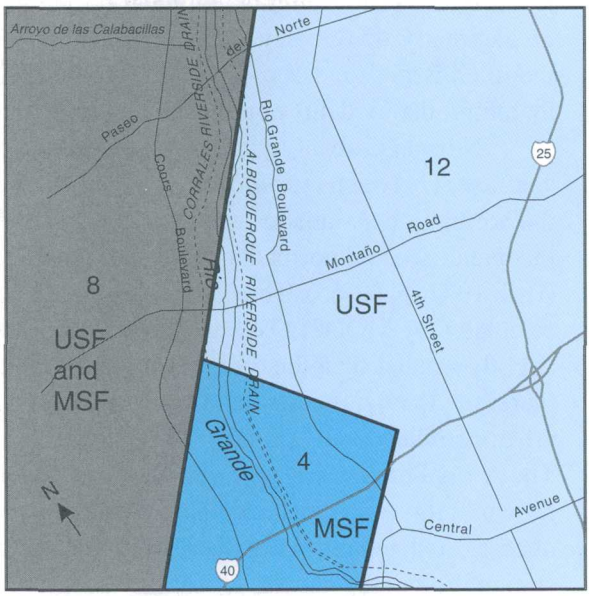

LAYER 7

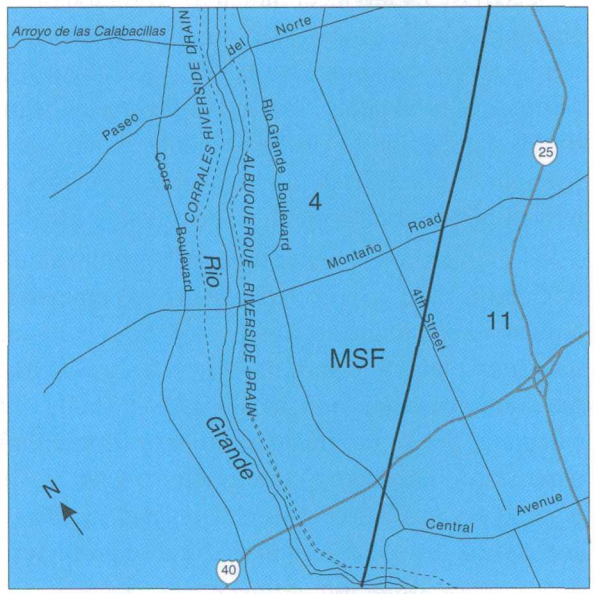

LAYER 8

EXPLANATION

HYDROSTRATIGRAPIC UNIT--Based on units described by Hawley and others (1995, p. 49)

- RA RIVER ALLUVIUM
- USF UPPER PART OF THE SANTA FE GROUP
- USF and MSF CONTAINS BOTH UPPER AND MIDDLE PARTS OF THE SANTA FE GROUP
- MSF MIDDLE PART OF THE SANTA FE GROUP

12 ZONE OF EQUAL HYDRAULIC CONDUCTIVITY--Number is hydraulic conductivity, in feet per day

INACTIVE PART OF MODEL--Part of model layer that represents an unsaturated part of the aquifer

0 1 2 3 MILES

0 1 2 3 KILOMETERS

Figure 10. Distribution of hydraulic conductivity in the model calibrated by nonlinear regression.

The validity of these parameter estimates are dependent on the assumption that the model correctly represents the zonation of the parameters and that model boundary conditions are correct. Given that the entire upper part of the Santa Fe Group in the vicinity of the well field was estimated as one zone, it is concluded that the estimates for K_{USF}, A_V, and S_s are valid estimates for the average of those aquifer properties in the vicinity of the Griegos well field. Because observed data for this aquifer test are available only for the immediate area of the well field and the values of these aquifer properties vary throughout the Albuquerque area, the estimates of these parameters may be in error near the perimeters of the modeled area.

The approximate linear 95-percent confidence intervals on the three estimates of hydraulic properties (K_{USF}, A_V, and S_s) lie within expected ranges of values for each of these parameters. A fairly large amount of uncertainty is associated with the estimate of P_5 as indicated by its large coefficient of variation (62 percent), but the estimates of pumping from the other model layers are somewhat better constrained. The estimate of total pumping (sum of parameter estimates for P_4, P_5, P_6, and P_7) differs by only about 7 percent from the average discharge measured during the test, indicating that total pumping is reasonably constrained.

Correlations greater than the absolute value of 0.95 (Hill, 1992, p. 65-66) between two parameters can indicate that a unique estimation of those parameters may not be possible with the observation data used in the nonlinear regression. MODFLOWP (Hill, 1992) calculates the approximate covariance matrix for the parameters. The largest correlation between any of the parameters was 0.90 between K_{USF} and P_4. This correlation is not large enough to cause problems with non-unique estimation of the parameters.

The composite scaled sensitivity for each parameter is dependent on the values of the parameters. Because the values of the estimated parameters changed in the nonlinear-regression calibration procedure, the sensitivity values also may change. The composite scaled sensitivities for the estimated parameters calculated using the optimal parameter estimates (table 5) are listed in table 6. Because the sensitivities for the parameters not estimated can change as a result of changes in the parameters that were estimated, their composite scaled sensitivities are included in table 6. The most sensitive parameter was the hydraulic conductivity of the upper part of the Santa Fe Group (K_{USF}). The parameters estimated still have the largest composite scaled sensitivity values of all the parameters (tables 4 and 6).

Model Linearity and Normality of Weighted Residuals

The linear 95-percent confidence intervals for the parameters are accurate if the model is effectively linear with respect to the parameters and the weighted residuals are normally distributed. The modified Beale's measure is used to assess the degree of linearity of the model near the estimated parameter values (Cooley and Naff, 1990, p. 187-189). The modified Beale's measure was calculated to be 0.26 using the program BEALEP (Hill, 1994, p. 45-54). The model is effectively linear if the modified Beale's measure is less than 0.04 and is highly nonlinear if the measure is greater than 0.45 (Cooley and Naff, 1990, p. 189). The modified Beale's measure is between these limits; therefore, the model is nonlinear to some degree.

Normal probability plots and the correlation coefficient between the ordered weighted residuals and the normal order statistics are used to assess the independence and normality of the weighted residuals (Hill, 1992, p. 62-65). The correlation coefficient was calculated by MODFLOWP to be 0.958. This is slightly smaller than the critical value of 0.960; therefore, the hypothesis that the weighted residuals are uncorrelated and normally distributed is rejected. The normal probability plot of weighted residuals is shown in figure 11. If the weighted residuals are uncorrelated and normally distributed, they plot on a straight line in the normal probability plot. The weighted residuals deviate somewhat from a straight line, which is consistent with the results using the correlation coefficient. Therefore, the weighted residuals are not strictly independent and normally distributed.

Table 6. Composite scaled sensitivity values calculated with the optimal parameter estimates

Parameter	Parameter identifier	Composite scaled sensitivity (dimensionless)
Estimated parameters		
Hydraulic conductivity of the upper part of the Santa Fe Group (zones labeled USF in fig. 5)	K_{USF}	11.6
Vertical to horizontal anisotropy ratio	A_V	2.83
Specific storage	S_s	2.43
Pumpage from model layer 4	P_4	7.35
Pumpage from model layer 5	P_5	1.31
Pumpage from model layer 6	P_6	3.13
Pumpage from model layer 7	P_7	4.55
Nonestimated parameters		
Hydraulic conductivity of the inner-valley alluvium (zone labeled RA in fig. 5)	K_{RA}	0.820
Hydraulic conductivity of zone 4 from figure 5 (zones labeled 4 and MSF in fig. 5)	K_4	1.01
Hydraulic conductivity of zone 8 from figure 5 (zone labeled USF + MSF in fig. 5)	K_8	0.105
Hydraulic conductivity of zone 11 from figure 5 (zone labeled 11 and MSF in fig. 5)	K_{11}	1.71×10^{-2}
Riverbed hydraulic conductivity	K_{RB}	3.37×10^{-4}
Riverside drain-bed hydraulic conductivity	K_{DB}	2.80×10^{-3}
Specific yield	S_y	0.608

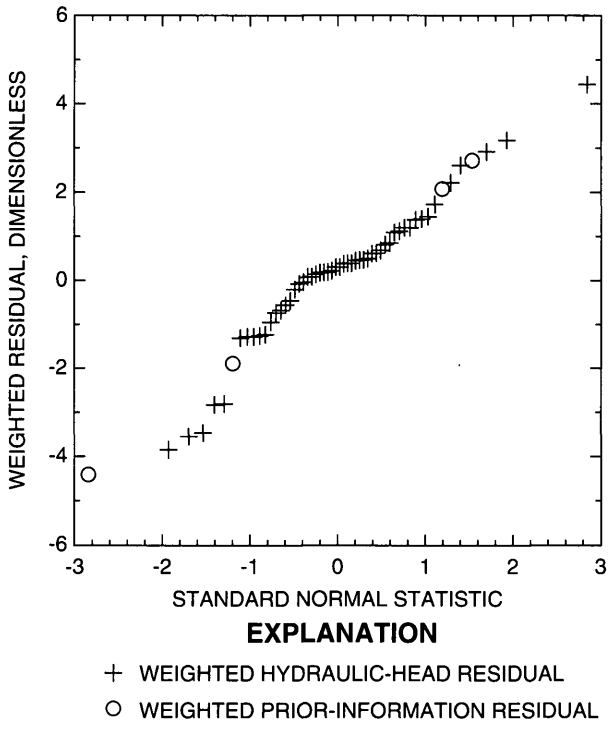

Figure 11. Normal probability plot of weighted residuals.

The method of generating uncorrelated random normal deviates and simulated residuals described by Cooley and Naff (1990, p. 168-170) was used to test whether correlation of the residuals could be the cause of the normal probability plot of weighted residuals not forming a straight line. Normal probability plots of uncorrelated random normal deviates and simulated residuals are very similar; therefore, the normal probability plot shown in figure 11 is unlikely to be greatly affected by correlation of the residuals and unequal variance (Cooley and Naff, 1990, p. 169-170). However, the trend in the normal probability plot of weighted residuals (fig. 11) differs from normal probability plots of simulated residuals. Therefore, the weighted residuals do not strictly conform to a normal distribution.

Because the model is nonlinear to some degree and the weighted residuals do not strictly conform to a normal distribution, the linear 95-percent confidence intervals for the estimated parameters are not strictly accurate. Therefore, they need to be considered approximate.

Drawdown of Hydraulic Head

The observed drawdown, simulated drawdown, and calculated residuals for the nonlinear-regression model are listed in table 7. Negative residuals indicate that simulated drawdown of hydraulic head is greater than observed drawdown, and positive residuals indicate that simulated drawdown is less than observed drawdown. The sum of squared weighted residuals is 134.58 for the drawdown observations and is 169.35 with drawdown observations and prior information. The sum of squared errors for the unweighted drawdown residuals is 67.30 feet squared.

Figure 12 shows the distribution of weighted drawdown residuals for times less than 6,000 minutes after pumping began, figure 13 shows the residuals for 10,000 minutes after pumping began, and figure 14 shows the residuals at the end of pumping (78,300 minutes after pumping began). Although the majority of the weighted residuals are relatively small, these figures and table 7 show a bias of the model to overpredict drawdown (residuals are negative) at most observation locations. The largest weighted residual (in absolute value) is -4.44 located at the Griegos 1 pumped well at the end of pumping. As described in the "Observations of drawdown" section, observations in Griegos 1 have the largest potential for error.

Table 7. Observed drawdown, simulated drawdown, residuals, and weighted residuals for the 52 drawdown observations used in the nonlinear least-squares regression

Well (fig. 2)	Time of observation, in minutes after pumping began	Observed drawdown, in feet	Simulated drawdown, in feet	Residual (observed-simulated), in feet	Weight	Weighted residual
Griegos 1	1,000	[1]40.00	41.69	-1.69	0.707	-1.19
Griegos 1	10,000	[1]41.60	45.29	-3.69	0.707	-2.61
Griegos 1	78,300	[1]39.90	46.17	-6.27	0.707	-4.44
Griegos 4	1,000	0.65	1.26	-0.61	5.20	-3.18
Griegos 4	10,000	3.13	3.20	-0.07	3.18	-0.22
Griegos 4	78,300	4.22	3.88	0.35	1.32	0.46
Montaño 1-deep	5,630	0.10	0.40	-0.30	3.81	-1.12
Montaño 1-deep	10,000	0.10	0.48	-0.38	3.18	-1.20
Montaño 1-deep	78,300	0.17	0.68	-0.52	1.32	-0.68
Montaño 1-intermediate	5,630	0.06	0.16	-0.10	3.81	-0.38
Montaño 1-intermediate	10,000	0.07	0.19	-0.12	3.18	-0.39
Montaño 1-intermediate	78,300	0.17	0.31	-0.14	1.32	-0.18
Montaño 1-shallow	5,630	0.02	0.07	-0.05	3.81	-0.18
Montaño 1-shallow	10,000	0.06	0.09	-0.02	3.18	-0.08
Montaño 1-shallow	78,300	0.11	0.18	-0.06	1.32	-0.09
Montaño 2-deep	1,000	4.17	3.43	0.74	5.20	3.85
Montaño 2-deep	10,000	5.79	4.67	1.12	3.18	3.55
Montaño 2-deep	78,300	6.77	5.78	0.99	1.32	1.31
Montaño 2-intermediate	1,000	1.19	1.47	-0.28	5.20	-1.45
Montaño 2-intermediate	10,000	2.05	2.14	-0.10	3.18	-0.30
Montaño 2-intermediate	78,300	3.17	3.52	-0.35	1.32	-0.46
Montaño 2-shallow	4,000	0.03	0.10	-0.07	4.15	-0.30
Montaño 2-shallow	10,000	0.13	0.28	-0.15	3.18	-0.47
Montaño 2-shallow	78,300	1.28	1.90	-0.62	1.32	-0.82
Montaño 3-deep	1,000	0.39	0.95	-0.56	5.20	-2.92
Montaño 3-deep	10,000	1.24	1.78	-0.54	3.18	-1.73
Montaño 3-deep	78,300	1.92	2.57	-0.64	1.32	-0.85

Table 7. Observed drawdown, simulated drawdown, residuals, and weighted residuals for the 52 drawdown observations used in the nonlinear least-squares regression--Concluded

Well (fig. 2)	Time of observation, in minutes after pumping began	Observed drawdown, in feet	Simulated drawdown, in feet	Residual (observed-simulated), in feet	Weight	Weighted residual
Montaño 3-intermediate	1,000	0.26	0.36	-0.10	5.20	-0.50
Montaño 3-intermediate	10,000	1.03	0.73	0.30	3.18	0.95
Montaño 3-intermediate	78,300	1.71	1.56	0.15	1.32	0.20
Montaño 3-shallow	5,630	0.07	0.06	0.01	3.81	0.04
Montaño 3-shallow	10,000	0.13	0.11	0.02	3.18	0.07
Montaño 3-shallow	78,300	0.65	0.96	-0.32	1.41	-0.45
Montaño 4-deep	1,000	0.01	0.13	-0.12	5.20	-0.61
Montaño 4-deep	10,000	0.16	0.50	-0.34	3.18	-1.09
Montaño 4-deep	78,300	0.57	0.87	-0.29	1.32	-0.39
Montaño 4-intermediate	78,300	0.36	0.47	-0.10	1.32	-0.14
Montaño 5-deep	1,000	0.20	0.46	-0.26	5.20	-1.38
Montaño 5-deep	10,000	0.69	1.13	-0.44	3.18	-1.40
Montaño 5-deep	78,300	1.00	1.47	-0.47	1.32	-0.62
Montaño 6-deep	1,000	2.72	3.14	-0.43	5.20	-2.22
Montaño 6-deep	10,000	7.59	7.19	0.40	3.18	1.26
Montaño 6-deep	78,300	8.68	8.17	0.52	1.32	0.68
Montaño 6-medium deep	1,000	4.55	4.41	0.14	5.20	0.73
Montaño 6-medium deep	10,000	9.23	8.34	0.89	3.18	2.83
Montaño 6-medium deep	78,300	10.24	9.27	0.97	1.32	1.28
Montaño 6-intermediate	1,000	6.88	6.92	-0.04	5.20	-0.19
Montaño 6-intermediate	10,000	11.00	10.61	0.39	3.18	1.23
Montaño 6-intermediate	78,300	11.88	11.46	0.42	1.32	0.55
Montaño 6-shallow	1,000	3.52	2.97	0.54	5.20	2.81
Montaño 6-shallow	10,000	5.27	4.18	1.09	3.18	3.47
Montaño 6-shallow	78,300	6.21	5.24	0.97	1.32	1.28

[1]Observed drawdown adjusted to estimate drawdown in model cell (see "Observations of drawdown" section).

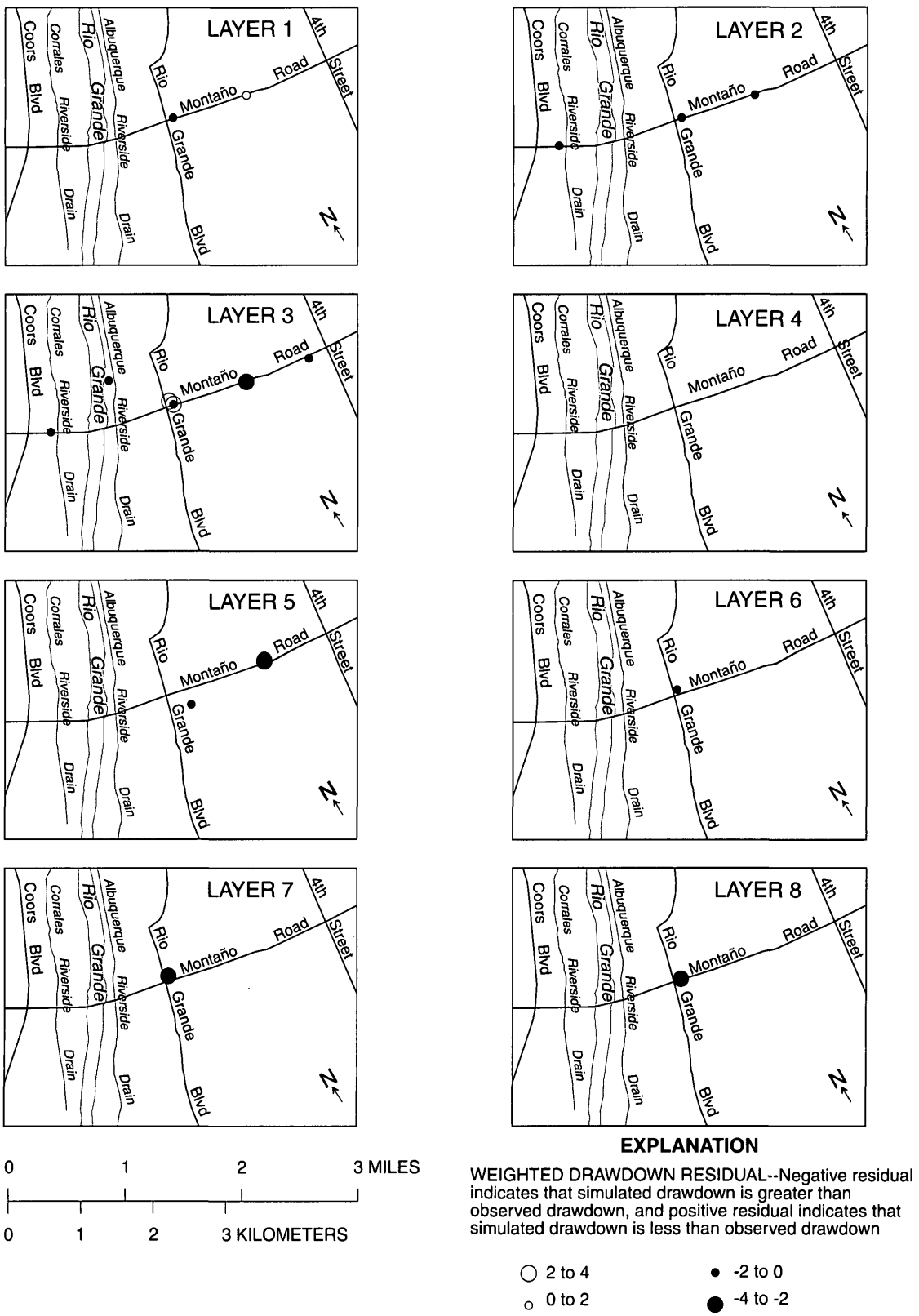

Figure 12. Distribution of weighted drawdown residuals for times less than 6,000 minutes after pumping began in the model calibrated by nonlinear regression.

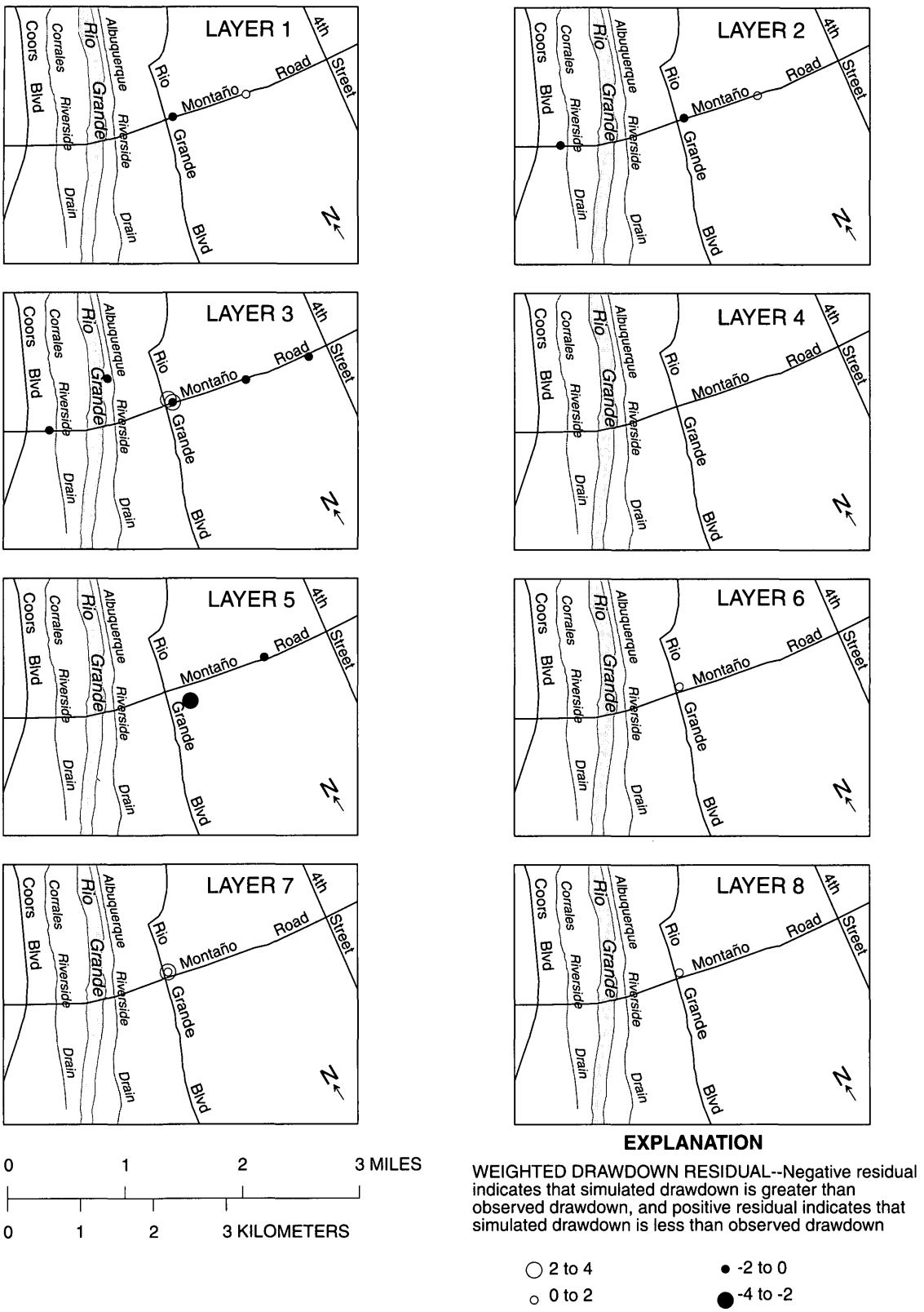

Figure 13. Distribution of weighted drawdown residuals at 10,000 minutes after pumping began in the model calibrated by nonlinear regression.

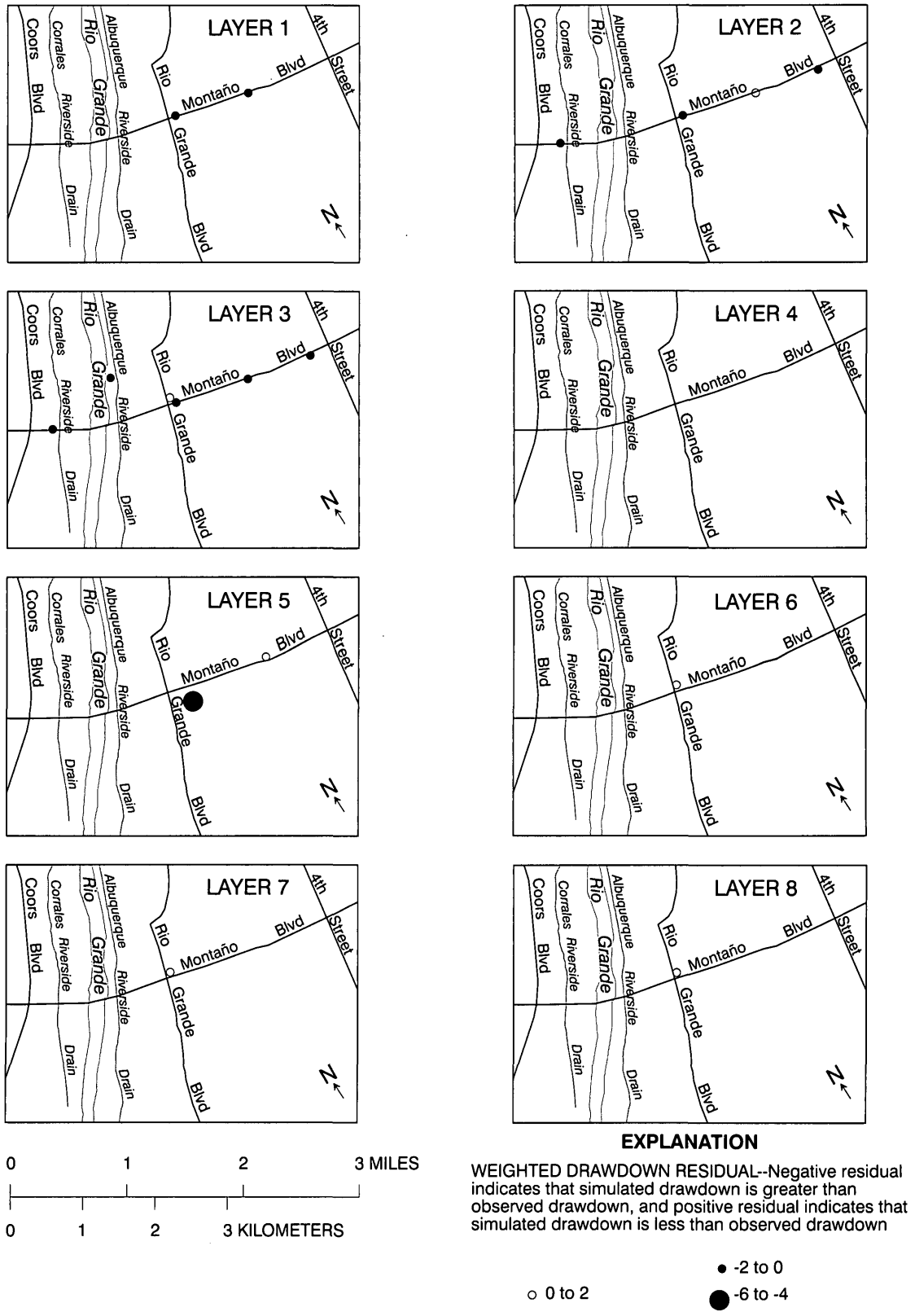

Figure 14. Distribution of weighted drawdown residuals at the end of pumping in the model calibrated by nonlinear regression.

To compare the fit of the model calibrated by nonlinear regression with the model calibrated by trial and error, table 8 lists simulated drawdown for the nonlinear-regression model for the time periods and locations shown in table 2. The nonlinear-regression model fits the observed drawdowns better than the trial-and-error model for all time periods. The nonlinear-regression model fit at the early time period is substantially better than that for the trial-and-error model (sum of squared errors of 6 feet squared compared with 24 feet squared). At the intermediate time period the nonlinear-regression model fit is also significantly better (sum of squared errors of 26 feet squared compared with 50 feet squared). At the end of pumping the nonlinear-regression model fit is only slightly better (sum of squared errors of 55 feet squared compared with 56 feet squared). The overall sum of squared errors is 87 feet squared for the nonlinear-regression model compared with 130 feet squared for the trial-and-error model. The model fit at the end of pumping is not substantially better than the trial-and-error model because the late-time observations were given substantially lower weights as a result of the potential for greater error in the observed drawdowns at late time (end of pumping; see "Observations of drawdown" section).

Curves of drawdown as a function of time for the observation wells are shown in figure 15. These curves may be compared with the curves shown in figure 6 for the trial-and-error-calibrated model. As was done in the model calibrated by trial and error, the simulated drawdown for Griegos 1 was adjusted using equation 2 to calculate drawdown in the borehole. One of the most noticeable differences is in the curves for Griegos 1 (figs. 6A and 15A). The nonlinear-regression model simulated the 27-minute power failure (fig. 15A), whereas the trial-and-error model assumed a constant pumping rate throughout the simulation. The effects of the power failure on most of the other curves are barely detectable. Although this adjustment occurred during the initial minutes of the test and was measured on the order of hundredths of feet, it illustrates the errors that can compound by projecting pretest trends in hydraulic head over the 54-day duration of the test (see "Observations of drawdown" section).

Although the overall sum of squared differences between simulated and observed drawdown shown in tables 2 and 7 is improved for the nonlinear-regression model (87 feet squared for the nonlinear-regression model compared with 130 feet squared for the trial-and-error model), only about half the curve matches shown in figure 15 for the nonlinear-regression model are an improvement over those for the trial-and-error model (fig. 6). The matches of the curve shapes are particularly improved in the Montaño 2-intermediate and -deep and Montaño 6-medium deep and -deep piezometers (fig. 15H, I, U, and V). Conversely, the simulated drawdown for the trial-and-error model (fig. 6C) fits the observed drawdown in Griegos 4 better than the simulated drawdown for the nonlinear-regression model (fig. 15C). As in the trial-and-error model, simulated drawdown in the nonlinear-regression model poorly matches observed drawdown in Griegos 3 (fig. 15B). As discussed previously, observations in Griegos 3 were not used to guide calibration of either model (see "Model calibration by trial and error" section); however, they are included in the sum-of-squared-errors comparison of the models (tables 2 and 8). Observation wells with small amounts of drawdown, particularly the Montaño 1-intermediate and -deep piezometers (fig. 15E and F), also have poor matches. The wells with relatively small drawdowns also tend to have relatively small simulated drawdowns, resulting in relatively small unweighted residuals. Based on the weighting used for the observations, these observations have a smaller influence on the nonlinear regression than do the observations with larger drawdowns (see "Observations of drawdown" section). Therefore, the match between simulated and observed curves for these wells is not significantly improved over the trial-and-error model.

The simulated drawdown for the nonlinear-regression model at the end of pumping is shown in figure 16 for all model layers. Simulations with no-flow and head-dependent-flux lateral boundaries are shown. As in the trial-and-error model, simulated drawdown in areas that have observation wells does not differ between the two boundary conditions. Flexures in the 0.1- and 0.5-foot lines of equal drawdown for layers 1 and 2 are shown near the Rio Grande and drains and are similar to those for the trial-and-error model (fig. 7). Slightly more pronounced flexures in the 0.1-foot line of equal drawdown near the drains and Rio Grande are shown for layer 2 in figure 16. This is likely the effect of a greater simulated vertical hydraulic conductivity between layers 1 and 2 in the nonlinear-regression model than in the trial-and-error model (vertical to horizontal anisotropy ratio of 1:82 rather than 1:140 applied to the same horizontal hydraulic-conductivity value for parameter K_{RA}), resulting in a greater influence of the surface-water system on simulated drawdown in layer 2.

Table 8. Comparison between observed drawdown and drawdown simulated using the model calibrated by nonlinear regression, by time of pumping

[--, data not used]

Well (fig. 2)	Observed drawdown, in feet	Simulated drawdown, in feet	Difference (observed-simulated), in feet
Early time--1,000 minutes after pumping began			
Griegos 1	64.73	[1]66.42	-1.69
Griegos 3	0.27	1.39	-1.12
Griegos 4	0.65	1.26	-0.61
Montaño 1-deep	0.00	0.11	-0.11
Montaño 1-intermediate	0.00	0.04	-0.04
Montaño 1-shallow	0.00	0.02	-0.02
Montaño 2-deep	4.17	3.43	0.74
Montaño 2-intermediate	1.19	1.47	-0.28
Montaño 2-shallow	0.00	0.02	-0.02
Montaño 3-deep	0.39	0.95	-0.56
Montaño 3-intermediate	0.26	0.36	-0.10
Montaño 3-shallow	0.00	0.01	-0.01
Montaño 4-deep	0.01	0.13	-0.12
Montaño 4-intermediate	--	0.04	--
Montaño 4-shallow	--	0.00	--
Montaño 5-deep	0.20	0.46	-0.26
Montaño 5-intermediate	--	0.08	--
Montaño 5-shallow	--	0.00	--
Montaño 6-deep	2.72	3.14	-0.42
Montaño 6-medium deep	4.55	4.41	0.14
Montaño 6-intermediate	6.88	6.92	-0.04
Montaño 6-shallow	3.52	2.97	0.55
Root-mean-square error			0.58
Sum of squared errors, in feet squared			6.03
Mean difference, in feet			-0.22
Mean absolute difference, in feet			0.38
Intermediate time--10,000 minutes after pumping began			
Griegos 1	66.33	[1]70.02	-3.69
Griegos 3	0.67	3.51	-2.84

Table 8. Comparison between observed drawdown and drawdown simulated using the model calibrated by nonlinear regression, by time of pumping--Continued

Well (fig. 2)	Observed drawdown, in feet	Simulated drawdown, in feet	Difference (observed-simulated), in feet
Griegos 4	3.13	3.20	-0.07
Montaño 1-deep	0.10	0.48	-0.38
Montaño 1-intermediate	0.07	0.19	-0.12
Montaño 1-shallow	0.06	0.09	-0.03
Montaño 2-deep	5.79	4.67	1.12
Montaño 2-intermediate	2.05	2.14	-0.09
Montaño 2-shallow	0.13	0.28	-0.15
Montaño 3-deep	1.24	1.78	-0.54
Montaño 3-intermediate	1.03	0.73	0.30
Montaño 3-shallow	0.13	0.11	0.02
Montaño 4-deep	0.16	0.50	-0.34
Montaño 4-intermediate	--	0.15	--
Montaño 4-shallow	--	0.03	--
Montaño 5-deep	0.69	1.13	-0.44
Montaño 5-intermediate	--	0.20	--
Montaño 5-shallow	--	0.03	--
Montaño 6-deep	7.59	7.19	0.40
Montaño 6-medium deep	9.23	8.34	0.89
Montaño 6-intermediate	11.00	10.61	0.39
Montaño 6-shallow	5.27	4.18	1.09
Root-mean-square error			1.20
Sum of squared errors, in feet squared			26.11
Mean difference, in feet			-0.25
Mean absolute difference, in feet			0.72
Late time (end of pumping)--78,300 minutes after pumping began			
Griegos 1	64.63	[1]70.90	-6.27
Griegos 3	0.95	4.18	-3.23
Griegos 4	4.22	3.88	0.34
Montaño 1-deep	0.17	0.68	-0.51
Montaño 1-intermediate	0.17	0.31	-0.14
Montaño 1-shallow	0.11	0.18	-0.07

Table 8. Comparison between observed drawdown and drawdown simulated using the model calibrated by nonlinear regression, by time of pumping--Concluded

Well (fig. 2)	Observed drawdown, in feet	Simulated drawdown, in feet	Difference (observed-simulated), in feet
Montaño 2-deep	6.77	5.78	0.99
Montaño 2-intermediate	3.17	3.52	-0.35
Montaño 2-shallow	1.28	1.90	-0.62
Montaño 3-deep	1.92	2.57	-0.65
Montaño 3-intermediate	1.71	1.56	0.15
Montaño 3-shallow	0.65	0.96	-0.31
Montaño 4-deep	0.57	0.87	-0.30
Montaño 4-intermediate	0.36	0.47	-0.11
Montaño 4-shallow	--	0.32	--
Montaño 5-deep	1.00	1.47	-0.47
Montaño 5-intermediate	--	0.31	--
Montaño 5-shallow	--	0.05	--
Montaño 6-deep	8.68	8.17	0.51
Montaño 6-medium deep	10.24	9.27	0.97
Montaño 6-intermediate	11.88	11.46	0.42
Montaño 6-shallow	6.21	5.24	0.97
Root-mean-square error			1.70
Sum of squared errors, in feet squared			54.81
Mean difference, in feet			-0.46
Mean absolute difference, in feet			0.91
Summary statistics for all observations			
Root-mean-square error			1.26
Sum of squared errors			86.96
Mean difference			-0.31
Mean absolute difference			0.67

[1]Simulated drawdown adjusted to represent drawdown in the pumped well.

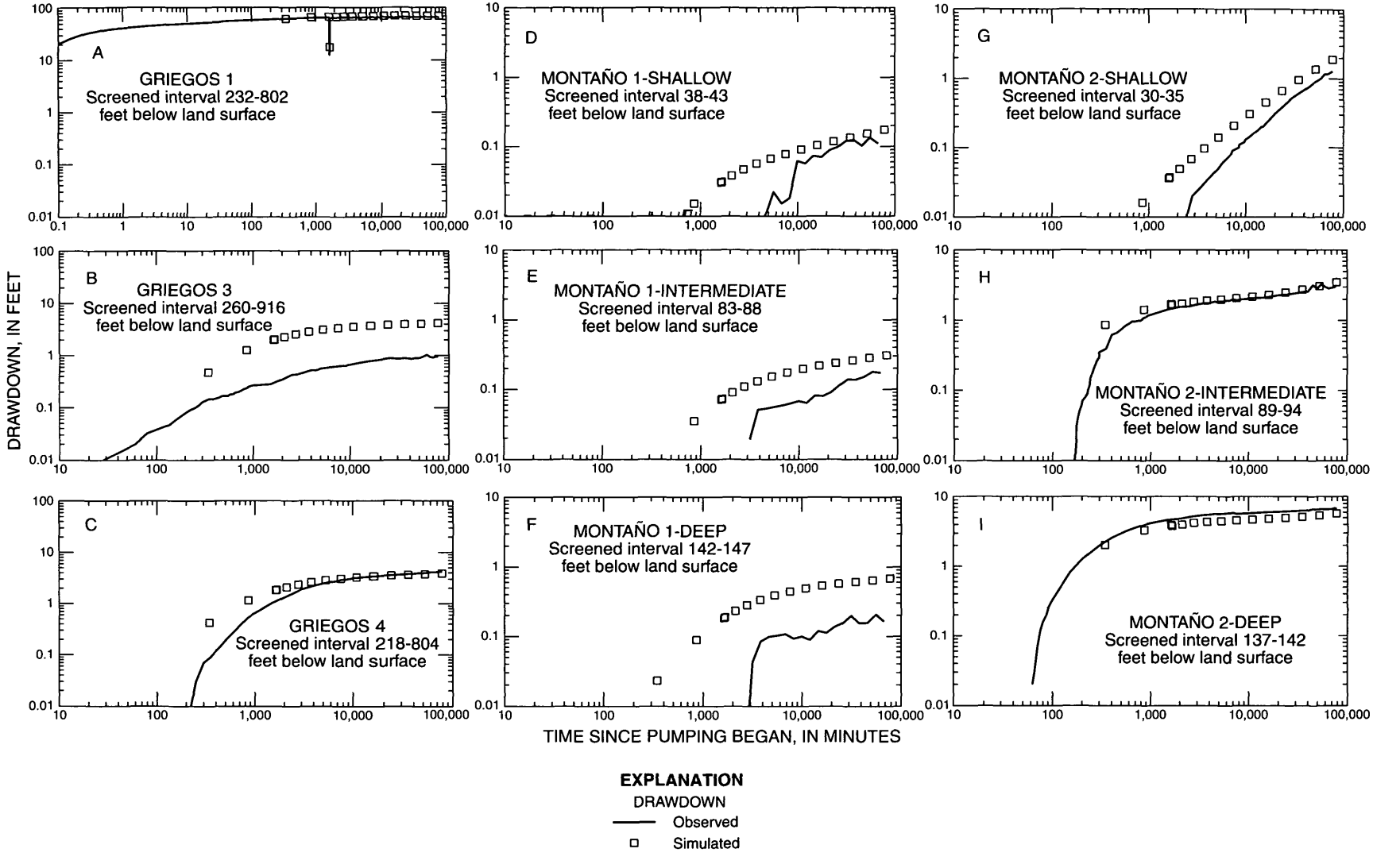

Figure 15. Comparison between observed drawdown and drawdown simulated using the model calibrated by nonlinear regression.

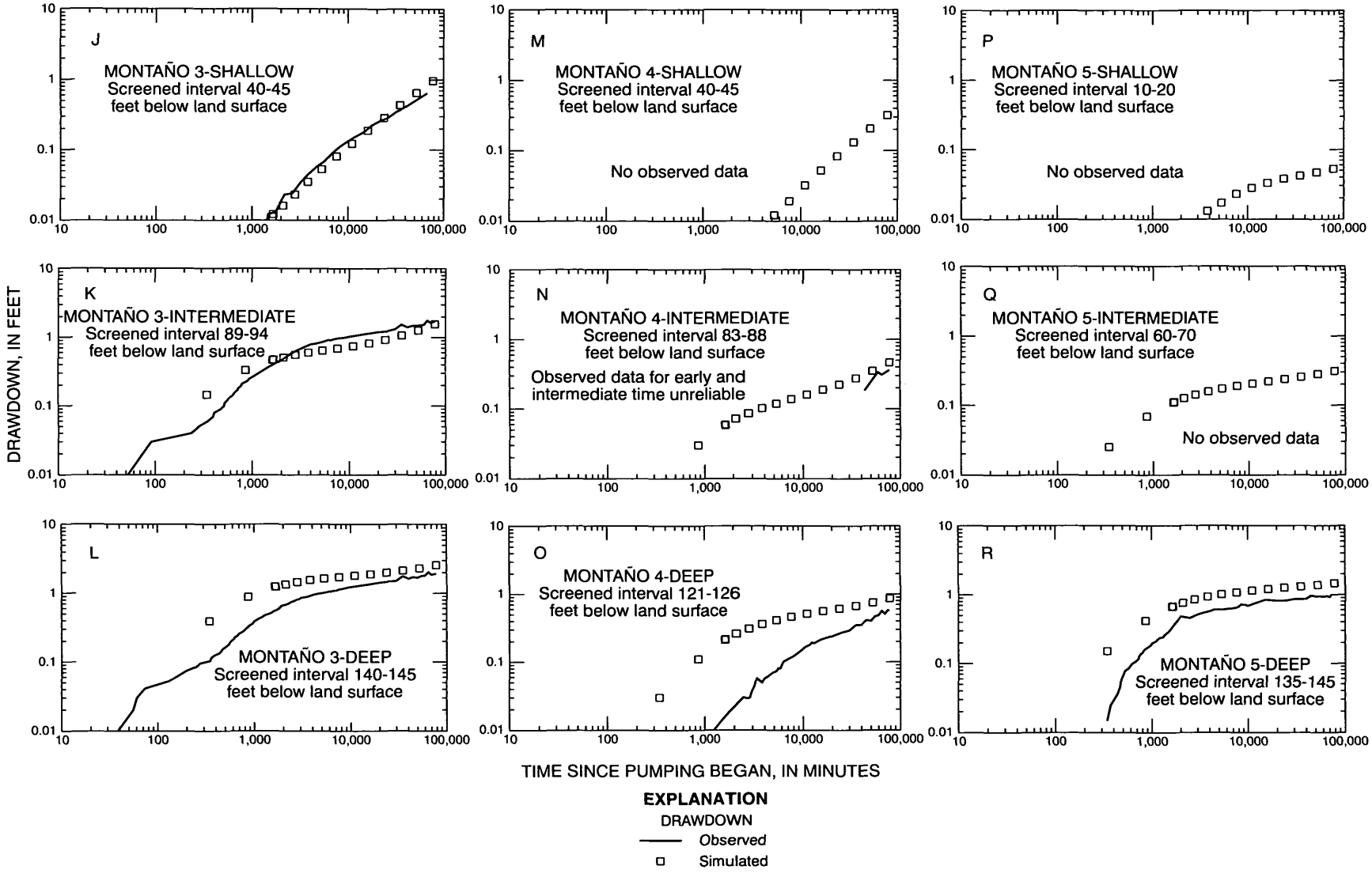

Figure 15. Comparison between observed drawdown and drawdown simulated using the model calibrated by nonlinear regression--Continued.

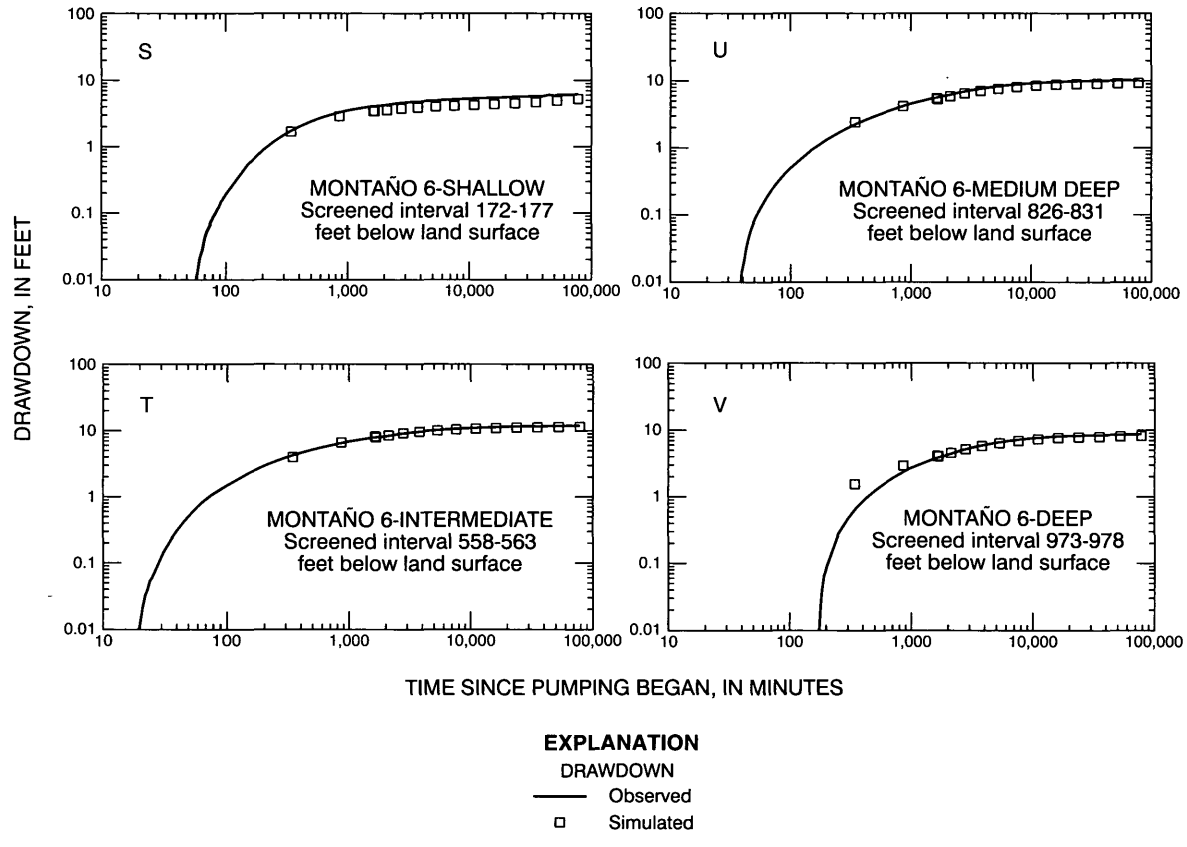

Figure 15. Comparison between observed drawdown and drawdown simulated using the model calibrated by nonlinear regression--Concluded.

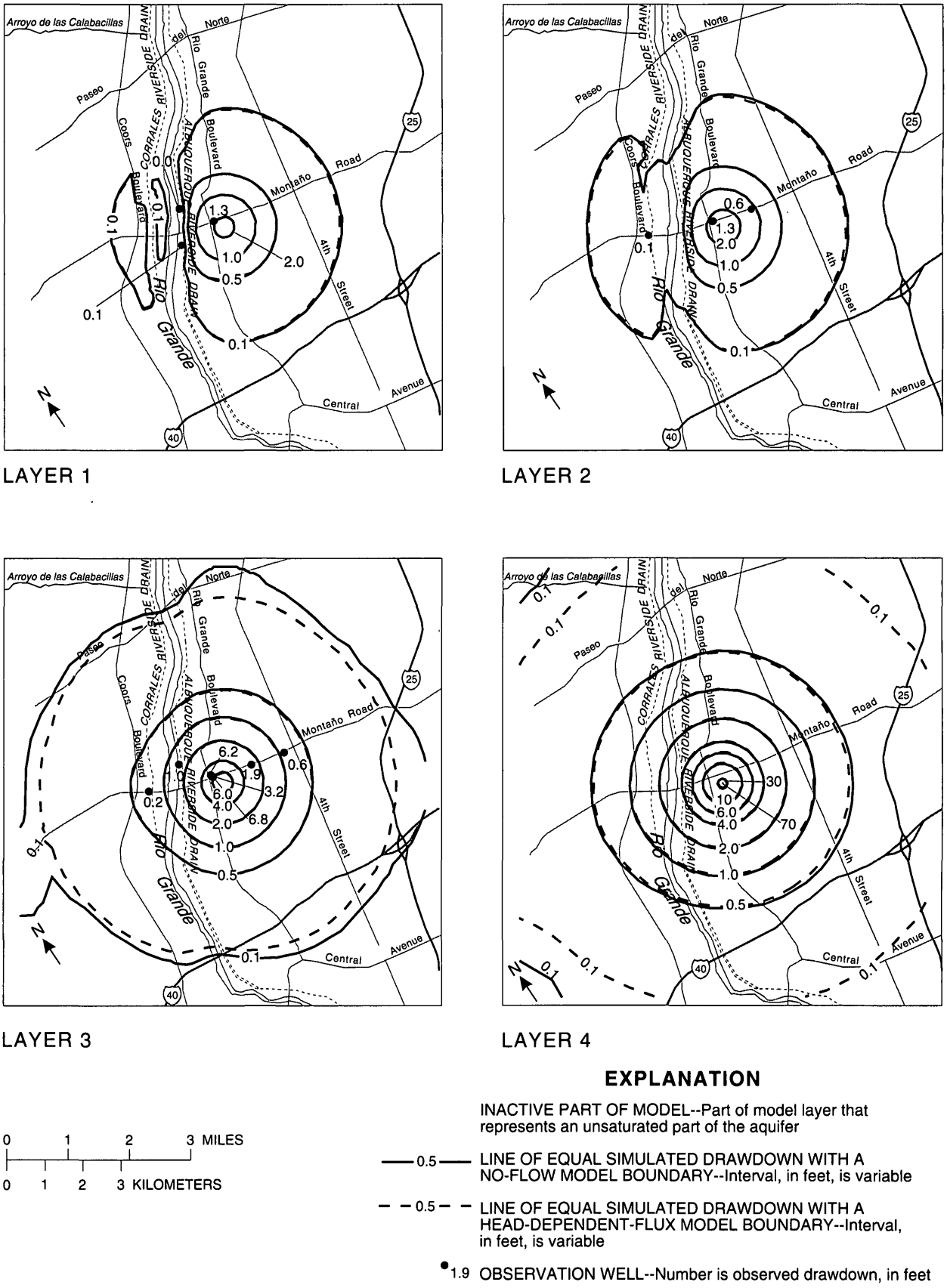

Figure 16. Observed drawdown and distribution of drawdown in the model calibrated by nonlinear regression.

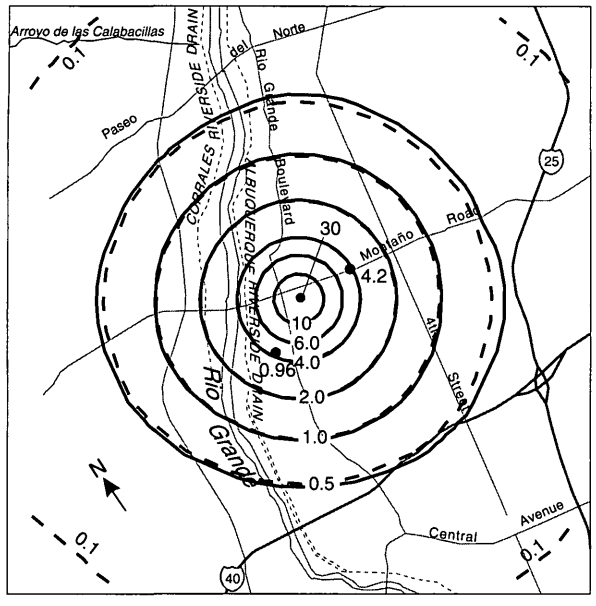

LAYER 5

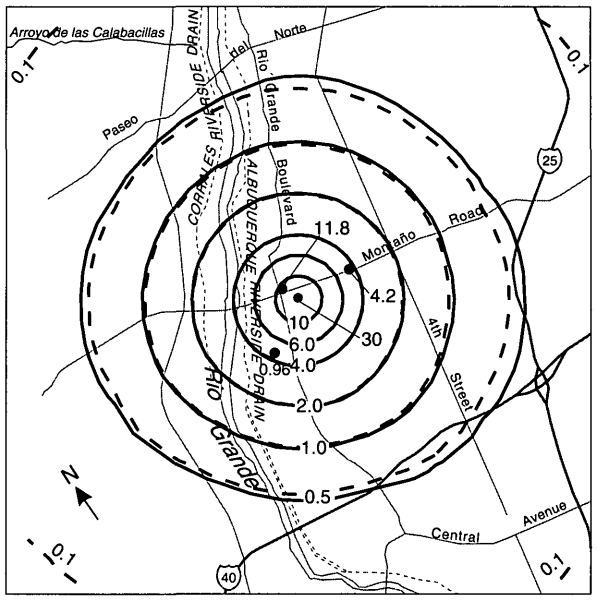

LAYER 6

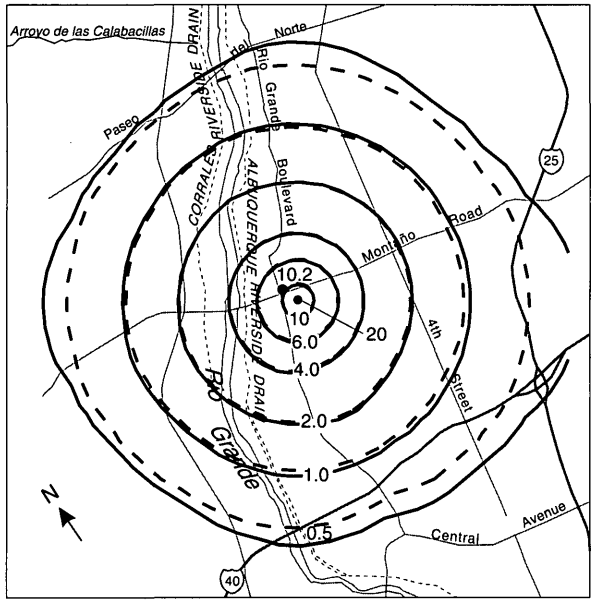

LAYER 7

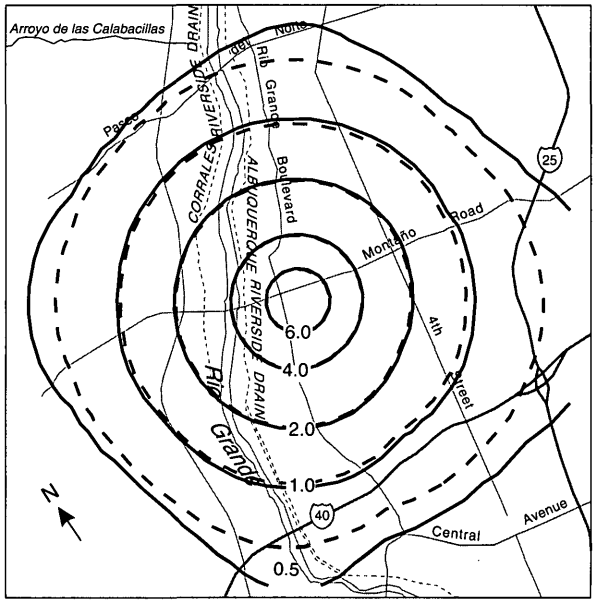

LAYER 8

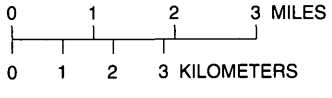

Figure 16. Observed drawdown and distribution of drawdown in the model calibrated by nonlinear regression--Concluded.

The vertical distribution of simulated drawdown is shown for the nonlinear-regression model in figure 17. Although more pronounced, flexures in the 0.1-foot line of equal drawdown in figure 17 are similar to those in the vertical section for the trial-and-error model (fig. 8). Again, the more pronounced flexures are the result of the larger riverbed hydraulic conductivity used in the nonlinear-regression model. The overall shape of the lines of equal drawdown in figure 17 differs from that in figure 8. At a given location, the nonlinear-regression model (fig. 17) has less difference in drawdown between the middle and lower layers (below layer 4) than the trial-and-error model (fig. 8). This results from a smaller vertical to horizontal anisotropy ratio in the nonlinear-regression model than in the trial-and-error model and from pumping applied to layer 7 of the nonlinear-regression model and none applied to layer 7 in the trial-and-error model.

Water Budget

The simulated water budget at the end of pumping is listed in table 9 for the nonlinear-regression model. Budgets for both a no-flow and a head-dependent-flux lateral model boundary are shown. In terms of percentage of withdrawal from the five sources, these water-budget values differ by 1.5 percent or less from those resulting from the trial-and-error model (table 3). The main difference between nonlinear-regression model budget values and trial-and-error model budget values is in ground-water withdrawal. Pumping rates by layer were included in the set of parameters estimated by nonlinear regression, resulting in an increase of about 6 percent in total pumping from the Griegos 1 well over that in the trial-and-error model.

The amount of simulated leakage from the river and riverside drains differs by 1 to 3 percent between the two lateral boundary conditions (table 9). As discussed for the trial-and-error model, the main difference between the two simulated water budgets using the nonlinear-regression model is the amount of water coming from storage at the end of pumping. The head-dependent-flux boundary condition (table 9) results in water coming from aquifer storage both within (aquifer-storage mechanism) and outside (head-dependent model-boundary mechanism) the modeled area. However, the difference between the two lateral boundary conditions in the total amount of water coming from aquifer storage (aquifer-storage and head-dependent model-boundary mechanism) is less than 0.5 percent. At the end of pumping, about 83 percent of the ground-water withdrawal rate was compensated by water from aquifer storage (aquifer storage inside and outside the model boundary), about 7 percent by river leakage, and about 10 percent by riverside-drain leakage (table 9). Of the cumulative amount pumped during the test, about 87 percent was simulated to have come from aquifer storage, 5 to 6 percent from river leakage, and 7 to 8 percent from riverside-drain leakage.

The simulated water budget over time is shown in figure 18 for the nonlinear-regression model. Because of the similarity of the water budgets for the two lateral boundary conditions, only the simulation with a no-flow boundary is shown. These curves and those shown for the trial-and-error model (fig. 9) have two main differences. The most noticeable difference is the change in the ground-water withdrawal rate for the 27-minute power failure simulated in the nonlinear-regression model (fig. 18A). The change in withdrawal rate was offset by an essentially equivalent change in aquifer storage. These changes in rate for that short time period had an insignificant effect on the cumulative water budget over the length of the test (fig. 18B). The second difference is the change in pumping rate between the two models, as discussed previously in this section. Except for these differences, the shapes of the curves in figure 18 are the same as those in figure 9. The discussion of pumping and the response in the budget components regarding figure 9 for the trial-and-error model applies to the nonlinear-regression model results (fig. 18) as well.

Sensitivity of Simulated Water Budget

The composite scaled sensitivity values discussed previously are a measure of the sensitivity of the simulated equivalents of observations used in the nonlinear-regression method to the model parameters. As shown in tables 4 and 6, the simulated values at the observation locations are very insensitive to riverbed and drain-bed hydraulic conductivity. However, no observations of flow between the aquifer system and the river or drain were available during the aquifer test.

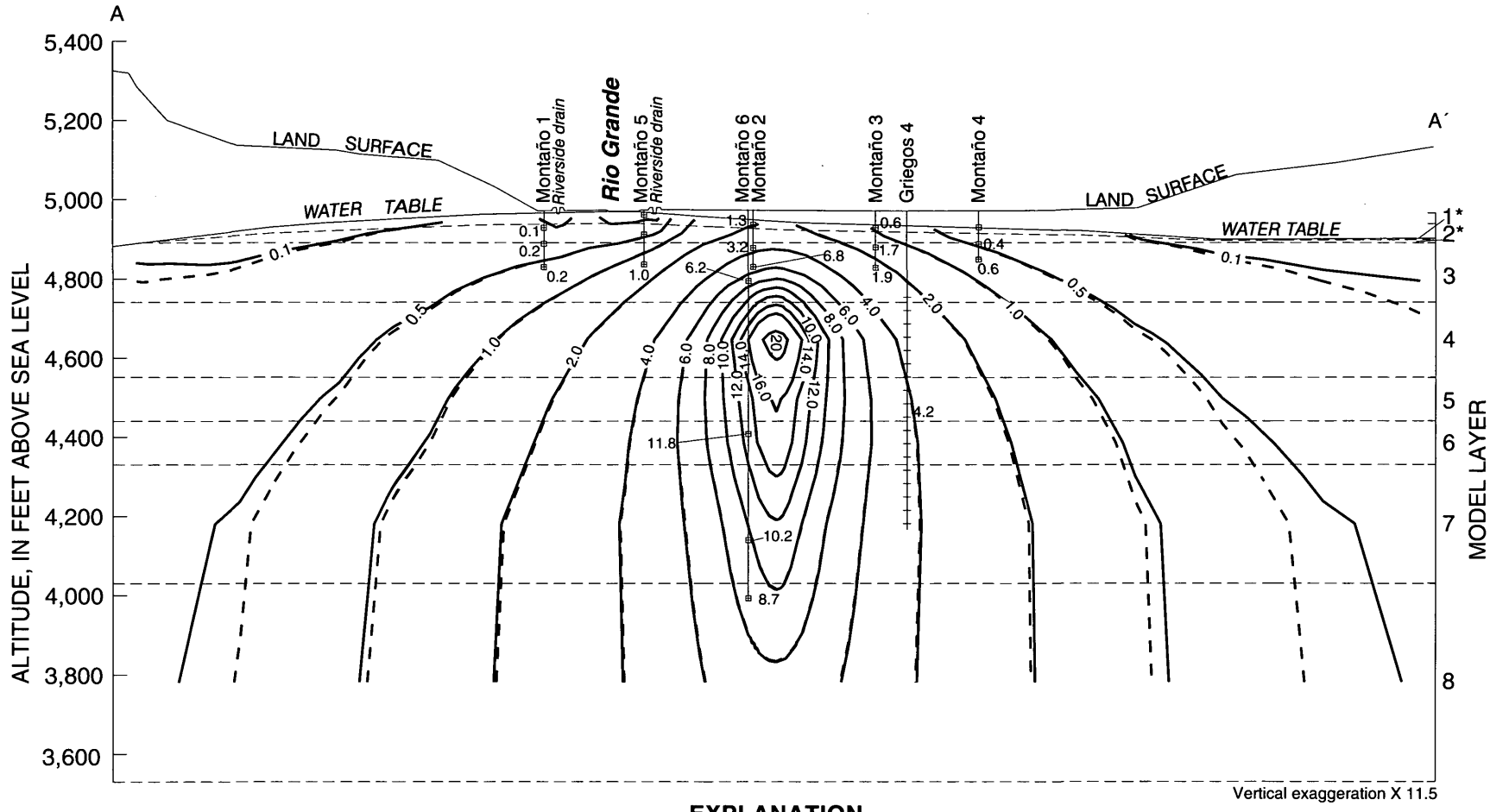

Figure 17. Generalized section A-A' showing the vertical distribution of drawdown simulated at the end of pumping using the model calibrated by nonlinear regression (location of section shown on plate 1).

Table 9. Simulated water budget at the end of pumping for the model calibrated by nonlinear regression

[Positive numbers indicate a source of water and negative numbers indicate a discharge of water]

Mechanism	Model with no-flow boundary				Model with head-dependent-flux boundary			
	Net flow rate		Cumulative net flow		Net flow rate		Cumulative net flow	
	Acre-feet per day	Sources as percentage of withdrawal	Acre-feet	Sources as percentage of withdrawal	Acre-feet per day	Sources as percentage of withdrawal	Acre-feet	Sources as percentage of withdrawal
Ground-water withdrawal	-10.92		-593.32		-10.92		-593.32	
River leakage	0.77	7.0	33.56	5.7	0.75	6.9	32.83	5.5
Riverside-drain leakage	1.13	10.4	44.70	7.5	1.11	10.2	43.85	7.4
Aquifer storage	9.01	82.6	515.06	86.8	8.48	77.7	492.12	82.9
Head-dependent model boundary	0.00	0.00	0.00	0.00	0.58	5.3	24.52	4.1
Total	-0.01	100.0	0.00	100.0	0.00	100.1	0.00	99.9
Percent discrepancy	0.09	0.00	0.00	0.00	0.00	0.10	0.00	0.10

Because these bed conductivities could influence the estimation of the amount and timing of infiltration from the river/drain system as a result of pumping during the test, the sensitivity of the simulated flow from these features was tested by adjusting the riverbed and drain-bed hydraulic-conductivity values in a series of simulations and comparing the resulting simulated water-budget values.

The simulated water budgets for sensitivity tests of riverbed and drain-bed hydraulic conductivity and the water budget for the standard simulation are listed in table 10. Table 10 shows the water budgets for two time periods: at the end of pumping (54.4 days after pumping began) and 160 days after pumping began. Because there is no aquifer-test pumping from Griegos 1 at 160 days, the budget rates show only the rates at which induced infiltration from the river and drain are replenishing aquifer storage. The cumulative amount of ground-water withdrawal for the two times is the same because no additional aquifer-test pumping was conducted after 54.4 days. Also, because the principle of superposition has been applied to the model (see "Model description" section) and only the effects of pumping during the aquifer test are simulated, continuation of the normal operation of wells in the aquifer-test area about 90 days after aquifer-test pumping began does not influence the results.

The sensitivity of simulated flow from the river and drain system to changes in the hydraulic conductivity of the riverbed and riverside-drain bed was tested by increasing and decreasing the conductivities by a factor of 2 (table 10). The increase (K_{RB} = 4 feet per day) and decrease (K_{RB} = 1 foot per day) in the simulated hydraulic conductivity of the riverbed results in as much as a 1.3-percent change in the rate and as much as a 1.8-percent change in the cumulative amount of river leakage for either of the two time periods. The increase (K_{DB} = 8 feet per day) and decrease (K_{DB} = 2 feet per day) in the simulated hydraulic conductivity of the riverside-drain bed results in as much as a 4.4-percent change in the rate and as much as a 6.0-percent change in the cumulative amount of drain leakage for the two time periods. Given that a 50- to 100-percent change in simulated hydraulic-conductivity values results in as much as a 6-percent change in simulated leakage, the leakage from these features seems to be slightly to moderately sensitive to the bed hydraulic conductivities. No detectable change in simulated drawdown at the observation locations resulted from the changes in simulated bed hydraulic conductivities. This result is consistent with the values of composite scaled sensitivity.

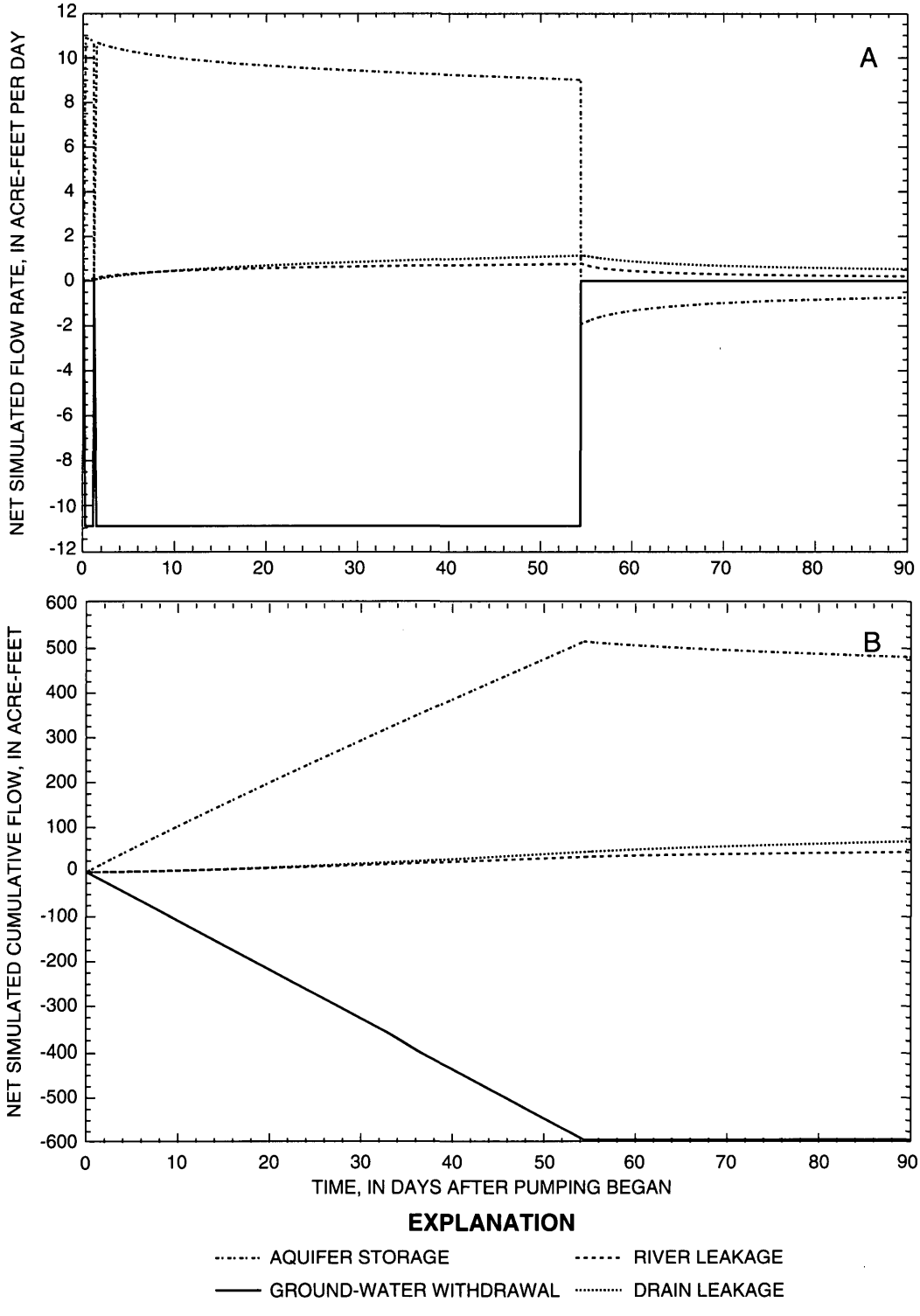

Figure 18. Net simulated flow rates (A) and cumulative flow (B) from the model calibrated by nonlinear regression. Positive numbers indicate a source of water and negative numbers indicate a discharge of water.

Table 10. Sensitivity of the simulated water budget to values of riverbed and drain-bed hydraulic conductivity

[Positive numbers indicate a source of water and negative numbers indicate a discharge of water. K_{RB} is riverbed hydraulic conductivity and K_{DB} is drain-bed hydraulic conductivity]

	Net flow rate, in acre-feet per day				Cumulative net flow since pumping began, in acre-feet			
	Groundwater withdrawal	River leakage	Drain leakage	Aquifer storage	Groundwater withdrawal	River leakage	Drain leakage	Aquifer storage
Budget components at the end of pumping (54.4 days after pumping began)								
Standard nonlinear-regression model with no-flow lateral boundaries (K_{RB}=2 feet per day; K_{DB}=4 feet per day)	-10.92	0.77	1.13	9.01	-593.32	33.56	44.70	515.06
Change made to standard model								
K_{RB}=4 feet per day	-10.92	0.77	1.13	9.01	-593.32	33.93	44.49	514.90
K_{RB}=1 foot per day	-10.92	0.76	1.14	9.02	-593.32	32.96	45.03	515.33
K_{DB}= 8 feet per day	-10.92	0.75	1.17	9.00	-593.32	32.99	46.32	514.00
K_{DB}= 2 feet per day	-10.92	0.79	1.08	9.05	-593.32	34.45	42.04	516.82
Budget components 160 days after pumping began (about 106 days after pumping ended)								
Standard nonlinear-regression model with no-flow lateral boundaries (K_{RB}=2 feet per day; K_{DB}=4 feet per day)	0.00	0.14	0.36	-0.50	-593.32	55.18	96.82	441.33
Change made to standard model								
K_{RB}=4 feet per day	0.00	0.14	0.37	-0.50	-593.32	54.36	97.51	441.46
K_{RB}=1 foot per day	0.00	0.14	0.36	-0.50	-593.32	55.68	96.38	441.25
K_{DB}= 8 feet per day	0.00	0.13	0.37	-0.50	-593.32	53.78	99.14	440.41
K_{DB}= 2 feet per day	0.00	0.15	0.35	-0.50	-593.32	57.46	92.97	442.88

AMOUNT AND TIMING OF INDUCED INFILTRATION FROM THE RIO GRANDE SURFACE-WATER SYSTEM

The amount and timing of induced infiltration from the Rio Grande surface-water system as a result of pumping during the aquifer test were estimated on the basis of simulated water budgets from the models described previously in this report. Estimates based on both the model calibrated by trial and error and the model calibrated by nonlinear regression are given. As described in the "Boundary conditions" section, partial barriers to ground-water flow in the aquifer system would likely affect the system in a manner intermediate to the effects resulting from the no-flow and head-dependent-flux lateral boundary conditions used in the models. Therefore, the projections of the amount and timing of induced infiltration from the surface-water system presented in this section are based on simulations using both boundary conditions with each of the two models. In this manner, induced infiltration in the aquifer system is likely bounded by the range of these projections.

Induced infiltration from surface-water systems has often been estimated using analytical methods. The Glover and Balmer (1954) analytical method with the addition of an impermeable boundary has been commonly used for estimating induced infiltration from the Rio Grande surface-water system as a result of ground-water withdrawal in the Albuquerque Basin (Summers, 1992). Estimates of induced infiltration as a result of aquifer-test pumping using this analytical method were compared with the estimates derived using the numerical models.

Numerical Model Estimates

Tables 3 (for trial-and-error model) and 9 (for nonlinear-regression model) list the simulated amounts of induced infiltration from the Rio Grande and the riverside drains at the end of aquifer-test pumping. The amounts differ somewhat between the two models because of the difference in the amount of pumping and the difference in some parameter values in the two models. In terms of pumping, induced infiltration from the river ranged from 5.5 to 5.8 percent of the amount pumped, and induced infiltration from the riverside drains ranged from 7.2 to 7.5 percent of the amount pumped. As described in the "Canals" section of this report, infiltration from canals cannot be significantly changed by pumping from the Griegos 1 well. The infiltration induced from the Rio Grande surface-water system is therefore the sum of the infiltration induced from the river and the drains. For both models with both boundary conditions, induced infiltration from the Rio Grande surface-water system was 13 percent (a range of 12.9 to 13.2 percent) of the total amount withdrawn at the time the pump was shut down. The source of the remainder of the amount pumped was from aquifer storage (from both inside and outside the modeled area in the simulations with head-dependent-flux boundaries; see the "Water budget" sections).

As time continues after the pump is shut down, induced infiltration from the surface-water system continues to replenish aquifer storage. Figure 19 shows the increase in induced infiltration from the Rio Grande surface-water system over time for all four model simulations. Whereas the simulated induced infiltration by the four simulations closely agrees during pumping and for a short time after pumping has stopped, the curves diverge over time after pumping has stopped. At late times the simulations with head-dependent-flux boundaries estimate less induced infiltration (58 to 60 percent of total withdrawal at 5 years; fig. 19, curves D and B) than the simulations with no-flow boundaries do (68 to 72 percent of total withdrawal at 5 years; fig. 19, curves C and A). The simulations with head-dependent-flux boundaries simulate less induced infiltration because inflow through the head-dependent-flux boundaries also replenishes the simulated depletion of aquifer storage within the model. The only source of water to replenish depletion of aquifer storage in the simulations with no-flow boundaries is induced infiltration from the surface-water system. As a result, the induced infiltration is larger.

The configuration of the aquifer system cannot be known with certainty. As a result, models cannot simulate the aquifer system without error. Although the model calibrated by trial and error and the model calibrated by nonlinear regression differ significantly in their simulated values of hydrologic properties and somewhat in model layer configuration, the most significant differences in their estimation of induced infiltration result from boundary-condition differences (fig. 19). Because these two boundary conditions represent extremes that could exist in the

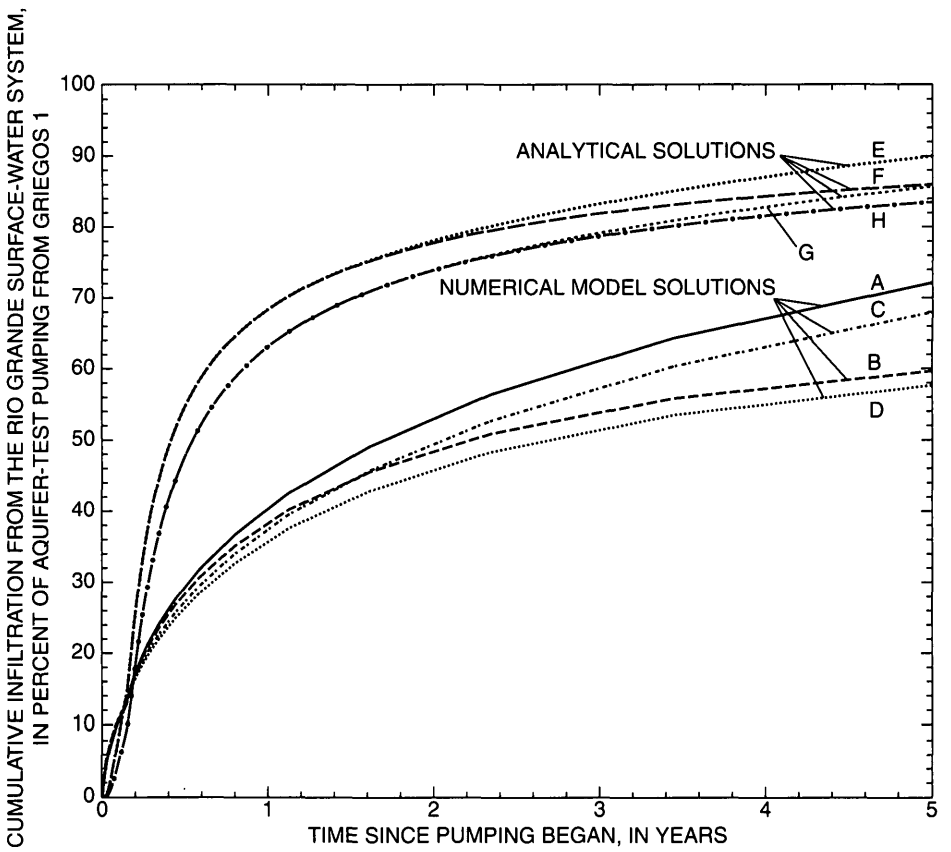

EXPLANATION

NUMERICAL MODEL SOLUTIONS

A — Trial-and-error-calibrated model with no-flow lateral boundaries

B — Trial-and-error-calibrated model with head-dependent-flux lateral boundaries

C — Model calibrated by nonlinear regression with no-flow lateral boundaries

D — Model calibrated by nonlinear regression with head-dependent-flux lateral boundaries

ANALYTICAL SOLUTIONS

E — Analytical solution using the horizontal transmissivity of the trial-and-error-calibrated model and a no-flow boundary at the location of the east model boundary

F — Analytical solution using the horizontal transmissivity of the trial-and-error-calibrated model and a no-flow boundary at the Sandia Mountain front

G — Analytical solution using the horizontal transmissivity of the model calibrated by nonlinear regression and a no-flow boundary at the location of the east model boundary

H — Analytical solution using the horizontal transmissivity of the model calibrated by nonlinear regression and a no-flow boundary at the Sandia Mountain front

Figure 19. Estimated infiltration from the Rio Grande surface-water system induced as a result of aquifer-test pumping from the Griegos 1 well.

aquifer system, the amount of induced infiltration as a result of aquifer-test pumping likely is somewhere between the values shown in the group of curves in figure 19 (A-D). These curves illustrate the uncertainties inherent in estimating induced infiltration using three-dimensional ground-water-flow models.

Analytical Estimates

Analytical methods require that complexities in the river/aquifer system be simplified so that the mathematical equations can be solved analytically. The simplifying assumptions of the Glover and Balmer (1954) method include (1) the river forms a straight line that is infinite in horizontal extent and extends to the entire depth of the aquifer, (2) the riverbed has no impedance to flow, (3) all ground-water flow is horizontal, (4) the aquifer is homogeneous and isotropic, (5) the well pumps from the entire thickness of the aquifer, and (6) aquifer transmissivity remains constant—that is, drawdown in the aquifer is insignificant compared to the thickness of the aquifer. The impermeable boundary (Summers, 1992, app. 1) is assumed to be a straight line parallel to the idealized river, also infinite in horizontal extent and extending to the entire depth of the aquifer. The aquifer system is, therefore, represented as an idealized two-dimensional system. As described in the "Model description" section, a three-dimensional numerical ground-water-flow model allows the complexity of the three-dimensional variation in boundary conditions and aquifer properties throughout the aquifer system to be included, eliminating the need for these simplifying assumptions.

For comparison to numerical model solutions, the hydraulic properties used in the analytical solutions were taken from the values used in the numerical models. The four analytical solutions that were made used (1) the horizontal transmissivity (22,180 feet squared/day over the 1,440 feet of simulated aquifer thickness) and specific yield (0.15) of the model calibrated by trial and error at the Griegos well field, and the impermeable boundary located at the east model boundary (4.1 miles from the Rio Grande) (curve E, fig. 19); (2) the same as (1) except that the impermeable boundary is located at the Sandia Mountain front (10 miles from the Rio Grande) (F, fig. 19); (3) the horizontal transmissivity (15,920 feet squared/day over the 1,440 feet of simulated aquifer thickness) and specific yield (0.15) of the model calibrated by nonlinear regression at the Griegos well field, and the impermeable boundary at the location of the east model boundary (4.1 miles from the Rio Grande) (G, fig. 19); and (4) the same as (3) except that the impermeable boundary is located at the Sandia Mountain front (10 miles from the Rio Grande) (H, fig. 19). Therefore, the analytical solutions differ only in the values of transmissivity and in the distance of the impermeable boundary from the river.

Comparison of Estimates

The analytical solutions are compared to the numerical model solutions in figure 19. In the early time after pumping begins (less than about 0.1 to 0.2 year), the numerical models estimate a greater percentage of induced infiltration from the river system than the analytical solutions. This results because the timing of the reduction of head in the aquifer reaching the river boundary is a function of the aquifer diffusivity (transmissivity or hydraulic conductivity divided by storage coefficient). Change in hydraulic head is transmitted through an aquifer system faster with larger diffusivity. The numerical models are three dimensional; therefore, all but the top layer simulate confined conditions. Because a confined storage coefficient is much smaller than the water-table storage coefficient (thickness times the magnitude of 10^{-6} compared to 0.15) and horizontal transmissivity is represented similarly, the diffusivity of all but the top layer is larger in the three-dimensional representation of the system than in the two-dimensional representation of the analytical method. Therefore, the reduced hydraulic head is transmitted quickly to the simulated river boundary from the middle model layers, where pumping occurs.

At any given time greater than about 0.2 year after pumping began, the analytical solutions estimate a significantly greater percentage of water coming from induced infiltration than the numerical models estimate. This is primarily because of the assumption of a fully penetrating river with unrestricted flow from the river to the aquifer system, which results in an overestimation of induced infiltration from the river over time (Sophocleous and others, 1995).

The six curves A, C, and E-H in figure 19 are solutions based on the assumption that the only source of water to replenish withdrawal from aquifer storage is

induced infiltration from the river system. Therefore, all water taken from aquifer storage will ultimately be replenished by induced infiltration. With similar aquifer properties, the two-dimensional representation of the analytical solutions will calculate that induced infiltration will reach a particular percentage of ground-water withdrawal significantly more quickly than will the three-dimensional representations of the numerical model solutions.

This is illustrated by comparing curve A with curve E and curve C with curve G in figure 19. The trial-and-error model with no-flow boundaries (curve A) estimated that induced infiltration would be 72 percent of the aquifer-test withdrawal 5 years after pumping began, whereas the analytical solution with the same horizontal transmissivity and boundary location (curve E) estimated that induced infiltration would be 72 percent of withdrawal 1.3 years after pumping began and would be 90 percent of withdrawal 5 years after pumping began. The nonlinear-regression model with no-flow boundaries (curve C) estimated that induced infiltration would be 68 percent of the aquifer-test withdrawal 5 years after pumping began, whereas the analytical solution with the same horizontal transmissivity and boundary location (curve G) estimated that induced infiltration would be 68 percent of withdrawal 1.3 years after pumping began and would be 86 percent of withdrawal 5 years after pumping began.

The four analytical solutions (fig. 19, curves E-H) show differences resulting from differences in transmissivity values and boundary locations used. Curves E and F differ in transmissivity values from curves G and H. With everything else equal, the analytical solutions show a greater estimated effect on the river system over time because of the larger values of transmissivity (curve E compared with curve G and curve F compared with curve H). With equal aquifer-transmissivity and storage values, a greater effect on the river system is estimated over time with decreasing distance of the impermeable boundary to the well and river (curve E compared with curve F and curve G compared with curve H). In these examples, however, the differences do not become noticeable until about 1.5 to 2 years after pumping began.

SUMMARY AND CONCLUSIONS

A long-term aquifer test was conducted near the Rio Grande in Albuquerque during January and February 1995 using 22 wells and piezometers at nine sites, with the City of Albuquerque Griegos 1 production well used as the pumped well. Griegos 1 was pumped for 54.4 days at about 2,330 gallons per minute. The purpose of this test was to estimate aquifer properties in the vicinity of the Griegos well field and the amount of infiltration induced into the aquifer system from the Rio Grande and riverside drains as a result of pumping during the test. A ground-water-flow model was developed for this analysis and calibrated by trial-and-error adjustments of the aquifer properties using the program MODFLOW. The model was adjusted for compatibility with the program MODFLOWP and recalibrated using the nonlinear least-squares regression technique implemented in that program. This report describes these finite-difference ground-water-flow models and the results of the analyses using the models.

The aquifer system in the vicinity of the aquifer test includes the middle Tertiary to Quaternary Santa Fe Group and Quaternary post-Santa Fe Group valley- and basin-fill deposits of the Albuquerque Basin. The upper part of the Santa Fe Group is the primary water-yielding zone in the aquifer-test area. The alluvium in the inner valley of the Albuquerque Basin consists of post-Santa Fe Group channel and flood-plain deposits, ranging from about 70 to 80 feet thick in the aquifer-test area. The Rio Grande and adjacent riverside drains are in hydraulic connection with the aquifer system.

The finite-difference model developed for trial-and-error calibration consisted of 57 rows, 65 columns, and 8 layers. The horizontal grid-cell dimensions ranged from a column width of 100 feet and a row width of 200 feet in the central part of the model to a column width of 2,800 feet and a row width of 1,500 feet at the margins of the model. The horizontal dimensions of the model were 7.2 miles on a side. The total modeled area was about 52 square miles. The layer thicknesses ranged from 30 feet or less for the top layer to 500 feet for the bottom layer, and the total thickness simulated was 1,440 feet. The Rio Grande and adjacent riverside drains were simulated as head-dependent-flux boundaries. The model analysis used the principle of superposition, so that all simulated changes in hydraulic head and water fluxes result from the simulated ground-water withdrawal from the aquifer-test pumping. Observed drawdowns used for

model calibrations were adjusted for any identifiable influences from stresses other than the aquifer-test pumping.

Hydraulic-conductivity values of the upper part of the Santa Fe Group resulting from the model calibrated by trial and error varied by zone in the model and ranged from 12 to 33 feet per day. The hydraulic conductivity for the zones representing the middle part of the Santa Fe Group were 4 and 11 feet per day. The hydraulic conductivity of the inner-valley alluvium was 45 feet per day. The vertical to horizontal anisotropy ratio was 1:140, except in the cell representing the pumped well, where it was assumed to be 1:5 because of the influence of the gravel-packed, 600-foot screened interval. Specific storage was 4×10^{-6} per foot of aquifer thickness and specific yield was 0.15 (dimensionless). The sum of squared errors between the observed and simulated drawdowns was 130 feet squared for the model calibrated by trial and error.

To apply MODFLOWP, the upper two layers of the model were adjusted so that layer 1 would not become unsaturated. MODFLOWP (version 2.13) does not support transient model simulations in which a layer becomes unsaturated and the water table passes to the next lower layer. The combined saturated thickness of layers 1 and 2 was split in the ratio of three-eights of the thickness to layer 1 and five-eights to layer 2, where previously layer 2 was 50 feet thick and layer 1 was saturated only if the water table was above the top of layer 2. This change assured that layer-1 cells never went from a saturated to an unsaturated condition.

The set of parameters used to estimate by nonlinear least-squares regression was selected on the basis of the value of the composite scaled sensitivity for each parameter. The parameters with large composite scaled sensitivity are more likely to be estimated by the regression procedure because the simulated values at the observation locations are most sensitive to these parameters. The set of parameters that could be estimated were the combined zones of hydraulic conductivity of the upper part of the Santa Fe Group (K_{USF}), vertical to horizontal anisotropy ratio (A_V), specific storage (S_s), and pumping rate from layers 4 through 7 (P_4, P_5, P_6, and P_7). The hydraulic conductivity of the inner-valley alluvium, middle part of the Santa Fe Group, riverbed, and riverside-drain bed and the specific yield had low composite scaled sensitivity values and therefore could not be estimated with use of the available drawdown data. The hydraulic conductivity of the upper part of the Santa Fe Group was estimated to be 12 feet per day, the vertical to horizontal anisotropy ratio was estimated to be 1:82, the specific storage was estimated to be 1.2×10^{-6} per foot, and the pumping rates were estimated to be 1,390, 197, 353, and 542 gallons per minute for layers 4 through 7, respectively.

The approximate linear 95-percent confidence interval for each parameter was calculated by MODFLOWP. Because the model is nonlinear to some degree and the weighted residuals do not strictly conform to a normal distribution, the linear 95-percent confidence intervals are not strictly correct and therefore need to be considered approximate.

The overall sum of squared errors between simulated values from the nonlinear-regression model and a common set of observations was 87 feet squared. This compares with 130 feet squared for the trial-and-error model and shows that the nonlinear-regression model is an overall better calibrated model. However, only about half the matches between curves of observed and simulated drawdown are better with the nonlinear-regression model. Several curves match better with the trial-and-error calibrated model, indicating that at least some of the modeled area is better represented by the trial-and-error model.

The amount and timing of induced infiltration from the Rio Grande surface-water system were estimated using both the trial-and-error and nonlinear-regression models. Two lateral boundary conditions (no flow and head-dependent flux) were used in each model for these simulations to represent the extremes of boundary conditions that could exist in the aquifer system. The boundary conditions caused little difference in simulated results at the drawdown-observation locations and in the simulated water budgets during the aquifer-test pumping period, which was used for calibration. However, projections of induced infiltration from the surface-water system beyond the end of pumping do show differences between the models and between the different lateral boundary conditions. The differences resulting from different boundary conditions are greater than the differences resulting from the two models. At the end of aquifer-test pumping (54.4 days after pumping began), 13 percent of the total amount of water pumped was compensated by induced infiltration from the Rio Grande surface-water system. The remainder was compensated by depletion of aquifer storage. After pumping stops, induced infiltration continues to replenish aquifer storage. Five years after pumping

began (about 4.85 years after pumping stopped), 58 percent (the nonlinear-regression model with head-dependent-flux lateral boundaries) to 72 percent (the trial-and-error model with no-flow lateral boundaries) of the total amount of water pumped was compensated by induced infiltration from the Rio Grande surface-water system. The true amount of induced infiltration resulting from aquifer-test pumping likely is between these values.

The amount and timing of induced infiltration from the surface-water system were also estimated using analytical methods. These analytical methods require that the complexities in the river/aquifer system be simplified and represented as an idealized two-dimensional system. The hydraulic properties used in the analytical solutions were taken from the values used in the numerical models. Comparison of these analytical estimates to the numerical-model estimates indicates that at any given time greater than about 0.2 year after pumping began, the analytical solutions estimate a significantly greater percentage of water coming from induced infiltration than the numerical models estimate. This is primarily because of the analytical-method assumption of a fully penetrating river with unrestricted flow from the river to the aquifer system, which results in an overestimation of induced infiltration from the river over time.

REFERENCES CITED

Bjorklund, L.J., and Maxwell, B.W., 1961, Availability of ground water in the Albuquerque area, Bernalillo and Sandoval Counties, New Mexico: New Mexico State Engineer Technical Report 21, 117 p.

Cooley, R.L., and Naff, R.L., 1990, Regression modeling of ground-water flow: Techniques of Water-Resources Investigations of the U.S. Geological Survey, book 3, chap. B4, 232 p.

Freeze, R.A., and Cherry, J.A., 1979, Groundwater: Englewood Cliffs, N.J., Prentice-Hall, 604 p.

Glover, R.G., and Balmer, G.G., 1954, River depletions resulting from pumping a well near a river: Transactions, American Geophysical Union, v. 35, no. 3, p. 468-470.

Groundwater Management, Inc., 1988, Pumping test data analysis, Griegos well field, City of Albuquerque, New Mexico: Consulting report, Kansas City, Kans., 22 p.

Hawley, J.W., 1996, Hydrogeologic framework of potential recharge areas in the Albuquerque Basin, central New Mexico, *in* Hawley, J.W., and Whitworth, T.M., eds., Hydrogeology of potential recharge areas and hydrogeochemical modeling of proposed artificial-recharge methods in basin- and valley-fill aquifer systems, Albuquerque Basin, New Mexico: Socorro, New Mexico Bureau of Mines and Mineral Resources Open-File Report 402-D, chap. 1.

Hawley, J.W., and Haase, C.S., 1992, Hydrogeologic framework of the northern Albuquerque Basin: Socorro, New Mexico Bureau of Mines and Mineral Resources Open-File Report 387, p. IX-7.

Hawley, J.W., Haase, C.S., and Lozinsky, R.P., 1995, An underground view of the Albuquerque Basin, *in* Ortega Klett, C.T., ed., The water future of Albuquerque and middle Rio Grande Basin: Proceedings of the 39th Annual New Mexico Water Conference, November 3-4, 1994, New Mexico Water Resources Research Institute WRRI Report No. 290, p. 37-55.

Hill, M.C., 1990, Preconditioned Conjugate-Gradient 2 (PCG2), a computer program for solving ground-water flow equations: U.S. Geological Survey Water-Resources Investigations Report 90-4048, 43 p.

Hill, M.C., 1992, A computer program (MODFLOWP) for estimating parameters of a transient, three-dimensional, ground-water flow model using nonlinear regression: U.S. Geological Survey Open-File Report 91-484, 358 p.

Hill, M.C., 1994, Five computer programs for testing weighted residuals and calculating linear confidence and prediction intervals on results from ground-water parameter-estimation computer program MODFLOWP: U.S. Geological Survey Open-File Report 93-481, 81 p.

McAda, D.P., 1996, Plan of study to quantify the hydrologic relations between the Rio Grande and the Santa Fe Group aquifer system near Albuquerque, central New Mexico: U.S. Geological Survey Water-Resources Investigations Report 96-4006, 58 p.

McDonald, M.G., and Harbaugh, A.W., 1988, A modular three-dimensional finite-difference ground-water flow model: Techniques of Water-Resources Investigations of the U.S. Geological Survey, book 6, chap. A1, variously paged.

Ortiz, David, and Lange, K.M., 1996, Water resources data, New Mexico, water year 1995: U.S. Geological Survey Water-Data Report NM-95-1, 628 p.

Ortiz, David, Lange, Kathy, and Beal, Linda, 1998, Water resources data, New Mexico, water year 1997: U.S. Geological Survey Water-Data Report NM-97-1, 574 p.

Reilly, T.E., Franke, O.L., and Bennett, G.D., 1987, The principle of superposition and its application in ground-water hydraulics: Techniques of Water-Resources Investigations of the U.S. Geological Survey, book 3, chap. B6, 28 p.

Roelle, J.E., and Hagenbuck, W.W., 1994, Surface cover maps of the Rio Grande floodplain from Velarde to Elephant Butte Reservoir, New Mexico: National

Biological Survey and U.S. Fish and Wildlife Service, atlas and maps for the National Wetlands Inventory, 57 p.

Sophocleous, Marios, Koussis, Antonis, Martin, J.L., and Perkins, S.P., 1995, Evaluation of simplified stream-aquifer depletion models for water rights administration: Ground Water, v. 33, no. 4, p. 579-588.

Summers, W.K., 1992, Effects of Albuquerque's pumpage on the Rio Grande and the rate at which Albuquerque will have to release San Juan-Chama water to offset them: City of Albuquerque memorandum, variously paged.

Thiem, Günther, 1906, Hydrologische methoden: Leipzig, J.M. Gebhart, 56 p.

Thorn, C.R., 2001, Analytical results of a long-term aquifer test conducted near the Rio Grande, Albuquerque, New Mexico, *with a section on* Piezometer-extensometer test results, by C.E. Heywood: U.S. Geological Survey Water-Resources Investigations Report 00-4291, 19 p.

Thorn, C.R., McAda, D.P., and Kernodle, J.M., 1993, Geohydrologic framework and hydrologic conditions in the Albuquerque Basin, central New Mexico: U.S. Geological Survey Water-Resources Investigations Report 93-4149, 106 p.

Trescott, P.C., Pinder, G.F., and Larson, S.P., 1976, Finite-difference model for aquifer simulation in two dimensions with results of numerical experiments: Techniques of Water-Resources Investigations of the U.S. Geological Survey, book 7, chap. C1, 116 p.

Wilson, B.C., 1992, Water use by categories in New Mexico counties and river basins, and irrigated acreage in 1990: New Mexico State Engineer Office Technical Report 47, 141 p.

☆ U.S. GOVERNMENT PRINTING OFFICE: 2001 — 673-092 / 54011 Region No. 8

GRAPHICS, EDITORIAL, AND TEXT PREPARATION TEAM
Darla E. Straka, Scientific Illustrator
Barbara J. Henson, Scientific Illustrator
Ben Garcia, Computer Specialist
Harriet R. Allen, Editor
Mary Montaño, Editorial Assistant

U.S. Department of the Interior
U.S. Geological Survey, WRD
5338 Montgomery Blvd. NE, Suite 400
Albuquerque, NM 87109-1311

BOOK RATE

D.P. McAda—SIMULATION OF A LONG-TERM AQUIFER TEST CONDUCTED NEAR THE RIO GRANDE, ALBUQUERQUE, NEW MEXICO—
U.S. Geological Survey Water-Resources Investigations Report 99-4260